Life Cycle Assessment Comparison of the Conventional Crystalline Silicon Solar Cell Versus the New, Potentially Revolutionary, Perovskite Solar Cell

By,
Taylor Camp
University of Colorado Boulder

A thesis submitted to the
University of Colorado Boulder
In partial fulfillment
Of the requirements to receive
Honors designation in
Environmental Studies
April 2019

Thesis Advisors:

Sarah Rogers, Environmental Studies Program, Committee Chair
Dale Miller, Environmental Studies Program
Sean Shaheen, Electrical, Computer & Energy Engineering Program
Eve-Lyn Hinckley, Environmental Studies Program

Abstract

In order to understand the environmental impacts associated with solar energy production, a life cycle assessment (LCA) comparison of two panel types is performed. Popular crystalline silicon photovoltaics (PV) are analyzed alongside the new perovskite PV material, currently being lab tested. Each panel type is analyzed individually using the LCA life cycle inventory (LCI) framework to gather information on the cradle to grave impacts. Following these LCI analyses, the two are compared on the utility scale using the LCA impact category framework. Natural resource depletion, energy payback time (EPBT), contribution to global climate change, land use, and human and ecosystem toxicity are the impact categories selected for this analysis as they are the most affected by solar installations today. This study finds that perovskite PV low embodied energy decreases the EPBT of solar on the utility scale, however the current relatively short lifetimes of this material increases the global warming potential (GWP), as compared to crystalline silicon PV. Although perovskite PV offers large upscaling potentials through print manufacturing, it does not address the immense land stress of utility scale solar. The current international standard for conducting a LCA does not specifically address ecosystem services and biodiversity impacts. Further research into decreasing the environmental impacts associated with big solar is suggested.

Acknowledgments

Though this study was one of the most challenging activities I have ever undertaken, it was also the most rewarding. Working with amazing professors at CU, I was able to develop my research and writing skills to a level I previously never thought possible. I would like to thank my advisors, Dale Miller, Sarah Rogers, Sean Shaheen, and Eve-Lyn Hinckley, for helping me throughout the entire process. You all offered unique perspectives and advise that helped both ease my mind and push me forward. A special thanks goes out to Sarah, you helped calm me and keep my thoughts straight as they went crazy right in front of your eyes. You not only helped me structure my thesis, but develop my opportunities as an intellectual to a place I never thought I would go. Thank you for pushing me and guiding me in our numerous discussions throughout this process while remaining supportive and sympathetic.

Another special thank you goes to my family as they have always supported me in everything I do. Thank you to my mom who single-handedly talked me off many metaphorical edges throughout my entire college experience (or my entire life). Thank you to my dad for always pushing me to be great and strive for more. You both inspire me every day and I could not have done it without either of you. Special shout-out to my little brother Ryder who is too young to know what any of this means but will one day surpass everything I have done. To all the rest of my family and friends, thanks for being there for me, listening to me, and guiding me. I love each and every one of you.

Preface

Energy consumption in the United States has grown so rapidly since the mid-20th century that many of us cannot imagine a world, or a life, without reliable sources of energy. As the public demand for stable energy systems continues to grow, so does our need for scientific understanding of the subsequent effects of each conventional or contemporary energy source. Great global energy dependence coupled with growing knowledge of negative anthropogenic environmental impacts creates a growing need for clean as well as reliable sources of energy. Solar PV power production is a renewable energy source experiencing expanding installed capacity throughout the entire world, with little end in sight. As solar installed capacity continues to grow, so does the need for an adequate understanding of the impacts of solar on our natural world. To understand the environmental impacts associated with this product/process is the fundamental reason why I decided to conduct a LCA.

As an environmental studies student, I have come to realize that although classes and professors often teach us of the immense benefits of renewable energy systems, they often avoid any conversation of adverse environmental impacts. With hopes of shedding light on the ecosystem stressors associated with this energy source while still supporting it, I have conducted a thorough LCA for the benefit of those interested in learning. Although this particular study can be seen from a negative viewpoint, I want to emphasize that renewable energy sources, as they become more cost effective and technologically advanced, are paving the way to a sustainable future. Reducing our environmental impact can be done through a variety of ways, but as a community, we must understand the role energy systems play in our natural world.

Table of Contents

Introduction

To understand the environmental impacts associated with any product or process, researchers create what is known as a life cycle assessment (LCA). A LCA study provides researchers with information about environmental effects that can ensue at every stage of a product or processes life cycle, from raw material extraction to disposal. Using this cradle to grave framework, this study compares the impacts associated with the conventional crystalline silicon solar cell against the new, potentially revolutionary, perovskite solar cell. In order to identify areas where this new, innovative technology alleviates or exemplifies harmful impacts, this study analyzes all inputs and outputs associated with each panel type before applying them to the predetermined impact categories. Comprehending how this technological innovation can assist in reducing environmental impacts associated with solar energy production will spark more innovation in the future, for the future.

Various background descriptions, including that of solar energy and LCAs, are provided first in order to help strengthen understanding of this topic and methodology. Using the LCA framework, a comparative analysis of the two panel types on the utility scale is developed. Crystalline silicon PV is analyzed first through the LCA life cycle inventory (LCI) framework because it is the most popular solar material in use today, producing energy at utility scale power plants globally. Perovskite PV LCI is analyzed second. There is no current installation using this material, therefore information learned during the LCI analysis of installed crystalline silicon is further applied to analyze the potential for perovskite. The two LCIs are evaluated and further applied to fit respective impact categories within the LCA impact category framework.

Categories from the LCA international standard that are most applicable to solar energy based on solar LCIs are preferred. Natural resource depletion is selected and subcategorized based on the individual panels use of raw materials and energy, then on the utility scale to measure the water used to maintain a solar site. Energy payback time (EPBT) falls within the natural resource category because it is calculated by comparing the previously identified energy inputs against the expected energy outputs of the solar site. Next, the contribution to global climate change is addressed using individual panel's global warming potentials (GWPs), as provided by previous solar LCAs. Land use, though also considered natural resource depletion, is separated into its own category because of the immense amount of land cover change required to install any utility scale solar power plant, regardless of the specific solar cell used. Land use is subcategorized into ecosystem stress, which follows a chain of events as they might unfold following extensive surface and subsurface alternations, as well as land use efficiency, based on the expected annual energy production of a solar site.

Using information from natural resource depletion, GWP, and immense land stress evaluated, the last impact category analyzes human and ecosystem toxicity associated with individual panels and utility scale solar. An interesting analysis of trees versus solar is presented for a carbon reduction comparison. Many of the lessons learned in each category overlap with others, as they impact each other through feedback systems. The results are discussed in detail to analyze the true differences between crystalline silicon and perovskite PV, while addressing the overwhelmingly under-analyzed issue of ecosystem stress from land cover change. This study concludes with panel installations and future research recommendations based on the analyzed data provided.

Background and Methods

This section offers insight into the growing solar industry through a brief history and current event synopsis. Following an introduction into solar, this section offers a brief history of LCAs, a framework from which this study was developed. Once the framework and requirements for LCAs are discussed in detail, the steps are further applied towards this specific study, thus providing a detailed methodology.

Solar Power

Although the solar PV technology used today was first seen as successful in 1954, it took nearly another 20 years before solar panels were made for public energy production. PV energy conversion efficiencies more than tripled during these 20 years, from 4% to 14%. Small-scale solar PV was implemented for a variety of uses, such as in-air satellite energy production and water pumping. In 1977, the U.S. Department of Energy (DOE) opened the Solar Energy Research Institute, now known as the National Renewable Energy Laboratory (NREL), located in Golden, Colorado. About five years later, the first MW-scale PV power plant went online in Hisperia, California (History of Solar n.d). Since this power plant was built, through the early 2000s, solar power production expanded very slowly as scientists and engineers worked to develop higher energy conversion efficiencies.

Since the early 2000s, PV technologies have become even more efficient and cost effective compared to conventional energy sources. The growth rate of solar energy adoption has increased rapidly, breaching on a 60% annual rising trend. Solar is used in almost every country in the world and has become a reliable source of clean energy (Solar Industry Research 2019).

According to the Energy Information Administration (EIA), solar energy accounts for around 1.6% of the United States total electricity generation, reaching a production capacity of nearly 70 billion kWh (kilowatt-hours) in 2018 (What is U.S. 2019). Worldwide, the International Energy Agency (IEA) reports that solar energy surpassed 398 GW (gigawatts) of installed capacity in 2017, generating more than 460 TWh (terawatt-hours) of electricity, accounting for around 2% of global total electricity generation (Solar energy n.d.). As global solar installed capacity continues to grow rapidly each year, it is of the utmost importance to understand the life cycle impacts of different PV technologies implemented at the utility scale.

Though there are a large variety of solar technologies on the market today, crystalline silicon PV accounts for the vast majority, over 90%, of the global solar installed market share (Srivastava 2016). Since Jan Czochralski's 1916 invention of growing crystallized structures from purified silicon, now known as the Czochralski Method, crystalline silicon PV has been at the forefront of solar research, development, and implementation (Uecker 2014). Energy conversion efficiencies of these technologies vary depending on the type of crystalline silicon PV, as well as the manufacturing methods used (Best Research-Cell Efficiencies 2019).

Multicrystalline silicon PV modules have ~20 % energy conversion efficiencies whereas monocrystalline silicon modules have ~25% (Uecker 2014). However, some research has suggested lab-tested efficiencies can reach up to 40% (Liu 2016). For the purpose of this study, an average conversion efficiency of 24% is assumed. These modules consist primarily of crystalline silicon structures but differ in wafer manufacturing and shape. Due to the vast installed capacity of crystalline silicon, understanding the various life cycle impacts of this particular PV technology creates a building block for future solar research.

Another PV technology taking up a wide portion of the global solar market share is thin film PV, accounting for around 30% of total solar installations worldwide (Gupta & Bais 2016). How do these market shares go beyond 100%? Multijunction solar cells, or crossbred solar cells, contain both thin film and silicon technologies. Combining these two panel types has achieved energy conversion efficiencies near 50% (Best Research-Cell Efficiencies 2019 & Philipps et al. 2018). For the purpose of this study, a focus is placed on mono or multi crystalline silicon PV alone, but combined PV technologies are important to understand. Figure 1 offers a design representation of the different solar PV technologies on the market today, note the location of perovskite solar cells. Perovskite PV is considered thin film solar because of the thin printing potential, discussed in detail later.

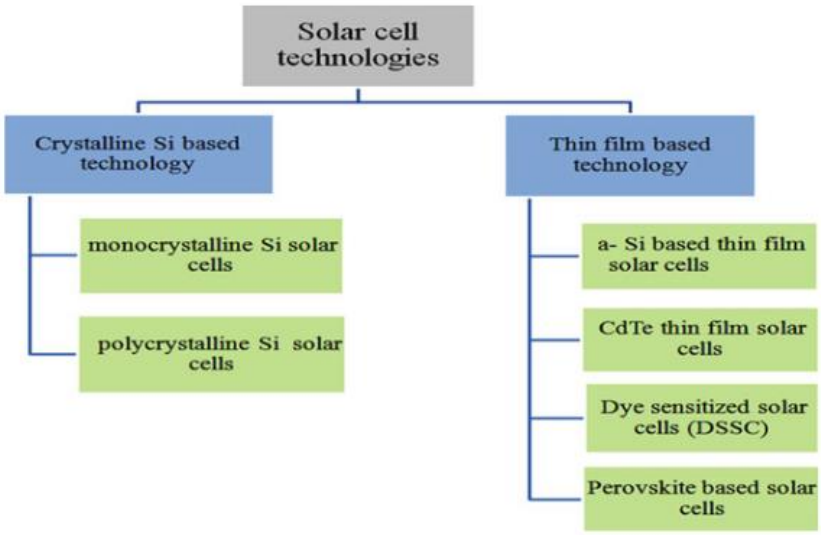

Figure 1: "Classification of Solar Cells by Technologies," from *Manufacturing Techniques of Perovskite Solar Cells*, by Kajal, Ghosh, & Powar 2018

Although these conventional panels offer energy conversion efficiencies greater than 20%, the desire for increased efficiencies and faster manufacturing methods have driven research into new, innovative solar technologies. Perovskite PV materials are a form of thin film solar cells that offer increased efficiencies alongside rapid increases in cell manufacturing rates. The potential for accelerating perovskite PV manufacturing through various techniques has driven research in a variety of ways by creating a more cost-effective technology with the potential to replace conventional silicon solar cells (Marsh 2019). Though the potential for perovskites is great, there are still many drawbacks to implementation, such as the use of toxic metals in the

cell material as well as the current relatively short lifetimes. Researchers aim to further develop perovskite PV technology for future utility scale solar installations.

Due to the lack of installed perovskite PV capacity, this study aims to fill the gaps in the research by comparing knowledge from the LCI of crystalline silicon to that of perovskite. In order to understand the full effects of this new technology, a theoretical LCA of utility scale perovskite is developed through the framework provided. It is important to note that due to the lack of installments, analyzing perovskite PV is difficult and comes with various limitations, i.e. it is hard to know the use lifetime of a product if it is not actually in use. Estimates from researchers and previous studies are used to find the average values associated with perovskites.

Life Cycle Assessments (LCAs)

In the late 1960s, as energy demands vastly increased alongside diminishing natural resources, growing concern for the environment led to the first LCA. Per industry request, the Midwest Research Institute (MRI) administered the first LCA of Coca Cola cans (Guinée et al. 2010). MRI researchers were successful in proving their hypothesis; that every aluminum can carried with it a plethora of negative environmental impacts. After the results of this study were made public, organizations began developing unique approaches to LCAs, however it was not until the mid-1990s that the International Organization for Standardization (ISO) developed two universal standards for LCAs. These standards are as follows:

1. ISO 14040 (2006E): 'Environmental management - Life cycle assessment - Principles and framework' (ISO 14040 1997)
2. ISO 14044 (2006E): 'Environmental management - Life cycle assessment - Requirements and guidelines' (ISO 14044 2006)

The first version of this new standard, Principles and Framework, was published in 1997 and included a loose guide for conducting a LCA. The standard described "the general framework, principles, and requirements for conducting and reporting" LCAs while opting not to "describe the [LCA] technique in detail" to allow more flexibility in the research within this growing field (ISO 14040 1997). Since conducting LCAs was a relatively new concept, the ISO refrained from placing too much restriction on the process in order to leave room for new methodologies while they worked on the second version of the standard. The Requirements and Guidelines version was published in 2006 and contained a detailed scope of LCA and Life Cycle Inventory (LCI) requirements while providing guidelines for conducting such an analysis (ISO 14044 2006). These standards also provided some suggestions for life cycle impact categories as they apply to cradle to grave frameworks.

Since the publication of these international standards, LCAs have grown more and more popular among scientific professionals concerned about environmental degradation and preservation. Researchers have expanded the framework used to examine the environmental impacts of soda cans into analyses that can change the course of any product or process in our global marketplace. Studies by various researchers either prove or disprove their hypothesis based on a comprehensive calculation of cradle to grave environmental impacts associated with the solar industry. Burkhardt, Heath, & Cohen (2012), Fthenakis & Kim (2011), and Peng, Lu, & Yang (2013) evaluate the inputs and outputs associated with solar panels to provide a complete understanding of the greenhouse gas emissions linked to panel life cycles. Studies by Parida, Iniyan, & Goic (2011) and Turconi, Boldrin, & Astrup (2013) use a LCA model to assess the performative efficiency and reliability of different solar panels. All forms of a LCA analysis

require background of the associated inputs and outputs at every stage of production in order to provide an educated answer to either support or contradict the hypothesis.

This study will use the LCA framework of LCIs to analyze environmental impacts associated with crystalline silicon and perovskite PV. Figure 2 offers a simplified schematic of the interactive, circular relationship between each part or step of a LCA analysis, as known and applied today.

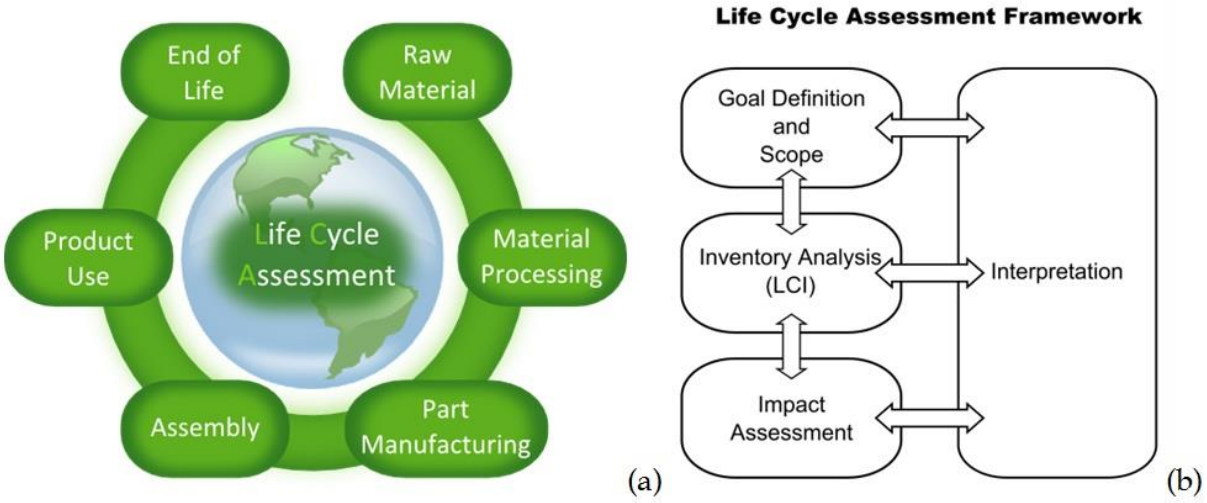

Figure 2: "(a) Cradle-to-grave Life Cycle Assessment and (b) LCA Framework according to ISO standards 14040 and 14044 (International Organization for Standardization 2006)," from *Life Cycle Assessment of Organic Photovoltaics*, by Anctil & Fthenakis 2011

LCAs highlight key areas of environmental impacts through four main phases; (1) goals and scope, (2) life cycle inventory (LCI) analysis, (3) life cycle impact assessment, and (4) interpretation, or further analysis (B Resource Guide 2008). Each stage needs to be completed in order to move on to the next stages. Identifying the goals and scope of the LCA provides a framework for the rest of the analysis. Analyzing the LCI of a specific product or process helps pinpoint all inputs and outputs associated at each stage of the life cycle. Classifying the variances of the LCI assists in identifying which impact categories are most affected by the production cycle. These relationships are analyzed and discussed, examining how LCIs and impact

categories intertwine and exploring possible solutions for alleviating harmful environmental impacts. This general LCA framework is applied to this study.

Goals and Scope

When beginning a LCA, the researcher or research team must first determine the goals and scope of the study, i.e. deciding which products, processes, environmental concerns, ongoing questions, etc. will be included in the study. For this study, a complete LCI of conventional crystalline silicon PV is presented first, followed by a LCI analysis of the potentially revolutionary perovskite PV. In order to understand the effects of implementing perovskite PV, an in-depth comparative LCA impact category analysis against utility scale crystalline silicon PV is completed following the individual LCI analyses. Analyzing crystalline silicon on the utility scale provides a look into the future for perovskites. Though they are lab-tested to be highly efficient and less impactful, perovskites have yet to be installed on the utility scale. Comparing utility scale crystalline silicon to perovskites provides an interpretation into varying environmental impacts to gain a better understanding of the side effects of these installations.

Life Cycle Inventory (LCI)

Identifying and measuring all inputs and outputs associated with a product or process is the basis of a LCI analysis. Inputs can include anything from the raw materials used to the required energy inputs to the recommended water or chemical use. Outputs refer to the stuff that comes from the analyzed product or process, i.e. waste, emissions, energy, etc. A LCI analysis can be split into three overarching categories; manufacturing, use, and decommissioning, however each of these three categories can be split up further. Manufacturing includes raw

materials acquisition, materials processing, and manufacturing, or material production. Although use inherently refers to the lifetime of a product or process, it can also refer to the installation and maintenance methods specific to the selected product. For solar panels, use refers to installation, energy production life cycle, and panel or site maintenance activities. The final stage of any product or processes life cycle is decommissioning, or disposal, which also includes waste treatments and recycling methods. The LCI research and analysis provides the groundwork for the next stage of Life Cycle Impact Assessment.

Life Cycle Impact Categories

Following descriptions of the cradle to grave inputs and outputs associated with the product or process, the Life Cycle Impact Assessment stage transforms this LCI data into "indicators for each impact category" (B Resource Guide 2008). Some common examples of impact category indicators are environmental aesthetics, climate change, resource depletion, human or ecosystem toxicity, eutrophication, etc. Once the proper impact categories are selected for the study, researchers use a multitude of data analysis techniques to calculate the total effect of the product or process on each of the categories separately and as a whole. Once the data analyses are completed, interpretation of the results either supports or rejects the original goals and scope of the LCA. The completed document then provides evidence of environmental impacts, areas for improvement, and recommendations for the future. Using previous solar LCAs, this study will find key areas of environmental impacts within the life cycle of utility scale solar panel production.

According to the Environmental Protection Agency (EPA), there are three overarching categories for which all impacts can reside. 'The first is natural resource impacts, which has six

main contributions within the category; the use, or depletion of, renewable resources, nonrenewable resources, and energy resources, as well as the use of solid, hazardous, and radioactive landfills. The abiotic ecosystem impact category follows with eight main contributions; global warming, stratospheric ozone depletion, photochemical smog, acidification, air quality, eutrophication, water quality, and radioactivity. The last main category refers to the potential human and ecosystem toxicity impacts, such as chronic human health effects, aesthetics, aquatic and terrestrial ecotoxicity, and so on' (Chapter 3 n.d.). Refer to Table 1 below. Though these categories are separated by the EPA, for the purpose of this study, the three will overlap with differing, yet similar, contributions. Solar production does not fit into, or contribute to, every impact category, therefore this study will analyze those that are relevant to PV manufacturing and utility scale solar sites. The impact categories described below were based on the impact categories given by the EPA, as well as those categories that have been used in previous LCAs of solar panels.

Table 1: Classification of Impact Categories Derived from the EPA's Established LCA Framework (Chapter 3 n.d.).

Natural Resource Impacts	**Abiotic Ecosystem Impacts**	**Potential Human and Ecosystem Toxicity**
Use of renewable resources	Contribution to global warming	Impacts on chronic human health effects
Use of nonrenewable resources	Contribution to stratospheric ozone depletion	Impacts on local aesthetics
Use of energy resources	Contribution to photochemical smog	Impacts on aquatic ecotoxicity levels
Use of solid waste landfills	Contribution to acidification	Impacts on terrestrial ecotoxicity levels
Use of hazardous waste landfills	Contribution to air quality issues	
Use of radioactive waste landfills	Contribution to eutrophication	
	Contribution to water quality issues	
	Contribution to radioactivity	

In order to provide a circular study of the life cycle impacts associated with both crystalline silicon and perovskite PV at the utility scale, the following impact categories were carefully selected and organized according to the level of connections to the respective LCIs. To begin the analysis, the impacts on our natural resources are separated based on the specific panel type or scale of production. The required energy inputs and raw materials for individual panel manufacturing are analyzed first. Using the energy input data for each panel type, the energy payback times (EPBTs) are calculated. Raw materials for utility scale installations are then analyzed alongside water requirements for site maintenance activities.

Following natural resources comes a comparative analysis of the contribution to global climate change. This is evaluated using previously identified global warming potentials (GWPs) for the individual panels. Land use, though also a depletion of available natural resources, is separated into its own impact category following GWPs due to the immense amount of environmental harm and degradation that occurs when land is prepared for a utility scale solar installation. The bulk of the land use section dives deep into a chain of events as they might unfold following immense land cover change in a specific ecosystem. As a subsection, land use efficiency is calculated by comparing the expected annual energy output of a site against the site acreage.

Using data collected from the previous impact categories, human and ecosystem toxicity impacts are assessed. This section addresses the underlying toxicity issues solar based on raw materials, energy requirements and GWPs before providing an interesting analysis of the tradeoff between land use for this carbon-free energy resource and natural carbon sequestration from dense trees. By evaluating all of these impacts, key areas of environmental stress are identified alongside future research interests.

Interpretation (Further Analysis)

Following the evaluation and application of the LCI measurements against the related impact categories, an interpretation of the calculated results is provided for further understanding of the future of perovskites and solar industry research. In this section, a comparative analysis of the key differences between crystalline silicon and perovskite PV is provided. Through this comparison, a panel installation recommendation is given. Following this recommendation, insight into the fundamental communications differences between engineers and ecologists is explored. Throughout much of the research, it becomes apparent that environmental concerns mean different things to researchers in different fields. The identification of this miscommunication provides insight into key areas of future research.

Discussion

Studying the development of the solar industry, individual panels, and LCAs themselves provides a base point for further research. Using the LCA framework and requirements, this study analyzes data presented in previous work and applies it on a much broader scale. In order to compare solar panel types, analyzing individual LCIs to apply both on a utility scale for impact categories offers a new perspective into a developing field. Offering a step-by-step comparison of the LCIs is something that has never been done before. Most studies complete perovskite LCAs and briefly compare certain aspects to crystalline silicon LCAs, without offering a side-by-side comparison, such as the one offered here. Figuring out environmental impacts associated with individual solar panels as well as utility scale solar developments will provide new ideas for further research to alleviate these impacts.

Methodology

Adapting the international framework of a LCA to fit my study specifically is the bulk of my methodology. Following in-depth research, I compiled enough data to produce an adequate analysis of the differences between these two panel types. Using this data, I formulated a rough structure for my argument of implementing solar energy on the utility scale. Developing the goals and scope of my study helped restructure LCA frameworks to fit my analysis specifically. Following an immense amount of practice writing, I developed a framework fit for this comparative analysis. Analyzing the LCI of both crystalline silicon and perovskite PV provided a base point for the rest of my research as I determined the best impact categories for my analysis. Once the impact categories were identified, adapting LCI findings to fit the categories provides the basis for the true evaluation. Using data and formulas from previous studies, average energy inputs, EPBTs, and GWPs are calculated. Discussing the areas where perovskite PV might exemplify or alleviate harmful environmental impacts provides fundamental information for the future of perovskite, if there are hopes to implement it on the utility scale. The following table is a list of calculation results further detailed in the impact categories.

Table 2: Crystalline Silicon Perovskite Comparison Table

Cell Type	Average Embodied Energy	Cell Energy Conversion Efficiency Range	Energy Payback Time (EPBT) Range	Life Expectancy	Average Global Warming Potential (GWP)
Crystalline Silicon PV	~ $\frac{451\ kWh}{m^2}$	22 to 27 %	2 to 6 years	~ 30 years	~ $\frac{49\ g\ CO_2\text{-eq.}}{kWh}$
Perovskite PV	~ $\frac{118\ kWh}{m^2}$	20 to 26 %	0.22 to 2 years	~ 5 years (need 10 years for implementation)	~ $\frac{100\ g\ CO_2\text{-eq.}}{kWh}$

Crystalline Silicon Photovoltaics

Life Cycle Inventory (LCI) Introduction

The LCI for crystalline silicon solar cells revolves primarily around material processing and manufacturing. “Polycrystalline silicon feedstock purification, crystallization, wafering, cell processing, and module assembly,” are the main focuses of crystalline silicon module manufacturing (Fthenakis, Kim, & Alsema 2008). These processes require a variety of material inputs and are extremely energy intensive. Following manufacturing processes, this LCI continues by evaluating crystalline silicon installations on the utility scale. As many utility scale solar installations will soon reach their end of life, understanding the site retirement processes is extremely important. This LCI closes by analyzing the various recycling methods for crystalline silicon as they become more publicly available. Once the LCI is complete, predetermined environmental influencers are split into various impact categories for further analysis.

Raw Material Acquisition, Material Processing, and Manufacturing

Although silicon is the primary material used to manufacture crystalline silicon solar cells, there are many other materials required during production. Modules consist of many layers with differing properties and purposes, production of each of these layers requires different raw materials as well as different energy demands. Manufacturing a complete crystalline silicon PV module has “four distinct processes: polysilicon production, ingot and wafer manufacturing, cell manufacturing and module manufacturing” (Photovoltaics Manufacturing 2016). By analyzing the inputs and outputs at each stage of the module production process, the first stage of the LCI begins.

For crystalline silicon PV, the basic raw material used for cell production is silica, sourced from silicon dioxide (SiO_2), a combination of Earth's two most abundant elements, silicon (Si) and oxygen (O) (Silica 2019). Silica can be collected easily via quartz sand (SiO_2), a naturally occurring, moderately pure material with worldwide mining availability. Higher, closer to electronic-grade purities of around 50%, are found primarily in quartz rock (Vatalis, Charalambides, & Benetis 2015). Following the procurement of quartz, the material is transported to a refinement facility that can use various dependent processes to produce a silicon-grade purification level acceptable for PV use (Kadro & Hagfeldt 2017). Crystalline silicon PV requires purities greater than 99%, preferably between 99.999% (5N) and 99.9999999% (9N) (Photovoltaics Manufacturing 2016). In order to cleanse quartz of metallic and nonmetallic impurities, refining facilities process the material in a variety of ways (Delannoy 2012). Figure 3 below is a flow chart imported from Green Rhino Energy's website depicting silicon refinement processes. Each step of the purification process is explained in detail in the following section.

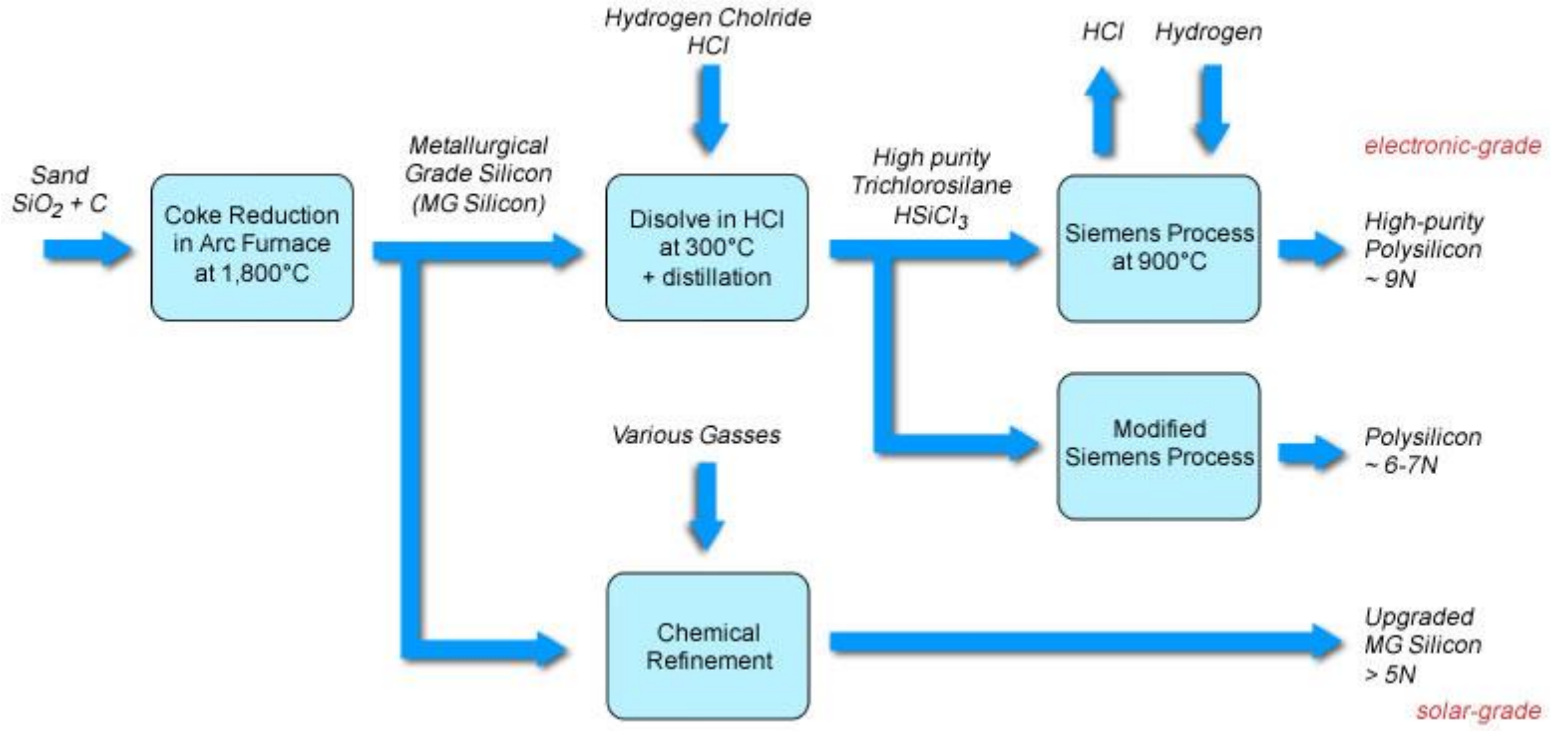

Figure 3: Manufacturing Silicon Flow Chart, from *PV Manufacturing*, by Green Rhino Energy

The refinement processes for quartz vary depending on the desired level of silicon purification, i.e. solar-grade silicon with purities greater than or equal to 5N, medium-grade polysilicon with purities between 6N and 7N, or electronic-grade polysilicon with purtities greater than or equal to 9N (Photovoltaics Manufacturing 2016, & Smith & Barron 2013). To begin the purification process for these three levels of PV-grade silicon, quartz is placed in an arc furnace at temperatures around 3,300°F (1,800°C) (Smith & Barron 2013). The high temperature requirements inherently result in high energy demands and thus, high costs for production. A carbon (C) base, usually in the form of coke, coal, charcoal, or wood, is also placed in the arc furnace for carbothermal reduction-smelting, where the additional carbon atoms help refine quartz and synthesize a purer version of silicon (Li et al. 2018, Ali et al. 2018, Smith & Barron 2013, & Chigondo 2018). The result is a ~98% purified silicon, commonly referred to as metallurgical-grade (MG) silicon (Chapter 3 n.d.). This MG silicon is not pure enough to be used in the production of crystalline silicon PV modules. Residual metallic impurities, such as aluminum and iron, as well as non-metallic impurities, such as phosphorous, boron, and carbon, within MG silicon requires further refinement steps for use in PV modules (Chapter 3 n.d., Fthenakis et al. 2008, Kadro & Hagfeldt 2017, & Steel - Raw Materials 2019).

Next steps depend on the desired level of purification, i.e. solar-, medium-, or electronic-grade silicon. For solar-grade silicon, otherwise known as upgraded MG silicon, with purities greater than or equal to 5N, some remaining impurities are processed out with gases. The next step varies depending on different panel manufacturers, but all involve some form of directional solidification, where many of the remaining "impurities are segregated to the melt" (Martorano et al. 2011). Following these further refinement strategies, the result is solar-grade silicon with purities acceptable for use in the production of PV modules. The following diagram (Figure 4)

represents the different processes used to produce crystalline silicon solar cells, two of which are followed and described in detail in the following section.

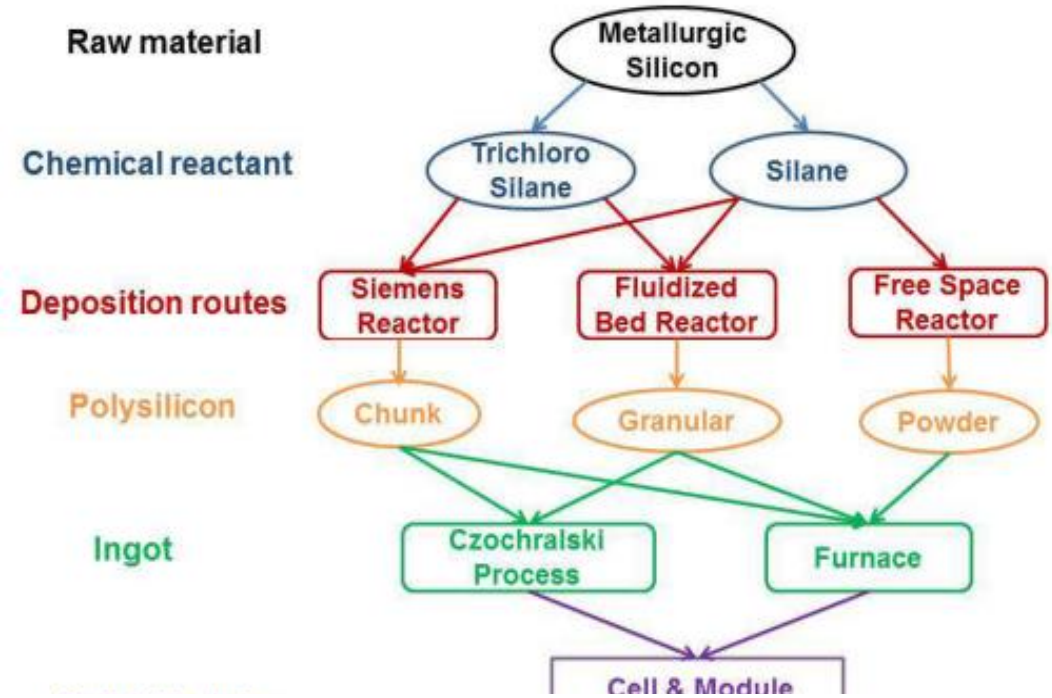

Figure 4: "Silicon Based Solar Cell Production Process," from *Producing Poly-Silicon from Silane in a Fluidized Bed Reactor,* by Ydstie & Du 2011

Higher purities increase the energy conversion efficiencies of the panels, therefore obtaining further silicon refinement is required for optimal energy production. To achieve either medium-grade (6-7N) or electronic-grade (≥9N) polysilicon, the next step entails distilling the remaining MG silicon in hydrogen chloride (HCl) at temperatures around 600°F (300°C) (Safarian, Tranell, & Tangstad 2012). The result is a highly pure silane gas, most commonly identified as trichlorosilane ($HSiCl_3$), formed through the further dissolving of leftover impurities. Following this distillation, the remaining silane gas and leftover HCl are put through some version of the Siemens process. This process is the oldest, most well known silicon refinement process, however it is extremely energy intensive as it requires very high

temperatures for further purification. The energy requirements also make this process extremely costly, therefore modified versions have been developed to reduce energy use and costs (Delannoy 2012). The version of the Siemens process that is selected is dependent on the manufacturer and desired level of purification, either medium- or electronic-grade polysilicon.

Achieving a purity level between 6N and 7N, or a medium-grade polysilicon, requires the remaining silane gas ($HSiCl_3$) to be put through a modified version of the Siemens process. One, less energy intensive and more cost-effective version involves the substitution of a fluidized bed reactor for the classic Siemens reactor. This offers reduced heat demands, resulting in reduced energy and cost requirements. The fluidized bed reactor preheats fluidizing gases, such as hydrogen and helium, in preparation for the addition of MG silicon into the reactor (Ydstie & Du 2011). Once silicon is added, chemical vapor deposition allows increased silicon seed particle growth, resulting in purified medium-grade polysilicon ready for crystallized growth (Ydstie & Du 2011, & Geng & Yu 2011). Figure 5 offers a comparison of the reactor processes via simple reactor diagrams. Using a modified Siemens process allows for more flexibility in the production output rates of the silicon solar cells, however it does not produce the highest silicon purification grade possible.

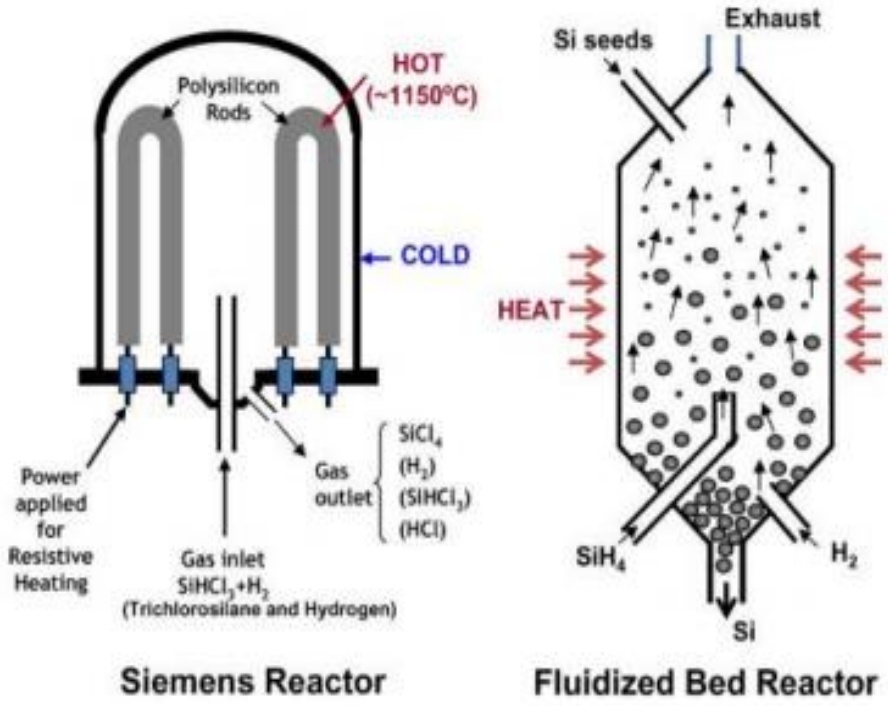

Figure 5: Comparative Reactor Diagrams, from *Silicon Wafer Technologies: Past & Future,* by Dixit, Agarwal, & Purohit 2017

To achieve a purification level greater than or equal to 9N for electronic-grade polysilicon, the remaining silane gas ($HSiCl_3$) and leftover HCl are put through the complete Siemens process. The silane gas ($HSiCl_3$) and leftover HCl are further broken down with the addition of hydrogen (H) atoms on a pure silicon bed (Takiguchi 2011). This further distillation process places materials in a Siemens reactor at temperatures around 2000°F (1100°C) with surrounding cool walls to prevent silicon deposition on the walls instead of on the bed (Delannoy 2012). During this process, HCl and H atoms are driven out alongside many of the other remaining impurities. HCl and H atoms are separated and recycled for further reuse in the same silicon production processes (Zadde et al. 2002). The result is electronic-grade polysilicon with purities greater than or equal to 9N, ready for crystallized growth for the use in solar cells.

Following the production of highly pure silicon or polysilicon, the process for manufacturing crystalline wafers begins. There are two different types of crystalline silicon wafers for PV modules that can be produced; monocrystalline or poly/multicrystalline silicon solar cells. Both monocrystalline and multicrystalline silicon solar cells require their own production processes, however both require the growing of crystallized silicon from the previously purified solar-, medium-, or electronic-grade silicon or polysilicon.

The first step for the production of monocrystalline silicon cells is the formation of single crystalline silicon, which is pulled from the previously purified PV-grade silicon (Dixit, Agarwal, & Purohit 2017). As briefly discussed in the background section, the process of growing crystallized structures from molten polysilicon is known as the Czochralski Method. This is the oldest, most commonly used method to produce crystalline silicon for use in solar cells. During this method, a small seed crystal is placed on top molten silicon to produce cylindrical shaped ingot of single crystalline silicon. The crystalline silicon cylinder is then ready

for slicing as well as further etching to produce the ideal shape. Cutting and shaping the wafers is usually done using a diamond saw which requires increased energy inputs (Photovoltaics Manufacturing 2016 & Dixit, Agarwal, & Purohit 2017). Once the ideal shape is achieved, the processed wafers are ready to be formulated into true energy producing circuit chips. To form multicrystalline silicon wafers, the previously purified polysilicon is melted to produce a cube-shaped ingot of monocrystalline wafers (Photovoltaics Manufacturing 2016 & Crystalline and Polycrystalline Silicon n.d.). These cube-shaped monocrystalline wafers are combined together to form multicrystalline wafers ready to be shaped or cut into circuit chips for solar cell use.

Finally, the mono or multicrystalline silicon circuit wafers are ready to be manufactured into full PV modules consisting of different layers dedicated to various operational tasks. There are two-layer module designs for crystalline silicon modules; the conventional multicrystalline silicon solar cell and the integrated back contact (IBC) monocrystalline silicon solar cell. The top layer for both types of cells is the same while the remaining layers differ. For the purpose of this study, the layers included in conventional crystalline silicon cells are described in detail, however Figure 6 on the following page is a DOE produced comparative diagram of the two different solar cell layers for reference.

In order to decrease the rate of 'lost' sunlight, or reflected light, a textured anti reflective coating (ARC) is applied to the top of the previously produced crystalline silicon wafer. An ARC usually consists of titanium dioxide (TiO_2) or silicon nitride (SiN) and is applied directly onto the silicon wafer surface (Crystalline Silicon Photovoltaics n.d.). The texture is primarily in the form of "micrometer-sized pyramidal structures, formed by a chemical etch process" (Ali et al. 2018). A conventional solar cell also applies a "screen-printed silver paste" on top of the ARC

for additional protection (Ali et al. 2018). These layers protect the inside cell structure from potential damage from outside forces, such as windblown debris or human-induced damages.

For a conventional multicrystalline silicon solar cell, the two layers beneath this textured ARC surface are dedicated to the production of a phosphorous-nitrogen interface. Figure 7 on the following page presents a high quality diagram of the p-n junction described in detail in the following section. To accomplish this "p-n junction, typically a phosphorous-doped n+ region is created on top of a boron-doped p-type silicon substrate" (Ali et al. 2018). An n-type silicon is created through the addition of atoms, such as phosphorus, which results in free moving excess electrons. By adding atoms, such as boron and gallium, a p-type silicon is produced alongside electron transport holes formed due to insufficient amounts of electrons (How a Solar Cell Works n.d.). The present electron surplus in the n-type

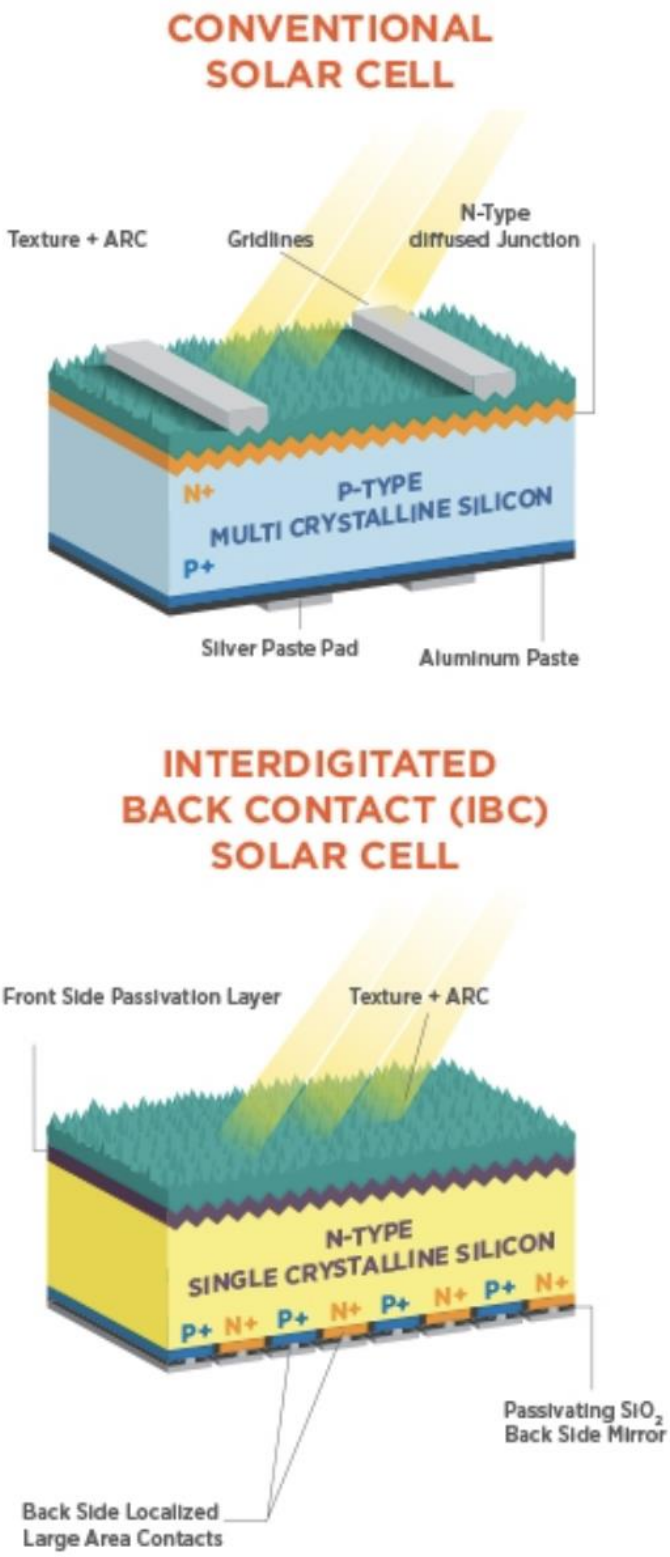

Figure 6: Comparative Layer Diagrams, from *Crystalline Silicon Photovoltaic Research,* by the DOE

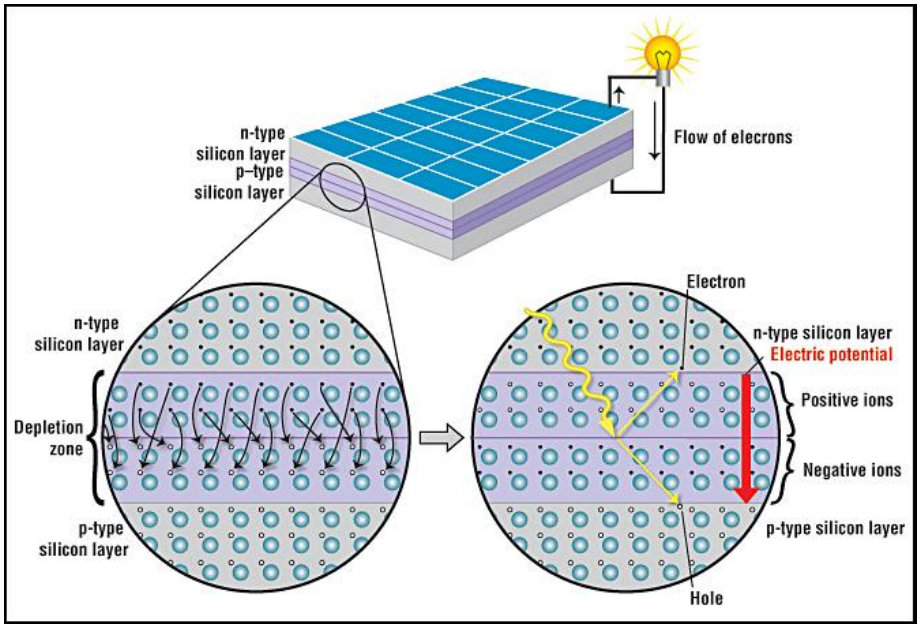

Figure 7: "Schematic representation of a solar cell, showing the n-type and p-type layers, with a close-up view of the depletion zone around the junction between the n-type and p-type layers," from *How a Solar Cell Works,* by Anthony Fernandez

region travels into available holes in the p-type region, thus creating the p-n junction, known as the depletion zone. Once the holes are filled with the excess electrons, the p-type side of the depletion zone carries negative charges while the n-type side carries positive charges. These opposite charges generate electricity, preventing further electron transport hole filling. Once sunlight hits the solar cell, electrons within the silicon regions are pushed out, passing through the depletion zone via a previously installed metallic wire and electricity is generated (Smith & Barron 2013 & How a Solar Cell Works n.d.). The electricity generated in the junction amplifies as the sunlight travels through the solar cell.

Underneath the p-n junction layers is an installed back contact layer for increased structural integrity and environmental impact protection (Fthenakis & Kim 2011). This layer is usually produced via a metal electrode, most commonly aluminum for crystalline silicon solar cells (Crystalline Silicon Photovoltaics n.d.). The aluminum back contact most often forms a sort-of frame surrounding the entire cell, on all four sides plus the back layer. A frame such as this not only offers additional protection from outside forces, but also makes installation much easier while providing increased structural integrity. Following the combination of all layers to produce a complete solar cell, the modules are ready to be transported to the installation site

from the manufacturing facility. The transport of materials along with the great energy requirements for silicon purification and module manufacturing result in emissions from fossil fuel resources, unless the manufacturing facility and transportation run off of renewable energy resources.

Installation and Use

Following module manufacturing, the materials are transported from the manufacturing facility to a fully prepared installation site, most commonly on the rooftop or utility scale. Figures 8 and 9 provide simple comparative schematics of the two solar site designs commonly used today. The size of these installations can range anywhere from a small 1 MW farm installation to a 5 MW multiple acre installation, depending on where the site is located and who the installer is (Utility-scale solar 2019). Changing lands in preparation for ground-mounted solar installations is a requirement no matter the size and results in an immense amount of new environmental pressures that create a negative chain of events, all of which are discussed in

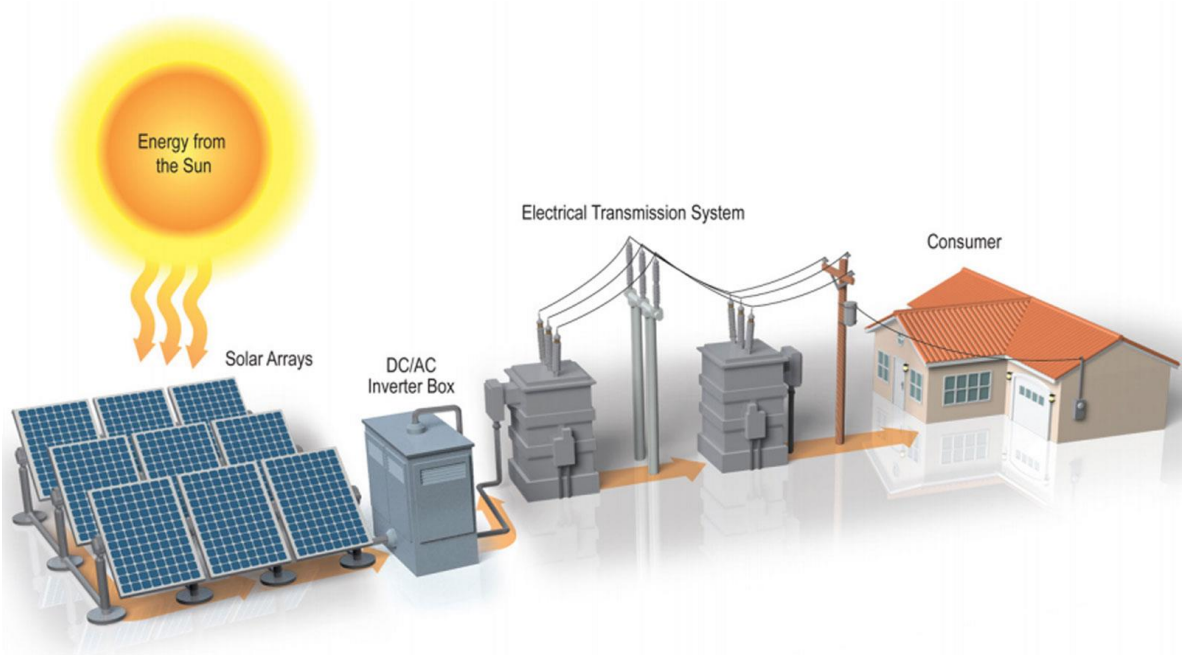

Figure 8: Grid Connected Solar Power Plants, from *Utility Scale Solar Farms in Wisconsin*, by Renew Wisconsin

detail in the impact category sections. Once installed, energy production outputs and site maintenance activities are the primary concerns for a utility scale solar site.

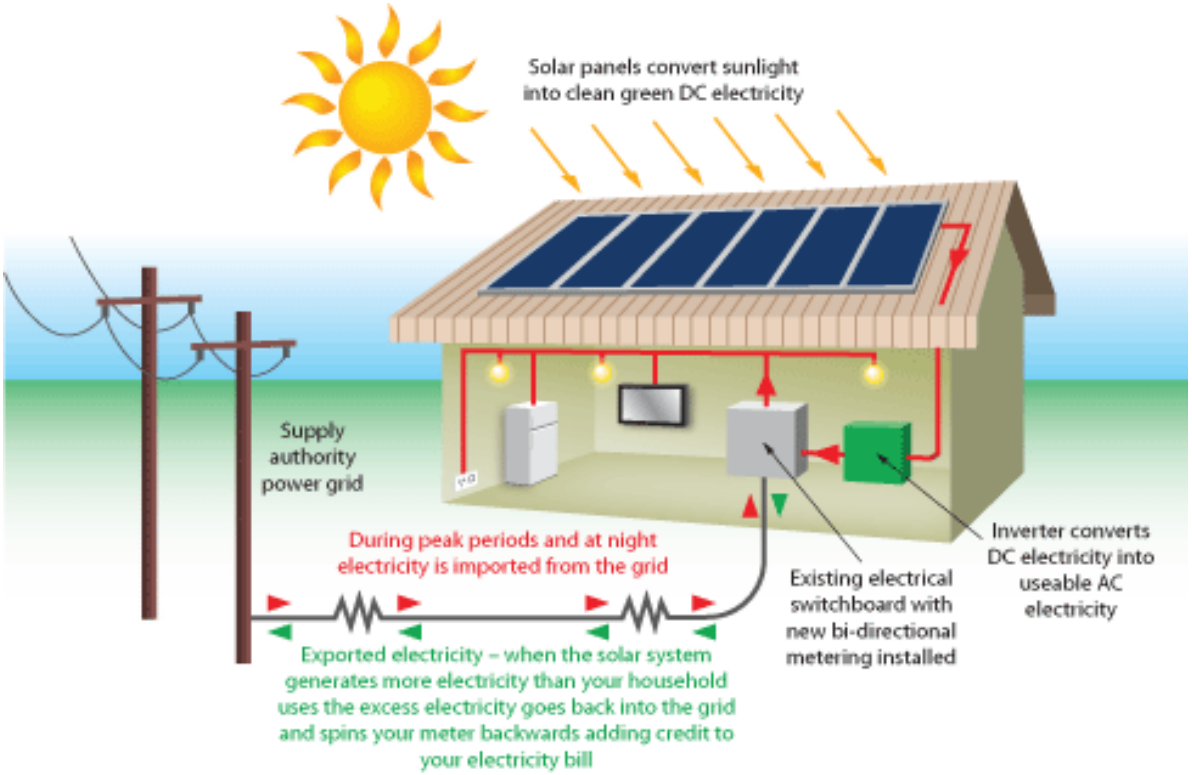

Figure 9: "Grid Connected Solar Panels," from *Renewable Resources Alternative Energies,* by Patrick Goliszewski

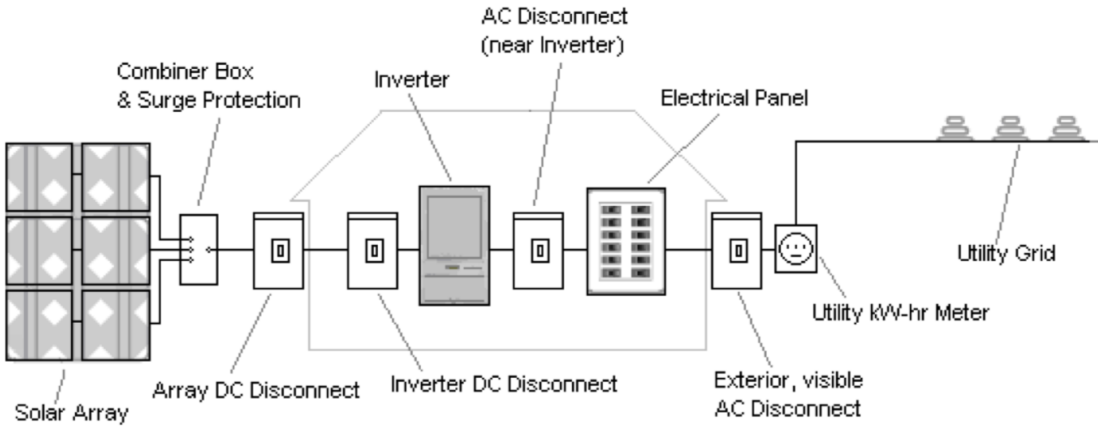

Figure 10: "Common Configuration of a Grid-Connected AC Photovoltaic System," from *Solar Electric System Design, Operation, and Installation,* by Carolyn Roos

Though the modules themselves are the energy producing materials, there are many other materials required to install a utility scale solar site. Figures 10 and 11 offer simple schematic representations of the necessary energy flow materials within the site itself. Ground-mounted

solar arrays require metal mounting structures. If standard ground-mounts are chosen, the panels are manually adjusted throughout the seasons to follow the peak sun, or a tracking system is also mounted to avoid these manual adjustments (Matasci 2019).

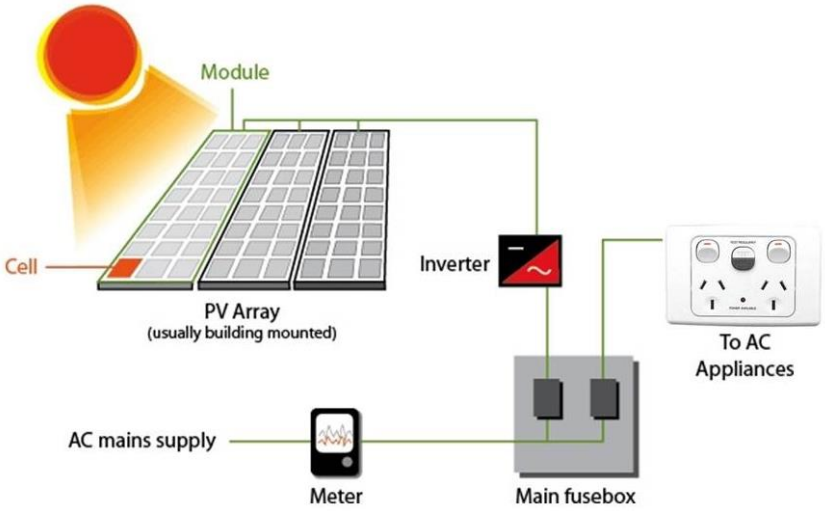

Figure 11: "Energy Transformation Flow Chart," from *Charts Collection*, by Charts Collection

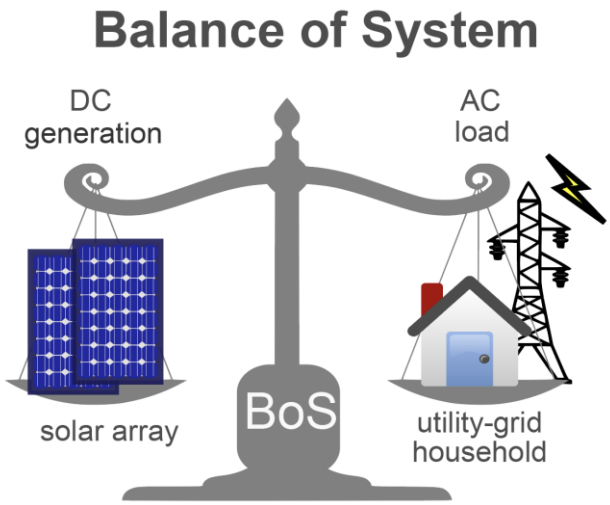

Figure 12: "The Balance of System Components of a Photovoltaic System," from *Balance of System,* by DOE

Balance of system (BOS) components refer to the materials necessary to transform the sunlight converted direct current (DC) energy into the utility used alternating current (AC) energy (Balance of System 2006). Figures 11 and 12 offer simple design schematics of the balance these components have to manage when converting DC to AC electricity. These components include wiring for direct electricity transfer, energy combiner boxes for current/voltage output management, inverters for DC to AC energy conversion, fuse-boxes for grid output management, and meters for energy production measurement (What is Photovoltaic 2018, Smalley 2015, Electrical and EMC Insulation n.d., Formisano 2018, & Net Metering 2019). Energy output management, though the primary lifetime management of a solar site, is not the only site management necessary during the use period.

During the roughly 30 year expected lifetime of the crystalline silicon solar cell itself, there is mandatory maintenance crucial to keeping energy production as high as possible.

Installations in arid regions will require more frequent panel washings due to dust accumulation, while installations in wet regions will require site mowings to counteract any shading from vegetation overgrowth. Aside from energy output management, panel washing, and site mowing, solar installations do not require consistent maintenance practices. Though the maintenance is limited, it accounts for all waste emitted during the production lifetime of a solar site. Emissions are discharged during maintenance team and material transport to and from the site as well as during the maintenance activities themselves. During the entire lifetime of a solar cell following installation, no excess waste is emitted from energy production, until decommissioning begins.

Energy production begins for the remaining lifetime of the site. The metal support structures have about a 60 year life expectancy. The solar cells themselves, inverters, and transformers last around 30 years, but there are often problems that arise during energy production periods that will require some part replacements (Fthenakis & Kim 2011). Problems include low efficiencies and damage from outside sources. Inverters and transformers often require replacements every 10 years (Safarian, Tranell, & Tangstad 2012). The replacement activities of a solar site depend greatly on the manufacturer as well as the site location as areas with high wind speeds can damage panels by throwing debris. Gunshots are another growing issue for the reliability of solar farms.

During the around 30 year lifetime of a solar site, the energy conversion efficiencies of the site depend on the panels selected for installation. In August of 2018, the highest efficiency levels found for crystalline silicon modules ranged between 22% and 26%. The highest efficiency for monocrystalline silicon solar cells was 26.7%, compared to 22.3% for multicrystalline cells (Philipps et al. 2018). These efficiency levels have nearly doubled in the past 10 years (Takiguchi 2011). In-lab testing records produce higher efficiencies than installed

solar sites, which are 25% for monocrystalline silicon solar cells and 20% for multicrystalline cells (Crystalline Silicon Photovoltaics n.d.). An average efficiency of 24% is used for impact category calculations. Energy conversion efficiencies are the main driver for PV research today.

Decommissioning, Materials Treatment, Disposal Methods, Recycling

As solar installations continue to develop, any outlook for the future must include strategies for proper disposal of panels, though there is great reuse potential for the site itself. Although there are many solar professionals and researchers concerned with the end of life of PV, retirement processes are often left out of PV LCAs. As there has yet to be a utility scale solar plant decommissioning, there is no universal plan for retirement yet. However, there are general plans being developed revolved around dissembling the plant, separating materials into groups based on their specific characteristics, treating the separate materials in different ways based on their built properties, and transporting these materials from the solar site to treatment facilities or landfills (Latunussa et al. 2016). Solar site components are separated into groups based on their primary materials and site functions, such as mounting structures, transformers, and the panels themselves.

There are two strategies for all site materials treatment following plant decommissioning: either they are buried in a landfill or recycled for future reuse (Gerbinet, Belboon, & Léonard 2014). The strategies selected for site decommissioning are determined by the solar site owner as well as the panel manufacturer. For the panels themselves, the strategies for disposal often depend on the panel manufacturers' preferred treatment methods. Unfortunately, the solar industry experiences extremely high rates of short lifetimes for panel manufacturers, primarily

due to bankruptcy (Wesoff 2015). Due to the quick rises and falls of manufacturers in the solar industry, developing a universal recycling method for panels is of the utmost importance.

According to the International Renewable Energy Agency (IRENA), global PV waste materials could be worth over $15 billion by 2050 as solar installed capacity continues to grow worldwide, therefore understanding the future of PV recycling is a research area gaining interest (Weckend, Wade, & Heath 2016). For the panels themselves, the recycling prospects are extremely high. Many of the different parts can be reused for the continued production of solar energy: the silicon solar cells, frames, glass, and wires can all be recycled (Marsh 2018). Once the panel is disassembled, the parts are separated for reuse or disposal. Without any required treatment, the metal, glass, and wires can automatically be reused for their original purposes in solar panels. The silicon cells themselves require processing to create a new cell for continued energy production (Marsh 2018).

The treatment strategies used to re-purify silicon cells depends on the recycling company's preferred methods. For the purpose of this study, three recycling techniques are discussed: pyrolysis-, solvent-, and compression-induced silicon separation and purification recycling. These all offer above 80% recovery rates of silicon and/or glass materials for future reuse (Latunussa et al. 2016). Pyrolysis refers to the decomposition of materials via very high temperatures and can be achieved by placing silicon materials in an arc furnace or fluidized bed reactor, utilizing similar techniques used during silicon cell manufacturing (Pyrolysis n.d.). With the addition of nitrogen and raising temperatures to around 900°F (450°C), silicon panel layers are separated to reclaim the silicon and glass materials (Frisson et al. 2000). In pyrolysis, 80% of the silicon materials and 100% of the glass materials are separated for further reuse in the solar

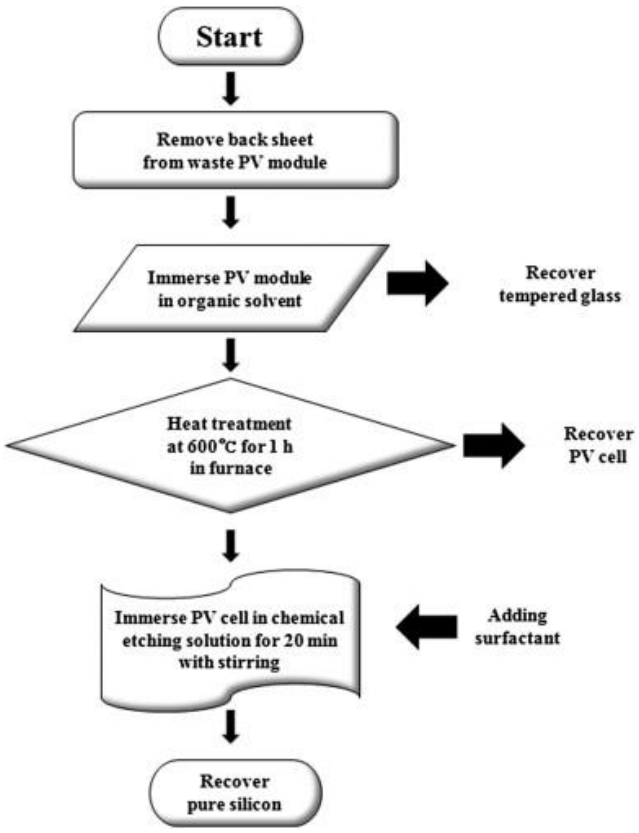

Figure 13: "Schematic Flow Chart Revealing the Recovery Processes of the Tempered Glass and the Silicon from the Waste PV Modules," from *Experimental investigations for recycling of silicon and glass from waste photovoltaic modules*, by Kang et al. 2012

industry (Latunussa et al. 2016). Pyrolysis-induced recycled wafers produce a 40% decrease in required energy inputs, greatly diminishing the EPBT of the solar site (Frisson et al. 2000).

Solvent-based recycling separates silicon modules with chemical etching. Figure 13 offers a simple schematic of this process. Similar to pyrolysis-induced approaches, heating the silicon cell itself is still required for further silicon purification. 86% of silicon materials are recovered and purified to ~5N (Kang et al. 2012).

Compression-based silicon PV recycling crushes modules using blade rotors. The silicon materials are then placed in a furnace at ~1200°F (650°C) (Granata et al. 2014). 85% of all glass is recovered, however this recycling method is not good for recovering the silicon materials (Latunussa et al. 2016).

Though these three recycling methods decrease the EPBT of a solar site, the necessary use of heat for silicon recovery and purification for further reuse requires an immense amount of energy and subsequently large production costs. These costs can be offset by recovering materials that would otherwise be lost to landfills, however unless the recycling facility runs off of renewable energy sources, emissions from fossil fuels contribute to global climate change.

With an estimated $15 billion solar material recovery value by 2050 expected via soon rapid decommissioning of utility scale solar power plants, there is great business interest. In France alone, installed solar capacity has grown around 35% each year, resulting in nearly

85,000 tonnes of materials used in 2017 (De Clercq 2018). In 2018, Veolia, an international environmental services agency, opened Europe's first solar panel recycling facility in France. This facility focuses on the recycling strategies for crystalline silicon PV, the most popular PV technology used in Europe today. Through a primarily robotic system, Veolia's plant dissembles the crystalline silicon panels and separates the metal, glass, wires, and silicon components for further treatment (De Clercq 2018). According to Veolia's Waste Solution CEO, 95% of the PV materials are recovered and redirected for use in a variety of industrial sectors (Harambillet 2018). Under the direction of PV Cycle, an international non-profit dedicated to implementing innovative PV waste management solutions, Veolia has undergone an extended contract to treat over 4,000 tonnes of PV waste material over the next 4 years (Bellini 2017 & About PV Cycle 2016). This is one of the world's first recycling facilities dedicated to only PV waste management. Following the end of the 4-year contract period, Veolia expects to be a successful example of PV recycling for profit, providing purified material excess that can be bought and reused for a variety of purposes.

Discussion

During manufacturing processes for crystalline silicon PV, there are high energy input demands, primarily for silicon purification and crystallized growth. These demands increase production costs, greatly affect the EPBT of the solar site and have pushed researchers to lab-test alternatives to this conventional solar technology.

Perovskite Photovoltaics

Life Cycle Inventory (LCI) Introduction

Perovskite is a solar innovation that aims to greatly surpass current low efficiency solar modules while offering massive upscaling potential alongside lowered manufacturing costs. Though there is great potential with perovskite, there are still many drawbacks inhibiting actual implementation or installation of perovskite PV for energy production. However, the potential reductions in these drawbacks have scientists on the edges of their seats, waiting for technological developments to help this innovation meet its true potential. The LCI of perovskite focuses on current manufacturing methods while pinpointing places in need of further development, if this new technology hopes to surpass its current competition. Due to the lack of perovskite installations, gaps in the life cycle are filled with information learned during the LCI of crystalline silicon PV. This information primarily comes during the installation and use subsection, as it can be assumed that perovskite PV will be installed in the same way as crystalline silicon PV, especially on the utility scale. To conclude this LCI, potential recycling of perovskites is presented.

Raw Materials Acquisition, Materials Processing, and Manufacturing

Perovskite is "an organic-inorganic hybrid compound [that has a] ABX_3 crystal structure," similar to the crystallized structure found in calcium titanium oxide ($CaTiO_3$), or calcium titanate (Kajal, Ghosh, & Powar 2018, Perovskite Solar Cell 2019, & Scott 2018). Perovskite minerals are most commonly mined from alkaline mafic rocks (Mineral Data Publishing 2001-2005). Alkaline mafic rocks contain the mineral properties of alkali, "a

chemical compound that neutralizes or effervesces with acids" (Definition of Alkali 2019). Most acids are in the form of anions, or negatively charged ions, whereas most ions found in perovskite/alkali structures are in the form of cations, or positively charged ions (Uptmor n.d. & Nace 2017). The immense amount of cations found within perovskite provides flexibility for altering the material to fit different industrial purposes (Gao 2016). However, the introduction of more negatively charged ions is required if perovskites PV aims to be at a competitive efficiency level to that of crystalline silicon PV.

There are many electrically applicable forms of perovskites, however halide perovskite solar cells (HPSCs) are most commonly used where PV technologies are concerned, due to the high energy conversion efficiencies (Celik et al. 2016 & Berry et al. 2017). Halide refers to the negatively charged acidic compounds formed through some sort of halogen synthesis, which when added, increases the efficiency of perovskite PV by allowing more movement for sunlight energy conversion within the material (Definition of Halogen 2019 & Hemman 2016).

Labs are testing processes for low-cost, low energy demand manufacturing of HPSCs. Due to the great potential for combination of materials, perovskite is most often combined with conventional crystalline silicon or thin film PV to produce an optimal level of energy conversion efficiency (Berry et al. 2017). Thin film combination is the focus of this study because of the printable potential for HPSCs. Figure 14 on the following page offers a brief comparative schematic of thin film versus silicon perovskite PV for reference. It is important to note that currently, researchers believe silicon-perovskite tandem devices will be the first wave of perovskite implementations on the commercial level due to the extremely high energy conversion efficiencies (Lab to fab n.d.). However, due to the lack of printability of this device,

thin film perovskite was chosen for this analysis to understand the impacts of future solar cell printing techniques.

Figure 14: Comparative Layer Diagrams, from *Perovskite Solar Cells*, by the U.S. Office of Energy Efficiency & Renewable Energy

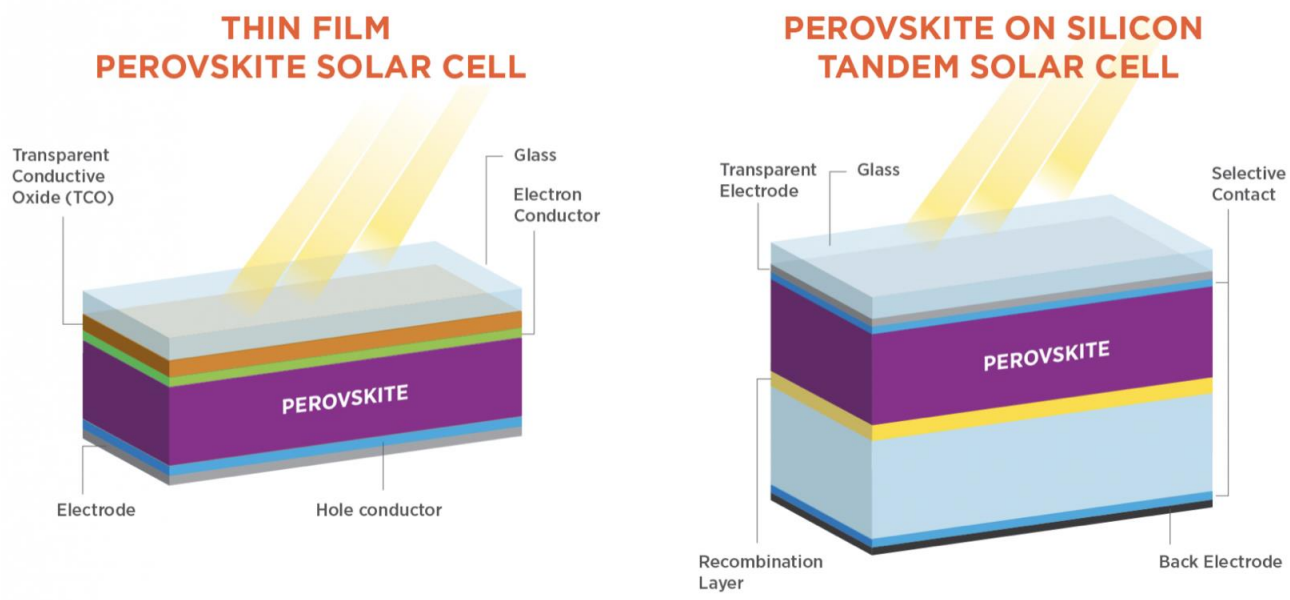

The most promising, low energy intensive and cost-effective thin film perovskite PV (HPSCs) manufacturing methods are referred to as solution processing, which can be achieved through either spin coating or roll-to-roll (R2R) manufacturing methods. Both of these are discussed in detail in the following section. Figure 15 helps visualize the differences among perovskite manufacturing techniques.

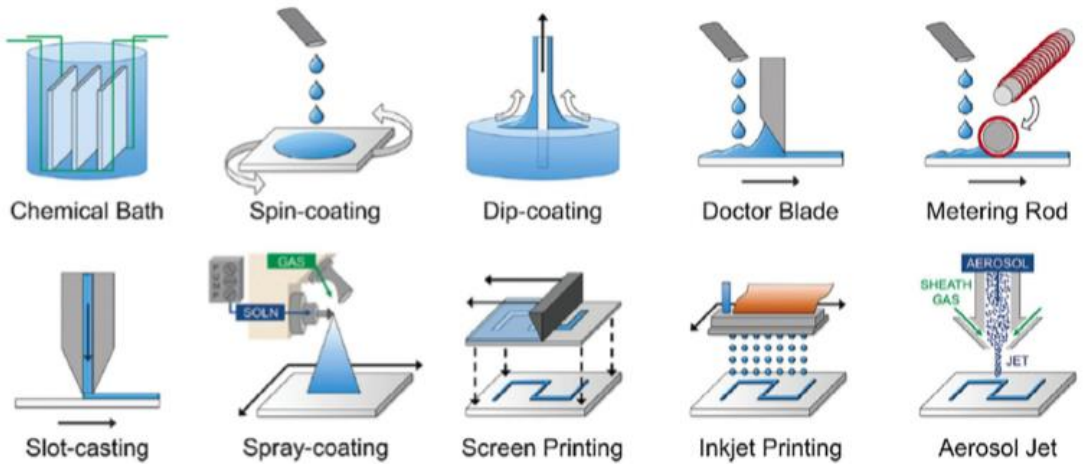

Figure 15: "Illustration of Various Solution Processing Methods," from *A Perspective on the Recent Progress in Solution-Processed Methods for Highly Efficient Perovskite Solar Cells*, by Chilvery, Das, Guggilla Brantley & Sunda-Meya 2016

Using solution processing methods to produce HPSCs has resulted in efficiencies greater than 20% (Zuo et al. 2018). For the purpose of this study, an average efficiency of 24% is assumed. Spin coating manufacturing was one of the first methods used to develop HPSC modules. This cost-effective production offers a basepoint for future perovskite developments, however due to the large amount of waste produced and rather slow process, spin-coating is inferior to R2R manufacturing (Kajal, Ghosh, & Powar 2018). Researchers foresee R2R manufacturing methods offering the opportunity to produce perovskite PV on the terawatt (TW) scale because of the print manufacturing potential (Berry et al. 2017). Lab-tested R2R-produced panel efficiencies have surpassed 15%, therefore this innovative production method is allowing HPSCs to become increasingly competitive with the conventional crystalline silicon PV module (Zuo et al. 2018).

Before either solution processing method can occur, the raw materials must go through pre-treatment for material cleansing. Perovskite materials can be refined at temperatures as low as ~215°F (~100°C). The material is placed in a comparatively inexpensive furnace with liquid solutions to assist in purification and to separate the ideal solar materials (Chandler 2019). Before manufacturing processes begin, perovskite materials are placed in an acetone and isopropanol bath for further refinement (Celik et al. 2016).

Spin coating involves several steps to produce HPSCs. First, a lead halide is spin coated to produce an active layer to be combined with a perovskite photoabsorber layer (Zuo et al. 2018). Once the lead halide cations are flattened on a spin coating board-like surface, a perovskite material, such as ammonium or formamidinium, is added on top of the flattened halide layer, then spin coated to produce a flattened perovskite layer (Kajal, Ghosh, & Powar 2018, & Zuo et al. 2018). Figure 16 on the following page offers a simplified schematic of this

spin coating technique. Once both layers are flattened with the perovskite sitting on top of the lead halide layer, they are heated to produce the ideal crystallized structure of perovskite PV (Kajal, Ghosh, & Powar 2018). Once heated, the perovskite PV layer is combined with four other HPSCs panel layers required to produce a full solar module. These additional layers are similar to that of the conventional crystalline silicon PV module.

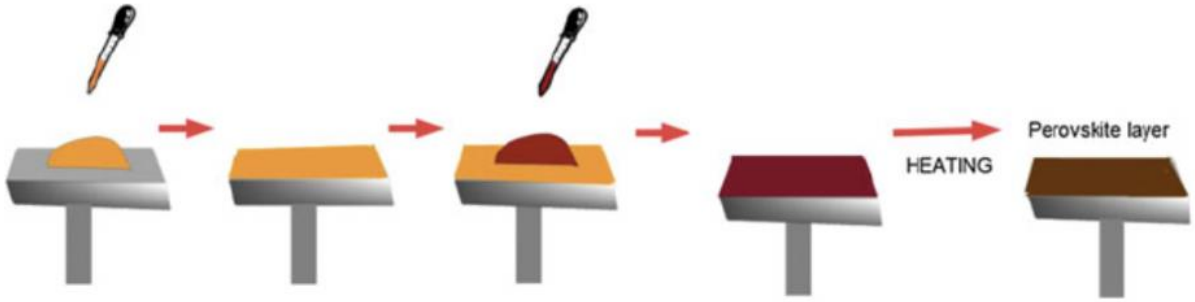

Figure 16: "Sequential Steps of Spin-Coating Process," from *Manufacturing Techniques of Perovskite Solar Cells,* by Kajal, Ghosh, & Powar 2018

Manufacturing methods for the perovskite photoabsorber layer vary depending on the facility, funding, and materials. However, the layout of a full HPSC panel is the same no matter the manufacturing method. For spin coating, once the lead halide and perovskite material layers are created, they are combined with the other four required module layers. The top layer of a perovskite PV panel is made from glass, to collect incoming solar electrons (Raghavan et al. 2018). Usually, this material layer is produced via easily procured flourine-doped tin oxides (Celik et al. 2016). For the purpose of this study, a general perovskite module structure is used and can be found in the previously provided Figure 14.

Below the top glass layer lies an electron transport layer (ETL) which transfers electrons from the above glass layer to the below perovskite photoabsorber layer. The ETL can be made from a variety of materials, but is primarily made of tin oxide or titanium dioxide. The low temperature requirements of tin oxide make it more desirable from a cost effective, energy

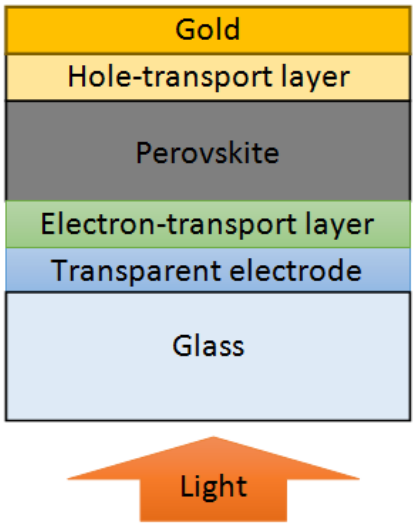

Figure 17: "The Thin-Film Perovskite Cell Structure," from *Perovskite-like Solar Cells*, by Raghavan, Avasthi, Muralidharan, & Ramamurthy 2018

saving perspective (Celik et al. 2016). As the incoming solar electrons flow through the ETL, they enter into the absorber layer, which transforms incoming sunlight into energy (Raghavan et al. 2018). The formation of this absorber is discussed in both the spin coating and R2R method descriptions.

Below the perovskite photoabsorber layer lies a hole transport layer (HTL) for increased energy conversion efficiencies through the recombination of electrons (Tress et al. 2014). The HTL is typically made from inorganic compounds to increase the efficiency of electron transport (Celik et al. 2016). The bottom of the panel serves as a back-layer contact to stop further electron transfer. For perovskite PV, this back layer is usually made up of a metal, either gold, silver, or aluminum. Although gold and silver offer the best energy production outputs, due to their extremely high prices aluminum is the cheaper, more common alternative (Celik et al. 2016). Once these layers are combined and wrapped around the perovskite absorber layer, the PV module is complete and ready for installation. Figure 17 offers a simplified schematic of the layers of thin film perovskite PV.

Although the spin coating method has been proven to produce HPSC energy conversion efficiencies greater than 20%, the loss in material and slow process creates barriers to optimal production (Zuo et al. 2018). During the spinning process, it has been calculated that around 90% of the added raw materials can be lost due to the fast speed of the spinning board processor (Celik et al. 2016). Along with great material loss, the spin coating process requires measurement, time, and care to the deposition of each material and may not be appropriate for large upscaling, due to the demand for highly efficient and cost-effective PV materials. With

large upscaling potential of new manufacturing methods, new perovskite PV production processes are being developed, with research focused on R2R print processing.

R2R manufacturing is a HPSC printing process being lab-tested to perfection. Efficiency rates increase alongside innovative production techniques. Due to the potential for high production outputs via quick printing techniques, R2R manufacturing is growing toward complete development and further implementation or installation. Following the same basic structure of the PV cell detailed above, R2R manufacturing creates a deposition process for the ETL, perovskite layer, HTL, and surrounding protective material (Kajal, Ghosh, & Powar 2018). These layers are applied one by one via a lined-up printing mechanism. Inkjet and slot die R2R printing processes can be adapted to produce solar cells on the terawatt scale while outputting next to no material waste (Kajal, Ghosh, & Powar 2018). Both R2R cell manufacturing techniques deposit the first three layers; ETL, perovskite, and HTL, then covers the layered material with a sort of lamination substance.

Prior to R2R manufacturing, the materials are thoroughly cleaned in 'boiling, deionised water' twice, then dried via compressed nitrogen application (Perovskite Solar Cells Fabrication n.d.). Following pretreatment activities, previously selected ETL material, perovskite precursor ink, and HTL material are placed into their predetermined ejection sites. Precursor ink refers to a metabolically-formed HPSC application substance. These materials are kept at temperatures around 160°F (~70°C) to ensure optimum material flexibility throughout the deposition process (Perovskite Solar Cells Fabrication n.d. & Kajal, Ghosh, & Powar 2018). Once materials are placed in ejection sites, the

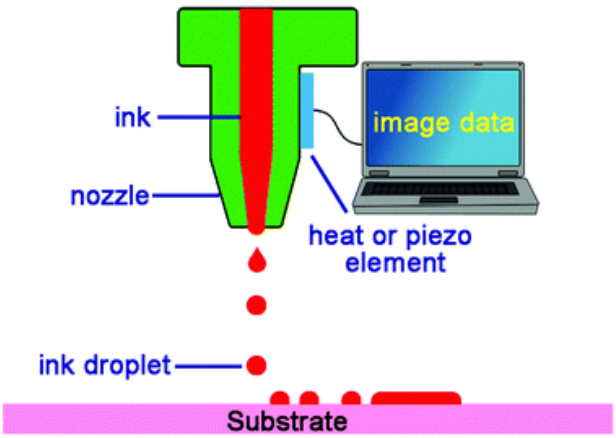

Figure 18: "Schematic Illustration of Inkjet Printing," from *Inorganic Nanomaterials for Printed Electronics: A Review*, by Wu 2017

machine may begin the printing process. Figure 18 on the previous page offers a schematic representation of a R2R perovskite inkjet printing process. Liquid filled ejection chambers squeeze the different materials out of their selective nozzles onto a previously selected substrate.

Due to the great thickness of materials, nozzle clogging is one of the main concerns for this R2R technique (Kajal, Ghosh, & Powar 2018). Researchers are still lab testing alternatives to nozzle driven R2R printing to reduce potential clogging. As a result, slot die R2R printing has grown in popularity as it reduces clogging while managing material deposition thickness.

Another R2R solution processed printing technique for terawatt scale production of perovskite PV is known as slot die coating. As with the other R2R HPSC inkjet printing mechanism, slot die coating involves the placement of previously selected ETL, perovskite layer, and HTL material into selective slot die coaters to ready the material for in-line deposition (Kajal, Ghosh, & Powar 2018 & Razza et al. 2016). Figure 19 offers a simplified schematic representation of the slot die R2R perovskite printing technique. As with inkjet printing, the material is squeezed out of the elongated slot die coaters onto a previously selected substrate, however unlike inkjet printing, the in-line printing process does not end with the HTL. Conductive paste and lamination materials are also placed into their selective in-line slot die coater.

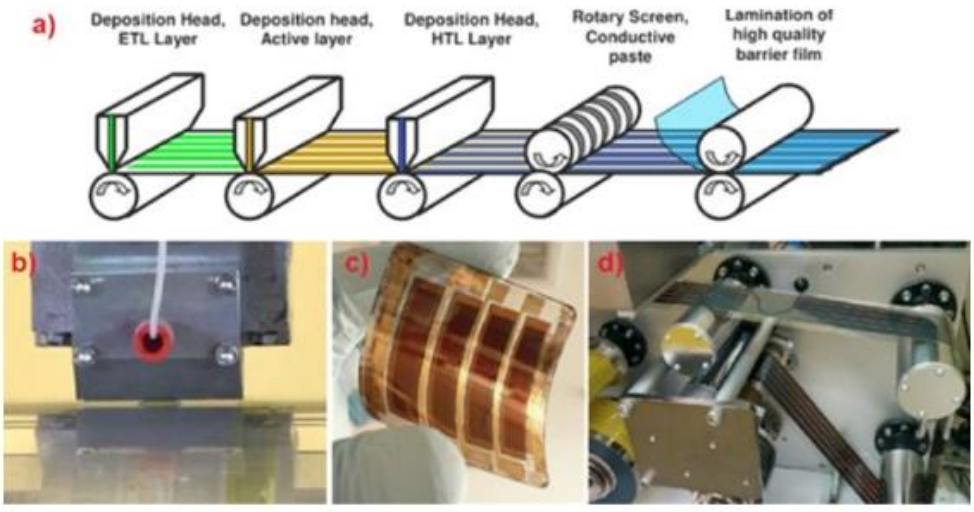

Figure 19: "(a) An example of a schematic of inline roll-to-roll manufacturing process for organic solar modules which is transferable also to perovskite solar cell fabrication: ETL, active, and HTL layers are deposited by slot-die technique whereas the back electrode is screen printed before lamination of a barrier film….. (b) PbI_2 layer deposited by slot-die process," from *Research Update: Large-Area Deposition, Coating, Printing, and Processing Techniques for the Upscaling of Perovskite Solar Cell Technology*, by Razza, Castro-Hermosa, Di Carlo, and Brown 2016

Once the ETL, perovskite layer, and HTL are applied to the selected substrate, the materials go further down the line of coaters and the conductive paste is applied, followed by the lamination material (Razza et al. 2016). Due to the complete process achieved via slot die R2R manufacturing as well as reductions in clogging potentials, this coating mechanism is preferred (Kajal, Ghosh, & Powar 2018). Following the deposition of all the layers to form the HPSC, the flat circuit is ready to be installed into or combined with the rest of the module materials to complete the HPSC. The front and back contact layers are added last to keep the circuit cell safe from outside stressors. As described above, the top contact layer of the perovskite solar cell is made from glass material while the back contact layer is most often aluminum. These perovskite printing techniques are most common in PV research and development at the moment, however upscaling PV manufacturing does not address some larger concerns for solar technology as a whole.

Installation and Use

The installation structure of a perovskite PV power plant will be the same as all other solar power plants installed today. Although the high energy conversion efficiency expectations (~ 24%) of perovskites have been lab tested and proven successful, there has yet to be any installed perovskite PV production capacity. Without any utility scale perovskite solar installations to study, analyzing the associated installation and use factors can be done by applying what was learned during the analysis of utility scale crystalline silicon installations. As with any utility scale solar power plant, perovskite PV plants will require an immense amount of site maintenance prior to installation, and various balance of system (BOS) components, such as wiring, inverters, mounting structures, etc.

Though the structure of the power plants will be the same, installing perovskite on the utility scale holds one key difference and potential harm than that of other solar installations. Due to the use of toxic lead material in the perovskite layer, many developers are concerned about implementing perovskite PV on the utility scale. As solar installed capacity continues to rise, addressing the growing toxicity issues is of the utmost importance. There are certain human and ecosystem toxicity risks that come along with using this toxic metal, discussed in detail in the impact category assessments. The cell itself is surrounded by the front and back contact layers, therefore only extreme cases are considered, such as high winds blowing hard objects and human induced gunshots hitting panels, potentially breaking the seal and allowing the lead to escape. Image 1 below shows an example of a wind or human caused breach of the top layer surface of a solar panel, revealing the circuit cell layer.

Image 1: Broken Solar Panel from Thrown Debris

Site maintenance activities, such as lawn mowings and panel cleanings, produce waste via emissions from trucks to transport workers and materials, emissions from mowers, and water

waste from washings. As with the previously analyzed utility scale crystalline silicon installations, panel washings are required to keep energy output at an optimal level. The panels themselves, however do not produce waste until the site has reached the end of its lifetime and is subsequently decommissioned, with necessary waste disposal mechanisms ahead. Currently, HPSCs have extremely short lifetimes (~ 5 years), calculated based on lab-tested efficiencies and small-scale installations (Kadro & Hagfeldt 2017). Though this is the estimated lifetime, without any current perovskite installations, it is hard to know if this is accurate. Researchers believe a minimum of a 10 year lifetime is required for actual commercialization. Luckily, with the further development of perovskite printing techniques, manufacturing perovskite PV solar cells can be extremely quick, counteracting the short lifespan with fast replacement technology. However, with lifespans so low and replacement techniques so high, there is growing concern for environmental impacts and end of life management of perovskite solar.

Decommissioning, Materials Treatment, Disposal Methods, Recycling

Recycling utility scale solar sites can greatly reduce the environmental impacts and energy payback time (EPBT) of solar. There is opportunity to reuse many of the materials, as well as the site location for future solar energy installations. All electrical equipment will require replacement, while mounting structures may last longer. If the site is to be completely decommissioned, almost all materials (nearly 99%) included in mounting structures, wiring, inverters boxes, the panels themselves, etc., can be recycled through various techniques (Kadro & Hagfeldt 2017). Perovskite panels front and back contact layers can be separated from the circuit cell, recycled, and reused for a variety of industrial purposes. Perovskite circuit cells themselves raise concerns due to the use of lead. Researchers are developing alternatives by lab testing tin as a lead substitute. Though tin might seem ‘better’ than lead, the low natural

occurrences alongside great environmental impacts from substance acquisition creates new ecotoxicity concerns. The impacts of tin are also addressed in the impact category assessment. Studying the recycling methods of conventional solar panels can give insight into the methods that might be used during the end of life processes of perovskite PV.

As provided in the crystalline silicon LCI decommissioning section, PV Cycle is an international agency dedicated to recycling PV waste. PV Cycle takes all kinds of PV modules for further separation and treatment for the reuse of many of the substances. PV Cycle has presented data showing the reclaiming of up to 96% of all materials within a solar cell for future use in different industrial sectors, but primarily the solar sector (Kadro & Hagfeldt 2017). It is important to note at least one recycling method specific to perovskite PV being lab tested today.

Perovskite recycling methods have to strategize the isolation of lead materials within the panels. One study developed a step by step recycling procedure to ensure safe toxicity levels while saving as much material as possible. Figure 20 is a schematic representation of this circular recycling method. The steps are as follows,

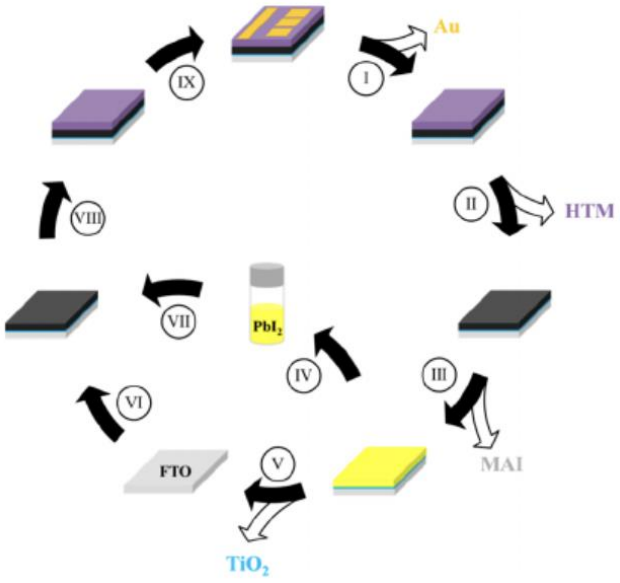

Figure 20: "Recycling Procedure for Perovskite Solar Cells," from *Recycling Perovskite Solar Cells to Avoid Lead Waste*, by Binek, Petrus, Huber, and Bristow 2016

1. Remove back contact layer with adhesive tape
2. Separate HTL by submerging the remaining material in chlorobenzene
3. Convert photoabsorber layer into iodide (PbI_2) and methylammonium iodide (MAI) by submerging the material in a bed of double distilled water
4. Submerge the remaining material in dimethylformamide (DMF) for further lead removal

5. Continue DMF submergence to separate ETL, leaving behind the glass top layer only (Binek, Petrus, Huber, & Bristow 2016). Though there are other ways to recycle PV materials, research shows that the addition of chlorobenzene, ethanol, and DMF are necessary for the separation of perovskite PV layers and protective lead isolation measures (Tsao 2016). The projected cost savings associated with using recycled PV materials, along with the lowered manufacturing energy demands creates an ideal outlook for the future of PV recycling.

Discussion

As perovskite solar cells continue to go through lab testing to find optimal levels of efficiencies alongside better substance use and longer life expectancies, the projection for installation continues to rise. The potential for massive upscaling of perovskite PV manufacturing through printing techniques creates an interesting environment for this growing industry. Are manufacturing techniques the only large concern for PV life cycles? This is explored in the impact category discussion section on both the individual panel and utility scale installation levels.

Impact Categories

Introduction

Though impact categories are separated by their primary effects, many overlap when PV modules and utility scale solar are being considered. During module manufacturing, the primary impacts are resource use during production, contribution to global climate change, land use, and human and ecosystem toxicity levels. These four impact categories combine data from required energy and materials use during production to understand the overall contributions. If modules are installed on rooftops, there are minimal installation, or use, impacts to consider outside of the initial impacts during manufacturing and anticipated panel washings. However, following installation on the utility scale, there are many more impact categories to consider, primarily due to immense land stress. Following installation, one of the main concerns for this renewable energy source is the energy payback time (EPBT). How long does it take for the solar site to produce an energy amount equal to that required during the manufacturing processes?

The following impact categories consider solar installations on the utility scale while discussing contributions specific to crystalline silicon and perovskite PV module manufacturing, use, and decommissioning. Some categories are discussed in a more general manner, such as land stress, as the impacts are associated with any utility scale solar plant, while some categories are discussed by directly comparing crystalline silicon and perovskite PV. The impact categories and subsections selected for this study are provided in the table on the following page.

Table 3: List of Selected Impact Category Sections and Discussions

Natural Resource Depletion	**Contributions to Global Climate Change**	**Land Use**	**Human and Ecosystem Toxicity**
Crystalline Silicon PV Material and Energy Requirements	Global Warming Potentials (GWPs)	Ecosystem Stress	Emissions
Perovskite PV Material and Energy Requirements		Land Use Efficiency	Use of Toxic Materials
Energy Payback Time (EPBT)			Trees vs Solar
Utility Scale PV Material and Energy Requirements			
Water Use			

Natural Resource Depletion

In reference to all PV installations, the natural resources used involve raw materials and energy requirements necessary for production, as well as mandatory water quantities for solar site maintenance. The raw material requirements for manufacturing of a solar site are described on a per panel basis, i.e. materials necessary for crystalline silicon versus perovskite PV, then on the utility scale. Energy requirements are analyzed based on each panel's individual manufacturing processes. Using energy input data and expected energy output, the energy payback times (EPBTs) are calculated. Using recycled PV material can greatly reduce the EPBT of the solar site. Water quantities are analyzed based on the amount of water necessary for periodic cleaning of solar panels.

Crystalline Silicon PV Material and Energy Requirements

Throughout the lifetime of crystalline silicon PV, there is a variety of required natural resource inputs. Natural high abundances of most input materials reduce concerns of substance diminishment. The inputs for crystalline silicon PV were analyzed in the LCI and are as follows;

Table 4: Raw Materials Required for Crystalline Silicon PV Production

Raw Material	**Production Purpose**
Quartz sand (silica, SiO_2)	For silicon production
Carbon (C) base (coke, coal, charcoal, wood)	For carbothermal reduction-smelting
Various gases	For Metallurgical Grade (MG) silicon refinement
Hydrogen Chloride (HCl)	For MG silicon distillation
Hydrogen (H) atoms	For the Siemens Process to further purify silicon
Small crystal seeds	For the Czochralski Method of growing crystalline silicon
Titanium dioxide (TiO_2) or silicon nitride (SiN)	For the textured anti reflective coating (ARC)
Screen-printed silver paste	For additional protection on front layer
Phosphorous-doped n+ region	For phosphorous-nitrogen (p-n) interface
Boron- (or gallium-) doped p-type region	For p-n interface
Aluminum	For back contact layer of solar cell

During the manufacturing of crystalline silicon PV, various energy requirements increase the embodied energy of the material, subsequently increasing the EPBT of the solar site. The great energy demands for silicon purification and crystallized growth during module manufacturing are the main concern for crystalline silicon PV, however the following table depicts all energy requirements expected for current and future module production. See Appendix I for calculation information.

Table 5: Energy Requirements for Crystalline Silicon PV Manufacturing (Embodied Energy)

Source	**Carbon Smelting**	**Siemens Process**	**Czochralski Method**	**Further Manufacturing Methods**	**Metal Frame**	**Total**
Alsema & Nieuwlaar (2000)	-	~611 kWh / 1 m^2	~ 278 kWh / 1 m^2	~ 278 kWh / 1 m^2	~111 kWh / 1 m^2	~1278 kWh / 1 m^2
NREL's PV FAQS (2004)	-	-	-	-	-	~ 420 kWh / 1 m^2 to ~ 600 kWh / 1 m^2
Nawaz & Tiwari (2006)	~15 kWh / 1 m^2	~ 72 kWh / 1 m^2	~ 210 kWh / 1 m^2	~ 190 kWh / 1 m^2	-	~ 487 kWh / 1 m^2
Mann, et al. (2013)	-	~152 kWh / 1 m^2	~ 62 kWh / 1 m^2	~ 82 kWh / 1 m^2	-	~ 296 kWh / 1 m^2
Diaz & Batalle (2013-2014) RANGE	-	~202 kWh / 1 m^2 to ~666 kWh / 1 m^2	~ 120 kWh / 1 m^2 to ~ 664 kWh / 1 m^2	~ 190 kWh / 1 m^2 to ~ 451 kWh / 1 m^2	~ 66 kWh / 1 m^2	~ 578 kWh / 1 m^2 to ~1846 kWh / 1 m^2
Kim, et al. (2014)	-	-	-	-	-	~ 25 kWh / 1 m^2 to ~ 104 kWh / 1 m^2

From this embodied energy table, a distinct decreasing trend is found. In 2000, energy requirements for crystalline silicon module production reached almost 1300 kWh/m^2. Over the years, this number greatly decreased to under 100 kWh/m^2. Using the values in the table above, an average embodied energy value of ~450 kWh/m^2 is assumed. See Appendix I for calculation information.

Perovskite PV Material and Energy Requirements

During manufacturing processes for perovskite PV, the primary raw materials used increase levels of concern while the small energy demands create ideas for manufacturing improvements. The raw material inputs for perovskite PV were analyzed in the LCI and are as follows;

Table 6: Raw Materials Required for Perovskite PV Production

Raw Material	**Production Purpose**
Alkaline mafic rocks	For perovskite production
Acetone, isopropanol, and deionized water	For pretreatment / cleaning activities
Compressed nitrogen	For dry cleaning
Glass	For top layer of module
Fluorine-doped tin oxide or titanium dioxide	For electron transport layer (ETL)
Lead-halide	For absorber layer (HPSCs)
Perovskite material (i.e. ammonium)	For absorber layer
Inorganic compounds	For hole transport layer (HTL)
Metals (gold, silver, aluminum)	For back contact layer
Conductive paste and lamination materials	To connect and surround thin film cell

Natural high abundances of most materials reduce concerns of materials diminishment, however the use of lead in the cell itself raises concerns for the level of human and ecosystem toxicity while guiding research towards other metal alternatives. Tin alternatives to lead have been lab tested. Though tin is appealing for the lack of direct toxicity effects, mining the substance releases toxicity levels with global warming potentials (GWPs) far beyond that of lead. Tin also occurs in rather small quantities naturally, therefore depleting the resource would not take long (Kadro & Hagfeldt 2017). Although the use of lead within the material can be of some concern, the extremely small amount can counteract most concerns.

Along with raw materials needed for production, there are some energy requirements associated with manufacturing perovskite PV. These requirements are far smaller than that of crystalline silicon PV production, but still relevant to this study. For perovskite PV, the various manufacturing methods and raw materials that can be selected greatly impact the embodied energy of the modules. These results are expressed in the following table. Please refer to Appendix II for calculation information.

Table 7: Energy Requirements for Perovskite PV Manufacturing (Embodied Energy)

Source	**Manufacturing Process Analyzed**	**Material Embodied Energy**	**Deposition Energy Requirements**	**Total Embodied Energy**
Celik, et al. (2016)	Solution Processing	-	-	~ $\frac{184.72\ kWh}{1\ m^2}$
Celik, et al. (2016) RANGE from EcoInvent Database	Solution Processing	-	-	~ $\frac{16.4\ kWh}{1\ m^2}$ to ~ $\frac{134.4\ kWh}{1\ m^2}$
Ibn-Mohammed, et al. (2017)	Vapor Deposition	$\frac{97.2\ kWh}{1\ m^2}$	$\frac{61.24\ kWh}{1\ m^2}$	~ $\frac{158.4\ kWh}{1\ m^2}$
Ibn-Mohammed, et al. (2017)	Spin Coating	$\frac{66.04\ kWh}{1\ m^2}$	$\frac{27.45\ kWh}{1\ m^2}$	~ $\frac{93.5\ kWh}{1\ m^2}$

From this information, the average embodied energy of perovskite PV is calculated. See Appendix II for detailed calculation. The average embodied energy of perovskite PV was calculated at ~118 kWh/m^2. This is significantly lower than the embodied energy found for crystalline silicon PV. The reason for this difference is the difference in energy requirements during module manufacturing, as crystalline silicon production is much more energy intensive than perovskite, due to the printability of perovskite PV.

Energy Payback Time (EPBT)

Many steps are involved in order to calculate the EPBT of a solar site. See Appendix IV for the detailed calculations of crystalline silicon and perovskite PV EPBTs.

1. Energy requirements during manufacturing must be calculated
    a. In the previous calculation, the energy requirements for both panels were,
        i. Crystalline silicon: ~451 kWh/m^2
        ii. Perovskite: ~118 kWh/m^2
2. Solar site expected annual energy output must be calculated
    a. Energy output is extremely location dependent due to variations in incoming solar radiation (insolation), therefore the annual outputs were calculated based on four different insolation locations
    b. For both panels, an energy conversion efficiency of 24% was assumed, therefore the following values for energy output were the same regardless of the panel
        i. Low annual insolation energy output: ~72 kWh/m^2/year
        ii. Medium-low annual insolation energy output: ~109 kWh/m^2/year
        iii. Medium-high annual insolation energy output: ~128 kWh/m^2/year
        iv. High annual insolation energy output: ~151 kWh/m^2/year
3. Cross reference each of these calculations to determine how long will it take the solar site to produce an amount of energy equal to that required during manufacturing and installation activities (location/insolation dependent)
    a. EPBT = embodied energy / expected annual energy output
    b. Using the two embodied energy values and four energy output values above, ranges for EPBTs were calculated for each panel

See Appendix IV for detailed EPBT calculation. For crystalline silicon PV, the average EPBT calculated was between 2 and 6 years, depending on the manufacturing processes used and the location of the solar site (Gerbinet, Belboom, & Leonard 2014). As expressed in the LCI, using recycled materials can decrease the EPBT of crystalline silicon PV by ~40% through reductions in energy demands during manufacturing (Frisson et al. 2000). On the other hand, the average EPBT of perovskite materials calculated was between 0.22 and 2 years, due to the extremely low energy demands during module manufacturing, as well as the location of the solar site (Celik et al. 2016).

Utility Scale PV Material and Energy Requirements

When installing any utility scale solar power plant, there is a variety of materials needed to complete the site. The following table presents LCI data of the most common BOS components and their related site responsibilities.

Table 8: Raw Materials Required for Utility Scale Solar Installations

Raw Material	**Production Purpose**
Metal mounting structures	For site stability
Copper-covered aluminum wiring	For direct electricity transfer
Energy combiner boxes	For current/voltage output management
Inverters	For DC to AC energy conversion
Fuse-boxes	For grid output management
Meters	For energy production management

Along with materials for installation activities, there is an immense amount of energy required for site preparation and installation. Some research suggests BOS components on the utility scale reach an embodied energy value of ~ 151 kWh/m^2 (Mason, Fthenakis, & Kim 2005). Others have suggested this value could be as low as ~ 40 kWh/m^2 or as high as ~ 500 kWh/m^2 (Zhou & Carbajales-Dale 2018 & Nawaz & Tiwari 2006). If the embodied energy of a utility scale solar site is added to the that of a specific panel, the EPBTs previously calculated would increase as a result.

Water Use

The depletion of water resources comes primarily during solar site maintenance specifically, panel cleaning. Throughout the lifetime of a solar site, the modules will require frequent washings to remove smog, dirt, dust, debris, etc. from the panel surface (Solar panel cleaning 2019). Panels covered in some sort of soiling layer will not produce as much electricity because the incoming sunlight will be blocked out. In 99% of cases, washing panels with plain water results in an adequate level of panel cleaning to increase energy output efficiency while decreasing the amount of grime left on the panels (Cleaning Your Solar Panels n.d.). In order to keep solar energy production at an optimal rate, panel washing is required, however the frequency of these washings depends on the location of the solar site and the rate of soiling increase over time. Deciding when to wash solar panels depends greatly on the previous and upcoming weather conditions, as well as the visible layer of debris on the panels (Krause 2014). It is hard to tell how much soiling actually affects the energy output of a solar array, however many studies have been conducted to do just that. Some studies suggest washing panels results in as high as a 50% increase in energy output while other studies have suggested that washing

panels does not change the energy output at all, unless there is an extremely thick layer of debris. In order to figure out the optimal washing schedule for solar sites in specific locations, you must first consider the weather conditions of that area.

In arid climates, such as the southwestern United States, with high rates of dust accumulation and dust transport alongside intermittent light rainfalls, panel washings are required more frequently. Aeolian dust soils panels, creating a layer of dry dust that can be easily washed away. Light rainfalls, though offering some relief for the layer of dry dust, often soil panels even further as they carry with them an array of particles ready to stick to the panels. In areas with wetter climates, frequent heavy rainfalls actually assist in washing away grime stuck on panels. However, these climates often experience some degree of snowfall as well which results in further panel soiling as snow carries particles from the atmosphere down to soil the panels. Although heavy rainfalls can help remove a layer of built up debris, most precipitation further soils panels, reducing the energy output efficiencies, and subsequently increasing the amount of required panel washings.

As a result of aeolian dust transport alongside location dependent precipitation rates, the general rule of thumb for panel washing is twice per year around the summertime (Zientara n.d.). In order to maximize the energy production rates, it is recommended to wash panels during peak sunlight months. Washings typically result in an immense amount of water resource depletion as utility scale solar sites can be incredibly large. Generally, washing panels uses around 20 gallons (gal) of water per 1 MWh of solar (Water Use Management n.d.). Frisvold & Marquez (2014) found an average of 51 gal/MWh energy production, however once the outliers were removed, the article found an average range of 0 to 33 gal/MWh for utility scale solar installations. Using these previously calculated averages, it is assumed that around 30 gal/MWh is needed to wash a

solar site. At the end of 2018, the Solar Energy Industries Association (SEIA) reported that the U.S. surpassed 60 GW of installed solar energy capacity (U.S. Solar Market Insight 2018).

To estimate the amount of water needed to wash all solar installations in the U.S., the following calculation is performed.

If 1 GW = 1,000 MW, then 60 GW = 60,000 MW of installed solar capacity in 2019

Each U.S. site requires 2 washings per year at 30 gallons of water per 1 MWh per wash

And 1 MW = 2,190 MWh

$$\frac{30\ \text{gal}}{\text{MWh/wash}} \times \frac{2{,}190\ \text{MWh}}{\text{MW}} = \frac{65{,}700\ \text{gal}}{\text{MW/wash}} \times \frac{2\ \text{wash}}{\text{year}} = \frac{131{,}400\ \text{gal}}{\text{MW/year}} \times 60{,}000\ \text{MW} =$$

= 7,884,000,000 gal/year

Therefore, the U.S. will require around 7,884,000,000 gallons of water each year to wash every solar site

In some locations, studies have found that washing panels results in around a 10-30% increase in energy output, if there is a visible layer of soiling on the panels beforehand (Why Clean Solar Panels? n.d. & Best Way to Clean Solar Panels n.d.). However, the rate of energy production increase greatly depends on the location and the amount of soiling on the panels beforehand, therefore not all washings will result in such a high energy production output increase. Many researchers today are trying to figure out whether the amount of energy output increase is worth the necessary water us for panel washings, as well as the costs of these washings.

Discussion

From this impact category analysis, it can be determined that when choosing a specific solar panel there are certain drawbacks that will come along with it. For crystalline silicon PV, the great energy demand during manufacturing increases costs as well as ecosystem toxicity and

subsequently, contributions to global climate change, if the manufacturing facility does not run on renewable energy sources. For perovskite PV however, the energy demands during manufacturing are far less than that of crystalline silicon but the use of toxic lead materials, creates barriers as society fears this specific toxicity. Following module manufacturing, the water demands during use are relatively the same as all utility scale solar sites have similar structures and materials, besides the specific panel.

Contribution to Global Climate Change

Many activities, from raw material extraction to site decommissioning, can play a great role in our climate system. During module production, maintenance, and transport, electricity and fuel primarily from fossil fuel sources contribute to our changing climate.

- Use of fossil fuels for energy production during manufacturing releases greenhouse gases (GHGs) into the atmosphere, thus exemplifying the greenhouse effect.
- Use of fossil fuels for worker and material transport also contributes to greenhouse effect
- Site clearing contributions to global dust-climate feedback system and eutrophication
- Site maintenance activities require mowers and other vehicles releasing GHGs

The following section analyzes the global warming potentials (GWPs) of crystalline silicon and perovskite PV using data from previously calculated studies.

Global Warming Potential of Crystalline Silicon and Perovskite PV

The EPA describes global warming potential (GWP) as a mathematical representation to compare the warming aspects of different emissions, such as carbon dioxide (CO_2), methane (CH_4), chlorofluorocarbons (CFCs), etc. “Specifically, [GWP] is a measure of how much energy

the emissions of 1 ton of a gas will absorb over a given period of time" (Understanding Global Warming 2017). For solar modules, a CO_2 equivalent is used to measure the GWP. From a variety of studies, information on the GWP for crystalline silicon and perovskite PV was collected and compared in the following tables.

Table 9: Global Warming Potential of Crystalline Silicon PV

Source	**Global Warming Potential (g CO_2-eq. / kWh)**
Fthenakis, Kim, & Alsema (2007)	~ 30 to 45 g CO_2-eq. / kWh
Hsu, et al. (2012)	~ 57 g CO_2-eq. / kWh
Gerbinet, Belboom, & Leonard (2014)	~ 39 to 100 g CO_2-eq. / kWh
Gong, Darling, & You (2015)	~ 40 g CO_2-eq. / kWh
Leccisi, Raugei, & Fthenakis (2016)	~ 30 g CO_2-eq. / kWh

Using this information, the average GWP for crystalline silicon PV was calculated. See Appendix V for calculation information. From this calculation, it can be assumed that on average, crystalline silicon PV releases ~49 g CO_2-eq. per kWh of solar panel energy production.

Table 10: Global Warming Potential of Perovskite PV

Source	**Global Warming Potential (g CO_2-eq. / kWh)**
Garcia-Valverde, Cherni, & Urbina (2010)	~ 55 to 110 g CO_2-eq. / kWh
Espinosa, et al. (2015)	~ 350 g CO_2-eq. / kWh
Gong, Darling, & You (2015)	~ 60 to 100 g CO_2-eq. / kWh
Celik, et al. (2016)	~ 99 to 147 g CO_2-eq. / kWh
Ibn-Mohammed, et al. (2017)	~ 90 to 160 g CO_2-eq. / kWh

Using this information, the average GWP for perovskite PV was calculated. See Appendix V for calculation information. From this calculation, it is assumed that the average perovskite panel has a GWP of ~ 100 g CO_2-eq. per 1 kWh of solar panel energy production.

Discussion

From these tables and related calculations, it is apparent that the GWP of perovskite is about double that of crystalline silicon. The reason for this larger contribution is primarily due to the rather short lifetimes of perovskite (~5 years right now). As researchers continues to strive for longer lifetimes (~ 10 years), it can be assumed that as the life expectancies increase, the GWPs will decrease. It is also important to note that in the following impact category sections various climate change contributions are analyzed as they relate to land cover change and human and ecosystem toxicity. These can include increased contributions to the dust-climate feedback system, decreased carbon sequestration, increased emissions, and so on.

Land Use

Due to the large size of utility scale solar power plants, environmental stressors from large land use change can be depicted using a chain of events-like framework. In the following section, the chain of events that might unfold as a result of land cover change for big solar, no matter the panels used, is analyzed. The great changes come along with great environmental impacts, all of which are discussed in detail. Once the site is developed, the reversibility of the land for other uses decreases as a result of the land surface and subsurface changes. Activities as preparation for installation through a chain of events, all the way to decommissioning and calculating land use reversibility, are included in the ecosystem stress subsection. The second

subsection involves calculating the land use efficiency of utility scale solar sites. This depends on the expected annual energy output as well as the site acreage. Both subsections provide an in-depth analysis into the great adverse environmental impacts associated with large scale solar installations, regardless of the specific solar cell used.

Ecosystem Stress

In order to install a utility scale solar power plant, a lot of changes must occur to create an ideal surface and subsurface land environment. For the purpose of this study, the following section analyzes a chain of events as they might occur from this land cover change. This chain of events correlates closely with North American Forests and the Great Plains. Both of these ecosystems provide services necessary for the preservation of our natural world. Forests are rich with biodiversity and ecosystem services, such as carbon sequestration and storage, nutrient cycling, and water purification (Forest ecosystem products 2017). The Great Plains house the nations vast grasslands and playas, both of which have great biodiversity and contribute necessary ecosystem services. These services include, but are not limited to, flood control, soil preservation, nutrient regulation, waste management, and carbon sequestration (Ecosystem Services from National n.d. & Ecosystem Services and Playas n.d.). Altering these environments for utility scale solar installations greatly impacts the area, potentially causing irreversible damage. The following section dives deep into the possible outcomes from clearing these lands for solar installations. The selection process used to determine ideal ecosystems to analyze is detailed in Appendix VI.

In preparation for installation, an immense amount of land cover change is required, such as vegetation clearing and soil maintenance (Utility-Scale Solar 2015 & Hernandez et al. 2014).

Great changes to lands cause adverse ecological effects that could take hundreds of years to be reversed (Beatty et al. 2017). Changing lands can result in adverse environmental effects for both the local land and water resources. The local ecosystem can experience decreases in local biodiversity, increases in the risks of soil erosion, increases in aeolian dust transport and subsequent increases in contributions to the global dust-climate feedback system. Along with land risks, effects on the local water resources can include increases in surface runoff, increases in eutrophication, and increases in water stress.

All of these negative impacts can result in decreases to the land use efficiency as well as the land use reversibility. These effects represent the biggest environmental concerns when implementing utility scale solar plants, regardless of the panel type installed. All of these effects are inherently related to each other, exemplifying one another down a chain-like system of degradation (Hernandez et al. 2014). The following section will follow this chain of events as they might unfold during the preparation, installation, use, and decommissioning of a utility scale solar site in either forest or grassland areas to provide a well-rounded understanding of the adverse effects of altering these landscapes.

While preparing the landscape for the development of a large ground-mounted solar site, developers and construction teams must change the land in a variety of ways. Land cover change often involves many methods to attack different 'problems' associated with the surface and subsurface. First, the land must be cleared of nearly all of the existing vegetation, soil, and underground roots. The above- and below-ground vegetation and roots are cleared using various machines, such as hogs, shears, and grapples (Vegetation 2019). The topsoil is the top layer of soil, containing the organisms, nutrients, characteristics, etc. essential for supporting the growth of vegetative life (Best Management Practices 2011). This uppermost soil layer is stripped using

machinery and stockpiled in a location either near or far from the solar installation site (Beatty et al. 2017). Once the topsoil is stockpiled, it has around 6 months to be reused before all of the essential ingredients for vegetation growth die out as a result of this landscape change (Best Management Practices 2011).

Following these various clearing strategies, the land is further graded, or leveled, before machine-driven soil compaction occurs (Beatty et al. 2017). Soil compaction refers to the landscape preparation method of applying a large amount of force to the surface soil. Contractors apply this method to further resist the infiltration of various natural mechanisms to the surface and subsurface soil, such as water, air, plant roots, etc. (Wolkowski & Lowery 2008). Without proper infiltration rates, lands experience rises in the potentials for landscape biodiversity diminishment, soil erosion progression, and storm water runoff advancement, all of which cause even more adverse ecosystem effects.

When developing a solar site, the various forms of landscape fragmentation required to achieve an ideal landscape result in adverse effects on the local ecosystem. Landscape change causes decreases in local biodiversity from the creation of new ecological barriers preventing different species from moving around and taking root (Hernandez et al. 2014). In other words, this vegetation clearing and soil grading can cause great changes to the ecological landscape by decreasing opportunities for biological expansion. Native plant species die out with a new, unwelcoming environment, allowing exotic invasive plant species to take root. Eventually, invasive species push native plant species completely out, taking over the environment (Beatty et al. 2017). Due to the probability of decreasing local biodiversity through the development of new ecological barriers, solar sites must be located outside endangered or vulnerable species habitats. The use of toxins, such as herbicides for land preparation and dust suppressants for maintenance

activities, also cause great habitat loss and subsequently, great reductions in local biodiversity (Hernandez et al. 2014). Along with barriers for biological expansion, clearing land impacts surface and subsurface soil properties, allowing for even more adverse environmental processes to take place.

Once the site is cleared of all remaining vegetation, the land becomes extremely hostile and barren as plant species die out to create an ideal environment for a utility scale solar site. Ideally, the land would be completely cleared of vegetation to decrease future maintenance activities centered around vegetation management. In other words, frequent mowings to reduce vegetation shading of panels can be diminished through the complete clearing of all vegetation from the premises. However, when vegetation is completely cleared out and the soil is compacted, other ecological problems rise in concern as they can too affect the outcome or output of the solar site. Barren landscapes result in extremely dry soil or dirt which contribute to increases in land erosion potential, aeolian dust transport, global dust-climate feedback systems, and storm water runoff contributions to eutrophication and great water stress.

As the land is cleared and compacted, the soil is left dry, which inherently means the soil is left weak. Weak soil can be impacted greatly by outside sources such as wind, water, human activity, and so on. These natural or anthropogenic forcings can negatively impact the surface or subsurface soils which, in turn, negatively impacts the energy production potential of a utility scale solar site. Dust can reduce the efficiency of a solar site through a variety of ways but primarily through the increased risk of landscape erosion as well as increased contributions to aeolian dust transport pathways and subsequently, contributions to the global dust-climate feedback system. In the case of solar sites, land erosion refers to the movement of surface and subsurface soil through the increase in natural forcings, such as wind and water (Evers 2018).

Erosion can shift an entire site, destroying parts and immensely decreasing the energy production output. Although the risks of land erosion on a solar site are known, strategies for erosion prevention are often forgotten as solar developers aim to keep installation costs low (Erosion Control 2019). Though erosion can cause the most damage to a solar site, it occurs the least often as panel soiling and weathering increases due to airborne dust transport, therefore developers are often more concerned with dusts contributing to advanced panel degradation rates rather than full site erosion potentials.

When lands are altered in various forms to create an ideal environment for a solar site, the amount of localized dust increases as a result. As weather conditions change with the seasons, wind speeds and frequencies increase, resulting in increased contributions to the amount of aeolian dust transport. Airborne dust can soil PV panels resulting in a layer of impurities on the module surface, weather panels resulting in decreased panel lifetimes, and contribute to the global dust-climate feedback system resulting in adverse climate change effects. A layer of soiling on the panels decreases the energy production output of the solar site and increases the rate of necessary panel washings. Wind-blown dust, dirt, and debris also increases the rate of panel weathering, which inherently refers to the aeolian soiling breaking down most material it comes in contact with (Evers 2018). This increased rate of weathering decreases panel efficiencies and lifetimes as it wears down the material necessary for adequate energy production outputs. Clearing vegetation dries out the lands, increasing the accumulation of dust and aeolian dust transport, increasing the contributions to the global dust-climate feedback system, while subsequently decreasing the energy production efficiency of the solar site.

Increases in dust contributes to the dust-climate feedback system, which can have adverse effects on our changing climate. The role dust plays in growing anthropogenic climate change

effects is still being explored, however there are specific effects that are well-understood among climate scientists. It is still unknown whether increases to the dust-climate feedback system might contribute to or take away from the global anthropogenic climate change effects seen today, however scientists can pinpoint key areas of concern (Kok, Ward, & Mahowald 2016 & Kok, Ward, Mahowald, & Evan 2018). Dust influences our climate system in a variety of ways, but its primary impacts are associated with variances in radiative properties as well as influences on the hydrologic cycle (Winckler 2010 & Highwood & Ryder 2014). Researchers are still studying the impacts of dusts have on our changing climate.

Compacted soil allows for little to no water absorption from a lack of filtration access from increased impervious surfaces. Due to the low absorbency property of compacted soil, barren landscapes experience increased rates of water runoff. Runoff most commonly refers to the flow of excess storm water along the surface, towards low lying land or bodies of water. As the water flows along the surface, it picks up various, potentially problematic, substances such as nutrients, bacteria, pesticides, chemicals, etc. (Perlman 2016). These natural or man-made substances travel along the water flow until they eventually deposit in a new environment. In most circumstances, the water runoff follows naturally occurring slopes or man-made paths into drainage pipelines, both of which empty into different bodies of water (Perlman 2016). If the water runoff carries an immense amount of new nutrients, the intake areas can experience increased rates of eutrophication and acidification.

The eutrophication process is as follows. Nutrients found in animal waste and fertilizers have very high concentrations of nitrogen and phosphorous, both of which fuel vegetative growth in the intake aquatic ecosystem (NOAA 2018). As these life-producing nutrients arrive in excess quantities to new underwater ecosystems, there is a sharp rise in plant and algae growth.

Spikes in aquatic vegetative growth result in the formation of incredibly dense algae blooms which end up blocking the necessary sunlight and intaking most of the available oxygen. Following decreases in sunlight and oxygen quantities, the local vegetation quickly dies off, creating a 'dead zone' where life can no longer thrive (Chislock, Doster, Zitomer, & Wilson 2013). Eutrophication can also result in increased rates of ocean acidification through the production of excess carbon dioxide from vegetative growth (NOAA 2018). Ocean acidification creates a more hostile environment for most marine wildlife, reducing the population of local fish, algae, etc. (Ireland 2015). As eutrophication rates increase worldwide, finding adequate prevention strategies remains incredibly important for the preservation of aquatic ecosystems.

Creating a barren, compacted landscape increases the rate of surface runoff carrying natural nutrients for vegetation growth and man-made chemicals for vegetation management, thus increasing the rate of eutrophication and acidification. The immense water stress from site preparation activities and vegetation management practices is of little concern to solar developers as they aim to keep installation costs low, therefore understanding the full effects of developing a utility scale solar site is of increasing importance. Figure 21 is a summary flow chart of the above chain of events, created specifically for this study.

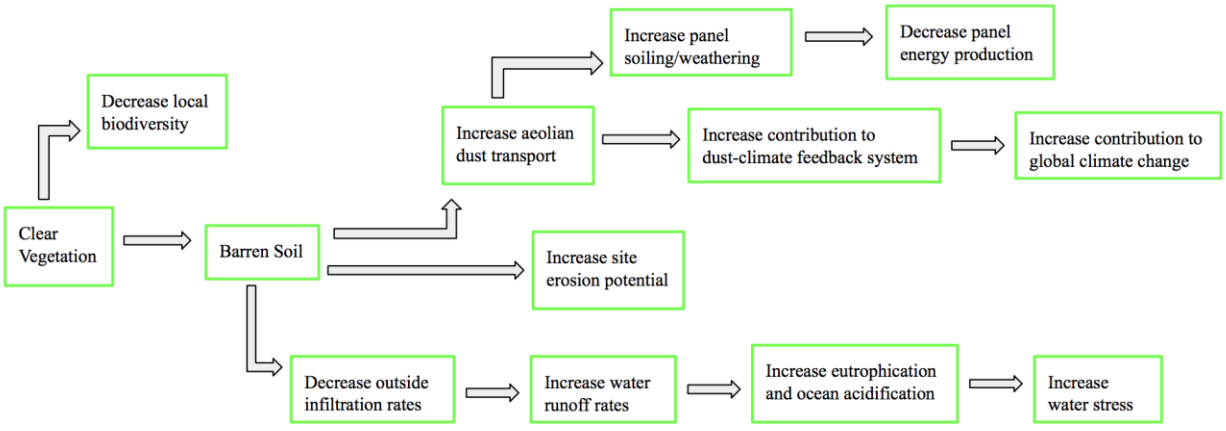

Figure 21: Adverse Environmental Chain of Events, by Taylor Camp

The collective restructuring of lands for utility scale solar use reduces the availability of that land for nearly any other activity for the foreseeable future. Land use reversibility or irreversibility can be calculated depending on the rate of ecosystem 'bounce-back' following the decommissioning of a utility scale solar power plant. Some changes to landscape result in irreversible damage and subsequent prevention for further uses. Though some changes can be irreversible, others can be reversible on a very long timescale (Hernandez 2014). The land use impacts associated with big solar are extremely concerning, however they are not the main point of research currently in the solar industry. It is important to note that as technological advancements for increased energy conversion efficiencies continue to prosper, focuses on land use impacts are rather minimal as the desire for renewable energy systems overshadows the associated negative environmental effects.

Another important ecosystem to consider when looking at downstream effects is The North American Deserts. Due to the immense amount of incoming solar radiation alongside relatively clear landscapes, deserts come across as the ideal place for a utility scale solar installation. However, this is far from true. Deserts provide unique ecosystem services from that of forests and grasslands. These services include, but are not limited to, resistance to desertification, gene pool protection, erosion protection, and nutrient cycle management (Taylor et al. 2017 & Monger 2009). Deserts also house unique plant species, necessary for the preservation of the local ecosystem. As demand for solar increases, understanding the different downstream effects based on the local ecosystems is of the utmost important. Preventing adverse ecosystem stress should be a top priority for solar installers, if this energy resource is to remain environmentally friendly as research continues.

Land Use Efficiency

In order maximize use of land for energy resources, researchers calculate the land use efficiency rates through a variety of techniques. For utility scale solar power plants, land use efficiency is often calculated by dividing the expected production output of the site by the total site acreage. Though this is the usual calculation strategy, studies vary depending on location and time scale, therefore presenting the data in a few different ways will give a more adequate understanding of the true land use efficiency of utility scale solar. By cross checking the energy conversion efficiencies with installed MW capacity and land coverage, studies have calculated average land use efficiency levels of around 35% for crystalline silicon PV (Hernandez, Hoffacker, & Field 2014). As energy conversion efficiencies are rather the same for crystalline silicon and perovskite PV, it can be assumed that land use efficiencies will be similar as well.

Discussion

As technological advancements for panels continue to inspire industry interests, the need for research into adverse environmental impacts is necessary. To understand the impacts of utility scale solar, regardless of the panel types used, this study analyzed the trickle down effects of clearing lands for site installation in forest or grassland areas, with a special note on desert ecosystems. It is important to note that as research prospers in this field, there has been very little concern for adverse ecosystem stress that results from immense land cover change. For research in the future, analyzing the effects on the utility scale is far more informative than analyzing on the per panel basis, though technological advancements can increase industry prosperity.

Human and Ecosystem Toxicity

During manufacturing processes, the emissions released vary depending on the facility and the panel being produced. Crystalline silicon manufacturing requires a lot more energy than perovskite manufacturing, however perovskite PV uses toxic lead materials within the panel. Following manufacturing, the emissions from material transport, site preparation, maintenance, installation, and decommissioning are all similar on the utility scale. Using emissions data, this section offers an interesting comparison between trees and solar, following detailed analyses of overall solar pollutant emissions and toxic material use.

Emissions

Toxic pollutants from solar life cycles can affect both human health and ecosystem quality. Hazardous pollutants are produced during manufacturing, transportation, land cover change, maintenance, and decommissioning services. The following bullets offer simplified information about emissions at each stage of the solar life cycle.

- Manufacturing Pollutants: greenhouse gas emissions as well as toxic metal emissions are released, causing harmful impacts to both humans and the surrounding environment
    - Pollutants such as toxic gases and heavy metals are produced on a larger scale during silicon material processing than that of perovskite
- Manufacturing Toxic Metal Use: use of lead in perovskite materials poses concern for increased toxicity levels as factory and site workers can be exposed to the toxic metal during manufacturing, maintenance, or decommissioning activities
- Transportation, Site Preparation, Installation, and Decommissioning: produce emissions via the use of gas for vehicle transport, tractor use, hog use, etc.

- Maintenance Activities: produces emissions via mowers primarily
    - According to the EPA, a conventional lawn mower emits pollution primarily in forms of volatile organic compounds (VOCs), nitrogen oxides (NOx), carbon monoxide (CO), carbon dioxide (CO2), and various sizes of particulate matter (PM) (Banks n.d., & Banks & McConnell 2015)
    - EPA emission calculations suggest lawn mowers emit more air pollution than most automobiles on the market today (Facts about the Environmental 2013)
    - Mowers can cause great noise pollution within a certain area as well as ground contamination from gasoline use (Fthenakis & Kim 2011)

These human and ecosystem increased toxicity levels from emissions are often overlooked as a part of this renewable energy resource.

Use of Toxic Materials

Although lead is often unexpectable to the general public, researchers have shown that the small quantities of lead in the panels is nearly insignificant. According to the EPA's Safe Drinking Water Act, the amount of lead tolerable and safe, per drinking water standards, is zero (Basic Information 2019). However, unless workers actually consume the panel material, coming in close contact with it is not necessarily unsafe. In other words, touching lead materials will not cause a worker harm but if they accidentally ingest the material it is toxic. This is proven by the amount of lead found naturally in soils, ranging from 10 to 50 mg/kg, meaning for every 1 kg of soil there is between 10 and 50 mg of lead (Wander n.d.). If other man-made lead sources are accounted for, there could be up to 10,000 mg/kg of lead in soils (Stehouwer 2010). Compare this to the amount of lead in perovskite PV of < 1 g/m^2 in the absorber layer, meaning for every 1

m^2 of cell material there is < 1 g of lead (Kadro & Hagfeldt 2017). If 1g/100g = 10,000 mg/kg, then it can be assumed, in the simplest of terms, that the amount of lead in the perovskite structure would near double the amount of lead in local soil if, on the off chance it is released through panel breakage.

Trees vs Solar

In 2016, it was estimated that a single tree can sequester ~400 pounds (lbs) of CO_2 in roughly 25 years time (Schildgen 2016). Divide 400 by 25 to get the estimated sequestration amount in 1 year to find that on average, one tree can sequester ~16 lbs (0.008 tons) of CO_2 from the atmosphere in a single year.

If an average forest houses ~100 trees/acre (Forest Inventory n.d.),

$$\text{then } \frac{0.008 \text{ tons } CO_2}{1 \text{ tree}} \times \frac{100 \text{ trees}}{1 \text{ acre}} = \frac{\sim 0.8 \text{ tons } CO_2}{\text{acre}}$$

In 2018, the EPA estimated that '0.85 metric tons of CO_2 are sequestered annually by one acre of average U.S. forest (Greenhouse Gases Equivalencies 2018).' Compare this number to the annual average reduction in CO_2 emissions from using a renewable energy resource, such as solar.

In 2019, it was estimated that choosing a renewable energy resource can counteract ~5,000 lbs of coal each year (Matasci 2019). According to the EIA, '1 short ton (2,000 lbs) of coal will generate ~5,720 lbs of CO_2 (Hong & Slatick 1994). If this estimate is true, then so is the following calculation.

$$\frac{5{,}000 \text{ lbs coal}}{1 \text{ year}} \times \frac{5{,}720 \text{ lbs } CO_2}{2{,}000 \text{ lbs coal}} = \frac{14{,}300 \text{ lbs } CO_2}{\text{year}} \times \frac{0.0005 \text{ ton}}{1 \text{ lb}} = \frac{7.15 \text{ tons } CO_2}{\text{year}}$$

In other words, choosing a renewable energy resource such as solar means ~ 7 tons of CO_2 will be kept out of the atmosphere from coal-fired energy production every year. Though this number is accurate, it is also extremely idealistic and has many limitations, however it can still be assumed that installing solar panels would keep more CO_2 out of the atmosphere than an entire acre of forest can sequester in one year. In order to install utility scale solar, acres of trees must be cleared. Is it worth the environmental cost?

Discussion

The very low energy demands required during manufacturing of perovskite PV, when compared to crystalline silicon, offer relief in the emission of fossil fuel resources, if the manufacturing facility does not run on renewables. However, the use of toxic metals in perovskite materials raises concerns for implementation on the utility scale. Even though the amount of lead in the perovskite material is extremely small, the public awareness, or fear, of lead in any amount can stall research and implementation. Although there are emissions released during the lifetime of solar, they are heavily outweighed by the emissions that are potentially saved from reducing fossil fuel energy production, estimated at ~7 tons of CO_2 per year, compared to the 50 to 100 g CO_2-eq./kWh produced from solar.

Discussion

With solar installed capacity continuing to rise each day, the need for an adequate understanding of the associated environmental impacts has never been more important. Although new advancements in PV manufacturing have created a more cost effective, fast paced production method, it hardly addresses the key issues of utility scale solar. As site installation

preparation activities stay the same, extreme downstream environmental effects come as a result. Some researchers have been testing different management practices as they hope to reduce these environmental effects, such as sheep grazing for vegetation management. While others, as this impact assessment points out, have focused on developing ‘better’ PV technology.

Even though the low energy demands during manufacturing and potential for great upscaling result in positive innovations, the use of lead within the perovskite materials along with the current short panel lifetimes raise questions on whether printing techniques are worth the potential savings. If manufacturing facilities run off of solar panels themselves, then do large energy demands for crystalline silicon matter as much as toxic metal use or short life times? Though these innovations are interesting and revolutionary, they do not address the true land use impact of big solar.

Interpretation

Using the data collected and calculated in the impact categories above, the following table was created as an overview of the fundamental differences between crystalline silicon and perovskite PV to formulate a future panel installation recommendation.

Table 2: Crystalline Silicon Perovskite Comparison Table

Cell Type	Average Embodied Energy	Cell Energy Conversion Efficiency Range	Energy Payback Time (EPBT) Range	Life Expectancy	Average Global Warming Potential (GWP)
Crystalline Silicon PV	~ $\frac{451\ kWh}{m^2}$	22 to 27 %	2 to 6 years	~ 30 years	~ $\frac{49\ g\ CO_2\text{-eq.}}{kWh}$
Perovskite PV	~ $\frac{118\ kWh}{m^2}$	20 to 26 %	0.22 to 2 years	~ 5 years (need 10 years for implementation)	~ $\frac{100\ g\ CO_2\text{-eq.}}{kWh}$

From this table and previous impact category assessment, the following can be determined.

1. High energy requirements for crystalline silicon manufacturing result in increased EPBTs
2. Current low life expectancy of perovskite PV increases GWPs

In order to make adequate panel recommendations these two dependent factors need to be considered through the lens of adaptive manufacturing techniques. As the energy requirements for manufacturing crystalline silicon PV have gone down over the past years, to less than 100 kWh/m^2 according to Kim et al. (2014), it is assumed that the EPBT has gone down as well. This results in an EPBT of ~2 years, which is close to the EPBT of perovskite, creating a near equal EPBT for both panel types. If this is correct, then the longer life expectancy alongside decreased GWP makes crystalline silicon the ideal PV material for commercialization.

On the other hand, as research continues to strive for longer life expectancies of perovskite PV, GWPs are expected to decrease. If this is to be assumed true, perovskite become a new ideal for the solar industry through the potential to print cells. However, until these life expectancies reach at least 10 years, implementing perovskite on any scale will be difficult. Once the ideal lifetimes are achieved, the printing capabilities associated with perovskites may completely dominate the solar market as the desire for renewable energy implementation continues worldwide. With installations continuing to rise, the manufacturing advancements become the center of most PV research. As a result, the land use impacts of big solar are often ignored.

As discussed in detail in the impact category section, the trickle down effects of altering landscapes for utility scale solar create new ecosystem stressors. Though some ecologists have studied these effects in a variety of ecosystems, there is often a disconnect between ecology research and engineering research, as engineers continue to focus on manufacturing advancements. While conducting this LCA, a lack of ecosystem framework was noticed. Though this is an international standard, concern for environmental or ecological impacts are in engineering terms, i.e. inputs and outputs, whereas ecologists often focus on downstream effects. This might be expected considering LCAs are more steered towards engineers, but as we strive for change towards a sustainable future, standards such as this must change along with it. LCAs in the future should include specific biodiversity and ecosystem services impacts, as they change alongside landscape alterations.

Though these effects are often overlooked by engineers, ecologists and philosophers have taken great interest in this research. As presented by Sovacool & Dworkin (2015), energy justice is an ethical perspective creating a framework for which energy systems should follow. These

authors describe the eight fundamental influencers for energy decision making; availability, affordability, due process, good governance, sustainability, intergenerational equity, intragenerational equity, and responsibility (Sovacool & Dworkin 2015). In accordance with the findings of this study, the sustainability aspect of energy justice is in jeopardy with utility scale solar installations. If land cover change results in irreversible damage from ecosystem stress, then solar fields may not be sustainable. This not only effects the current generation, but generations to come as they deal with landscape destruction from solar implementation.

As global solar installed capacity continues to rise, a need for an adequate understanding of the adverse ecological effects associated with big solar is necessary. For solar to continue to thrive as a clean energy source, alternatives to land clearing and soil compacting need to be considered. Sheep grazing is a promising management practice as it allows the solar installer to keep vegetation without fear of overgrowth shading the panels and decreasing energy production. Though there are other alternatives out there, such as low light or low growing crop integration, sheep grazing allows the installer to keep native plant species as they are, reducing local biodiversity impacts. Innovative, sustainable practices such as this should be the focus of solar research in the future, as lands continue to be developed for large scale installations.

Bibliography

About PV Cycle. (2016). Retrieved January 30, 2019, from http://www.pvcycle.org/organisation/about/

Ali, H. H. M., El-Sadek, M. H., Morsi, M. B., El-Barawy, K. A., & Abou-Shahba, R. M. Production of metallurgical-grade silicon from Egyptian quartz. (February 2018). Retrieved February 11, 2019, from https://www.researchgate.net/publication/325571725_Production_of_metallurgical-grade_silicon_from_Egyptian_quartz

Alsema, E. A. & Nieuwlaar, E. (November 2000). Energy viability of photovoltaic systems. Retrieved January 30, 2019, from https://www.sciencedirect.com/science/article/pii/S0301421500000872

Also Energy. (n.d.). Retrieved January 30, 2019, from https://www.alsoenergy.com/wp/

Anctil, A. & Fthenakis, V. (09 December 2011). Life Cycle Assessment of Organic Photovoltaics. Retrieved January 30, 2019, from https://www.intechopen.com/books/third-generation-photovoltaics/life-cycle-assessment-of-organic-photovoltaics

B Resource Guide: Conducting a Life Cycle Assessment (LCA). (February 2008). Retrieved February 11, 2019, from http://nbis.org/nbisresources/life_cycle_assessment_thinking/guide_life_cycle_assessment_bcorp.pdf

Balance of System. (05 January 2006). Retrieved January 30, 2019, from https://web.archive.org/web/20080504001534/http://www1.eere.energy.gov/solar/bos.html

Banks, J. L. (n.d.). National Emissions from Lawn and Garden Equipment, 15. Retrieved February 11, 2019, from https://www.epa.gov/sites/production/files/2015-09/documents/banks.pdf

Banks, J., & McConnell, R. (16 April 2015). National Lawn and Garden Equipment Emissions, 19. February 11, 2019, from https://www3.epa.gov/ttn/chief/conference/ei21/session10/banks_pres.pdf

Basic Information about Lead in Drinking Water. (28 March 2019). Retrieved April 5, 2019, from https://www.epa.gov/ground-water-and-drinking-water/basic-information-about-lead-drinking-water#regs

Beatty, B., Macknick, J., McCall, J., Braus, G., & Buckner, D. (May 2017). Native Vegetation Performance under a Solar PV Array the the National Wind Technology Center. Retrieved January 30, 2019, from https://www.nrel.gov/docs/fy17osti/66218.pdf

Bellini, E. (22 March 2017). Veolia opens solar module recycling facility in France. Retrieved January 30, 2019, from https://www.pv-magazine.com/2017/03/22/veolia-opens-solar-module-recycling-facility-in-france/

Bernardis, S. (February 2012). Engineering Impurity Behavior on the Micron-Scale in Metallurgical-Grade Silicon Production, 137. February 11, 2019, from https://pdfs.semanticscholar.org/3c1b/5fcbe4b48728ce7d6db9a639f1b423e672d6.pdf

Berry, J. J., van de Lagemaat, J., Al-Jassim, M. M., Kurtz, S., Yan, Y., & Zhu, K. (16 October 2017). Perovskite Photovoltaics: The Path to a Printable Terawatt-Scale Technology. *ACS Energy Letters*, *2*(11), 2540–2544. Retrieved February 11, 2019, from https://pubs.acs.org/doi/10.1021/acsenergylett.7b00964

Best Management Practices: Topsoil Management. (August 2011). Retrieved January 30, 2019, from https://apps.itd.idaho.gov/apps/env/BMP/PDF%20Files%20for%20BMP/Chapter%205/PC-33%20%20Topsoil%20Management.pdf

Best Research-Cell Efficiencies Chart. (03 January 2019). Retrieved February 11, 2019, from https://www.nrel.gov/pv/assets/pdfs/pv-efficiency-chart.20190103.pdf

Best Way to Clean Solar Panels. (n.d.). Retrieved January 30, 2019, from https://energyinformative.org/solar-panel-cleaning/

Binek, A., Petrus, M. L., Huber, N., Bristow, H., Hu, Y., & Bein T. (May 2016). Recycling Perovskite Solar Cells To Avoid Lead Waste. Retrieved January 30, 2019, from https://www.researchgate.net/publication/301941182_Recycling_Perovskite_Solar_Cells_To_Avoid_Lead_Waste

Brunisholz, M. J. (2019). Life Cycle Assessment of Future Photovoltaic Electricity Production from Residential-scale Systems Operated in Europe. Retrieved January 30, 2019, from http://www.iea-pvps.org/index.php?id=314

Burkhardt, J. J., Heath, G., & Cohen, E. (09 April 2012). Life Cycle Greenhouse Gas Emissions of Trough and Tower Concentrating Solar Power Electricity Generation: Systematic Review and Harmonization. *Journal of Industrial Ecology*, *16*, S93–S109. Retrieved February 11, 2019, from https://onlinelibrary.wiley.com/doi/full/10.1111/j.1530-9290.2012.00474.x

Canada, S. (April-May 2013). Impacts of Soiling on Utility-Scale PV System Performance. Retrieved January 30, 2019, from https://solarprofessional.com/articles/operations-maintenance/impacts-of-soiling-on-utility-scale-pv-system-performance#.XI8jbS2ZPEZ

Celik, I., Song, Z., Cimaroli, A. J., Yan, Y., Heben, M. J., & Apul, D. (November 2016). Life Cycle Assessment (LCA) of perovskite PV cells projected from lab to fab. *Solar Energy Materials and Solar Cells*, *156*, 157–169. Retrieved February 11, 2019, from https://www.sciencedirect.com/science/article/pii/S0927024816300605?via%3Dihub

Chandler, D. L. (07 February 2019). Unleashing perovskites' potential for solar cells. Retrieved March 1, 2019, from http://news.mit.edu/2019/perovskites-microstructure-solar-cells-0207

Chapter 3 of Desktop Computer Displays: Life Cycle Assessment; Volume 1. (n.d.). Retrieved February 11, 2019, from https://www.epa.gov/sites/production/files/2015-04/documents/ch3.pdf

Chigondo, F. (May 2018). From Metallurgical-Grade to Solar-Grade Silicon: An Overview. *Silicon*, *10*(3), 789–798. Retrieved February 11, 2019, from https://link.springer.com/article/10.1007%2Fs12633-016-9532-7

Chilvery, A., Das, S., Guggilla, P., Brantley, C., & Sunda-Meya A. (16 August 2016). A perspective on the recent progress in solution-processed methods for highly efficient perovskite solar cells. Retrieved January 30, 2019, from https://pdfs.semanticscholar.org/fb93/aa51d77e64ce0e043f6f5f9c1e98b8fd6186.pdf

Chislock, M. F., Doster, E., Zitomer, R. A., & Wilson, A. E. (2013). Eutrophication: Causes, Consequences, and Controls in Aquatic Ecosystems. Retrieved January 30, 2019, from https://www.nature.com/scitable/knowledge/library/eutrophication-causes-consequences-and-controls-in-aquatic-102364466

Ciftja, A., Engh, T. A., & Tangstad, M. (February 2008). Refining and Recycling of Silicon: A Review. Retrieved January 30, 2019, from https://edisciplinas.usp.br/pluginfile.php/2484614/mod_resource/content/1/Refining%20and%20Recycling%20of%20Silicon%20A%20Review.pdf

Cleaning Your Solar Panels. (n.d.). Retrieved January 30, 2019, from https://evergreensolar.com/how/cleaning/

Crystalline and Polycrystalline Silicon PV Technology. (n.d.). Retrieved January 30, 2019, from http://astro1.panet.utoledo.edu/~relling2/teach/archives/6980.4400.2011/20110224_PHYS_6980_4400.pdf

Crystalline Silicon Photovoltaics Research. (n.d.). Retrieved February 11, 2019, from https://www.energy.gov/eere/solar/crystalline-silicon-photovoltaics-research

De Clercq, G. (25 June 2018). Europe's first solar panel recycling plant opens in France. Retrieved January 30, 2019, from https://www.reuters.com/article/us-solar-recycling/europes-first-solar-panel-recycling-plant-opens-in-france-idUSKBN1JL28Z

Definition of Alkali. (2019). Retrieved February 11, 2019, from https://www.dictionary.com/browse/alkali

Definition of Halogen. (2019). Retrieved February 11, 2019, from https://www.dictionary.com/browse/halogen

Definition of Precursor. (2019). Retrieved January 30, 2019, from https://www.dictionary.com/browse/precursor

Definition of Pyrolysis. (2019). Retrieved January 30, 2019, from https://www.dictionary.com/browse/pyrolysis

Delannoy, Y. (December 2012). Purification of silicon for photovoltaic applications. Retrieved January 30, 2019, from https://www.sciencedirect.com/science/article/pii/S0022024811010256

Diaz, A. C. & Batalle, J. A. (2013 – 2014). Energy Life Cycle Assessment (LCA) of silicon-based photovoltaic technologies and the influence of where it is manufactured and installed. Retrieved January 30, 2019, from http://diposit.ub.edu/dspace/bitstream/2445/57523/1/TFM_MERSE_AlejandroCalderon.pdf

Dixit, N. K., Agarwal, A., & Purohit, M. (May 2017). Silicon Wafer Technologies: Past & Future. Retrieved January 30, 2019, from https://www.ijraset.com/fileserve.php?FID=7748

Ecoregions of North America. (12 November 2016). Retrieved April, 8, 2019, from https://www.epa.gov/eco-research/ecoregions-north-america

Ecosystem Services and Playas of the Great Plains. (n.d.). Retrieved April 10, 2019, from http://rwbjv.org/wp-content/uploads/2015/02/Ecosystem-Services-and-Playas-by-Loren-Smith.pdf

Ecosystem Services from National Grasslands. (n.d.). Retrieved April 10, 2019, from https://www.fs.fed.us/grasslands/ecoservices/index.shtml

Electrical and EMC Insulation Materials and Heat Dissipation Materials for Solar Inverters. (n.d.). Retrieved March 1, 2019, from http://www.fabrico.com/sites/default/files/Import_0/Import/Fabrico_SolarInverters_ApplicationSheet.pdf

Energy Transformation Flow Chart Examples. (n.d.). Retrieved March 1, 2019, from https://wordpresshostingsignals.com/177318_energy_transformation_flow_chart_examples_new/

Erosion Control for Solar Farms. (2019). Retrieved January 30, 2019, from https://worldwindsolar.com/utility-scale-solar-services/erosion-control-solar-farms/

Espinosa, N., Serrano-Lujan, L., Urbina, A., & Krebs, F. C. (June 2015). Solutions and vapour deposited lead perovskite solar cells: Ecotoxicity from a life cycle assessment perspective. Retrieved January 30, 2019, from https://www.sciencedirect.com/science/article/pii/S0927024815000744

Evers, J. (20 March 2018). Erosion. Retrieved January 30, 2019, from https://www.nationalgeographic.org/encyclopedia/erosion/

Facts about the Environmental Impact of Gas Powered Lawn Mowers 2013. (2013). Retrieved February 11, 2019, from https://cleanairyardcare.ca/sustainability/environmental-facts/

Forest ecosystem products and services. (28 February 2017). Retrieved April 10, 2019, from https://www.nrcan.gc.ca/forests/canada/sustainable-forest-management/13177

Forest Inventory "Cheat Sheet." (n.d.). Retrieved April 10, 2019, from http://forestry.wsu.edu/wp-content/uploads/Inventory_Cheat_Sheet.pdf

Formisano, B. (18 December 2018). A Visual Guide to Fuses and How They Work. Retrieved January 30, 2019, from https://www.thespruce.com/home-fuse-box-how-they-work-1824667

Frisson, L., Lieten, K., Bruton, T., Declercq, K., Szlufcik, J., De Moor, H., Goris, M., Benali, A., & Aceves, O. (01-05 May 2000). Recent Improvements in Industrial PV Module Recycling. Retrieved January 30, 2019, from https://www.researchgate.net/profile/Jozef_Szlufcik/publication/228810136_Recent_improvements_in_industrial_PV_module_recycling/links/0c9605239447994b4e000000.pdf

Frisvold, G. B. & Marquez, T. (03 February 2014). Water Requirements for Large-Scale Solar Energy Projects in the West. Retrieved April 5, 2019, from https://onlinelibrary.wiley.com/doi/full/10.1111/j.1936-704X.2013.03156.x

Fthenakis, V. M., & Kim, H. C. (August 2011). Photovoltaics: Life-cycle analyses. *Solar Energy*, *85*(8), 1609–1628. Retrieved February 11, 2019, from https://www.sciencedirect.com/science/article/pii/S0038092X09002345?via%3Dihub

Fthenakis, V. M., Kim, H. C., & Alsema, E. (06 February 2008). Emissions from Photovoltaic Life Cycles. *Environmental Science & Technology*, *42*(6), 2168–2174. Retrieved February 11, 2019, from https://pubs.acs.org/doi/abs/10.1021/es071763q

Gao, P. (04 December 2016). Perovskites: crystal structure, important compounds properties. Retrieved February 11, 2019, from https://gmf.epfl.ch/wp-content/uploads/2018/10/Perovskites_crystal_structure_important_compounds_properties.pdf

Garcia-Valverde, R. Cherni, J. A., & Urbina, A. (15 April 2010). Life cycle analysis of organic photovoltaic technologies. Retrieved January 30, 2019, from https://onlinelibrary.wiley.com/doi/full/10.1002/pip.967

Geng, S. & Yu, A. (11 May 2011). Production of Polysilicon using a Modified Siemens Process. Retrieved January 30, 2019, from https://eng.umd.edu/~austin/enes489p/projects2011a/PolysiliconProcess-FinalReport.pdf

Gerbinet, S., Belboom, S., & Lifconard, A. (October 2014). Life Cycle Analysis (LCA) of photovoltaic panels: A review. *Renewable and Sustainable Energy Reviews*, *38*, 747–753. Retrieved February 11, 2019, from https://www.sciencedirect.com/science/article/pii/S136403211400495X?via%3Dihub

Global Market Insights. (14 June 2018). Thin Film Solar Cells Market to Grow at 16% CAGR From 2016 to 2024. Retrieved January 30, 2019, from https://solarmagazine.com/thin-film-solar-cells-market-to-grow-at-16-cagr-from-2016-to-2024/

Goliszewski, P. (n.d.). Renewable Resources – Alternative Energies. Retrieved January 30, 2019, from https://www.tes.com/lessons/KsVCzpvyg4Ha8w/renewable-resources-alternative-energies

Gong, J., Darling, S. B., & You, F. (2015). Perovskite photovoltaics: life-cycle assessment of energy and environmental impacts. Retrieved January 30, 2019, from https://pubs.rsc.org/en/content/articlelanding/2015/ee/c5ee00615e#!divAbstract

Granata, G., Pagnanelli, F., Moscardini, E., Havlik, T., & Toro, L. (April 2014). Recycling of photovoltaic panels by physical operations. Retrieved January 30, 2019, from https://www.sciencedirect.com/science/article/pii/S092702481400018X

Greenhouse Gases Equivalencies Calculator - Calculations and References. (18 December 2018). Retrieved April 10, 2019, from https://www.epa.gov/energy/greenhouse-gases-equivalencies-calculator-calculations-and-references

Guinée, J. B., Heijungs, R., Huppes, G., Zamagni, A., Masoni, P., Buonamici, R., Ekvall, T., & Rydberg, T. (02 September 2010) Life Cycle Assessment: Past, Present, and Future - Environmental Science & Technology (ACS Publications). Retrieved February 11, 2019, from https://pubs.acs.org/doi/10.1021/es101316v

Gupta, A. & Bais, A. S. (December 2016). Thin Film Solar Cells Market Size By Component (Cadmium Telluride (CDTE), Amorphous Silicon (A-Si), Copper Indium Gallium Diselenide), By Connectivity (On-Grid, Off Grid), By Application (Residential, Commercial, Utility), Industry Analysis Report, Regional Outlook (U.S., Canada, Mexico, UK, Germany, Spain, France, China, India, Japan, Australia, UAE, South Africa, Brazil, Chile, Argentina), Price Trends, Competitive Market Share & Forecast, 2016 – 2024. Retrieved March 9, 2019, from https://www.gminsights.com/industry-analysis/thin-film-solar-cells-market

Harambillet, B. (05 July 2018). Veolia opens the first European plant entirely dedicated to recycling photovoltaic panels. Retrieved January 30, 2019, from https://www.veolia.com/en/newsroom/news/recycling-photovoltaic-panels-circular-economy-france

Hemman, J. (06 April 2016). How halogen atoms compete to grow 'winning' perovskites. Retrieved January 30, 2019, from https://www.sciencedaily.com/releases/2016/04/160406133632.html

Hernandez, R. R., Easter, S. B., Murphy-Mariscal, M. L., Maestre, F. T., Tavassoli, M., Allen, E. B., Barrows, C. W., Belnap, J., Ochoa-Hueso, R., Ravi, S., & Allen, M. F. (January 2014). Environmental impacts of utility-scale solar energy. *Renewable and Sustainable Energy Reviews*, *29*, 766–779. Retrieved February 11, 2019, from https://www.sciencedirect.com/science/article/pii/S1364032113005819?via%3Dihub

Hernandez, R. R., Hoffacker, M. K., & Field, C. B. (18 December 2013). Land-Use Efficiency of Big Solar. Retrieved January 30, 2019, from https://pubs.acs.org/doi/10.1021/es4043726

Highwood, E. J. & Ryder, C. L. (28 June 2014). Radiative Effects of Dust. Retrieved January 30, 2019, from https://link.springer.com/chapter/10.1007/978-94-017-8978-3_11

History of Solar Timeline. (n.d.). Retrieved February 11, 2019, from https://www1.eere.energy.gov/solar/pdfs/solar_timeline.pdf

Hong, B. D. & Slatick, E. R. (August 1994). Carbon Dioxide Emissions Factors of Coal. Retrieved April 10, 2019, from https://www.eia.gov/coal/production/quarterly/co2_article/co2.html

How a Solar Cell Works. (n.d.). Retrieved February 11, 2019, from https://www.acs.org/content/acs/en/education/resources/highschool/chemmatters/past-issues/archive-2013-2014/how-a-solar-cell-works.html

Hsu, D. D., O'Donoughue, P., Fthenakis, V., Heath, G. A., Kim, H. C., Sawyer, P., Choi, J., & Turney, D. E. (19 March 2012). Life Cycle Greenhouse Gas Emissions of Crystalline Silicon Photovoltaic Electricity Generation. Retrieved January 30, 2019, from https://onlinelibrary.wiley.com/doi/full/10.1111/j.1530-9290.2011.00439.x

Ibn-Mohammed, T., Koh, S. C. L., Reaney, I. M., Acquaye, A., Schileo, G., Mustapha, K. B., & Greenough, R. (December 2017). Perovskite solar cells: An integrated hybrid lifecycle assessment and review in comparison with other photovoltaic technologies. Retrieved January 30, 2019, from https://www.sciencedirect.com/science/article/pii/S1364032117307311

Ireland, P. (13 August 2015). What You Need to Know About Ocean Acidification. Retrieved January 30, 2019, from https://www.nrdc.org/stories/what-you-need-know-about-ocean-acidification

ISO 14040: International Standard: Environmental management – Life cycle assessment – Principles and framework. (15 June 1997). Retrieved February 11, 2019, from https://web.stanford.edu/class/cee214/Readings/ISOLCA.pdf

ISO 14044: International Standard: Environmental management – Life cycle assessment – Requirements and guidelines. (01 July 2006). Retrieved February 11, 2019, from https://www.saiglobal.com/pdftemp/previews/osh/iso/updates2006/wk26/iso_14044-2006.pdf

Kadro, J. M., & Hagfeldt, A. (06 September 2017). The End-of-Life of Perovskite PV: Joule. Retrieved February 11, 2019, from https://www.cell.com/joule/fulltext/S2542-4351(17)30020-X

Kajal, P., Ghosh, K., & Powar, S. (January 2018). Manufacturing Techniques of Perovskite Solar Cells. Retrieved January 30, 2019, from https://www.researchgate.net/publication/321396151_Manufacturing_Techniques_of_Perovskite_Solar_Cells

Kang, S., Yoo, S., Lee, J., Boo, B., & Ryu, H. (November 2012). Experimental investigations for recycling of silicon and glass from waste photovoltaic modules. Retrieved January 3, 2019, from https://www.sciencedirect.com/science/article/pii/S0960148112002716

Kim, B., Lee, J., Kim, K., & Hur, T. (January 2014). Evaluation of the environmental performance of sc-Si and mc-Si PV systems in Korea. Retrieved January 30, 2019, from https://www.sciencedirect.com/science/article/pii/S0038092X13004684

Kok, J. F., Ward, D. S., & Mahowald, N. M. (December 2016). Estimation of the dust-climate feedback. Retrieved January 30, 2019, from http://adsabs.harvard.edu/abs/2016AGUFM.A33G0320K

Kok, J. F., Ward, D. S., Mahowald, N. M., & Evan, A. T. (16 January 2018). Global and regional importance of the direct dust-climate feedback. Retrieved January 30, 2019, from https://www.nature.com/articles/s41467-017-02620-y

Krause, M. B. (14 April 2014). Do You Wash Your Solar Modules Often Enough? Retrieved January 30, 2019, from https://www.greentechmedia.com/articles/read/do-you-wash-your-solar-modules-often-enough#gs.02wiq7

Lab to fab. (n.d.). Retrieved April 8, 2019, from https://www.oxfordpv.com

Land Use Efficiency. (n.d.). Retrieved January 30, 2019, from http://webservices.itcs.umich.edu/drupal/recd/?q=node/105

Latunussa, C. E. L., Ardente, F., Blengini, G. A., & Mancini, L. (November 2016). Life Cycle Assessment of an innovative recycling process for crystalline silicon photovoltaic panels. *Solar Energy Materials and Solar Cells*, *156*, 101–111. Retrieved February 11, 2019, from https://www.sciencedirect.com/science/article/pii/S0927024816001227?via%3Dihub

Leccisi, E., Raugei, M. & Fthenakis, V. (26 May 2016). The Energy and Environmental Performance of Ground-Mounted Photovoltaic Systems - A Timely Update. Retrieved January 30, 2019, from https://www.mdpi.com/1996-1073/9/8/622

Li, F., Tangstad, M., & Ringdalen, E. (12 February 2018). Carbothermal Reduction of Quartz and Carbon Pellets at Elevated Temperatures. *Metallurgical and Materials Transactions B*, *49*(3), 1078–1088. Retrieved February 11, 2019, from https://link.springer.com/article/10.1007%2Fs11663-018-1195-x

Liu, Z. (2016). Global Energy Interconnection. Retrieved January 30, 2019, from https://www.sciencedirect.com/book/9780128044056/global-energy-interconnection

Maghami, M. R., Hizam, H., Gomes, C., Radzi, M. A., Rezadad, M. I., & Hajighorbani, S. (June 2016). Power loss due to soiling on solar panel: A review. Retrieved January 30, 2019, from https://www.sciencedirect.com/science/article/pii/S1364032116000745

Mann, S. A., de Wild-Scholten, M. J., Fthenakis, V. M., van Sark, W. G. J. H. M., & Sinke, W. C. (11 February 2013). The energy payback time of advance crystalline silicon PV modules in 2020: a prospective study. Retrieved January 30, 2019, from https://onlinelibrary.wiley.com/doi/full/10.1002/pip.2363

Marsh, J. (30 August 2018). Recycling solar panels in 2018. Retrieved January 30, 2019, from https://news.energysage.com/recycling-solar-panels/

Marsh, J. (21 January 2019). Perovskite solar cells: the future of solar? Retrieved January 30, 2019, from https://news.energysage.com/perovskite-solar-cells/

Martorano, M. A., Neto, J. B. F., Oliveira, T. S., & Tsubaki, T. O. (25 February 2011). Refining of metallurgical silicon by directional solidification. *Materials Science and Engineering: B*, *176*(3), 217–226. Retrieved February 11, 2019, from https://www.sciencedirect.com/science/article/pii/S0921510710006495?via%3Dihub

Mason, J. E., Fthenakis, V. M., & Kim, H. C. (28 September 2005). Energy Payback and Life-cycle CO2 Emissions of the BOS in an Optimized 3.5 MW PV Installation. Retrieved April 5, 2019, from https://onlinelibrary.wiley.com/doi/epdf/10.1002/pip.652

Matasci, S. (29 January 2019). Ground mount solar for your home. Retrieved March 1, 2019, from https://news.energysage.com/ground-mounted-solar-panels-top-3-things-you-need-to-know/

Matasci, S. (02 January 2019). Health & Environmental Benefits of Solar Energy. Retrieved April 10, 2019, from https://news.energysage.com/health-environmental-benefits-of-solar-energy/

McKenzie, R. H. (October 2010). Agricultural Soil Compaction: Causes and Management. Retrieved January 30, 2019, from https://www1.agric.gov.ab.ca/$department/deptdocs.nsf/all/agdex13331

Mineral Data Publishing: Perovskite. (2001-2005). Retrieved from http://www.handbookofmineralogy.org/pdfs/perovskite.pdf

Monger, H. (01 April 2009). Desert Soils: Ecosystem Services and Human Impacts. Retrieved April 10, 2019, from https://portal.nifa.usda.gov/web/crisprojectpages/0217661-desert-soils-ecosystem-services-and-human-impacts.html

Nace, T. (27 November 2017). Scientists Discover “Miracle” Mineral That Could Make Internet 1,000-times Faster. Retrieved February 11, 2019, from https://www.forbes.com/sites/trevornace/2017/11/27/scientists-discover-miracle-mineral-that-could-make-internet-1000-times-faster/#51e894b97f45

Nawaz, I. & Tiwari, G. N. (November 2006). Embodied energy analysis of photovoltaic (PV) system based on macro- and micro-level. Retrieved January 30, 2019, from https://www.sciencedirect.com/science/article/pii/S0301421505001680

Net Metering. (2019). Retrieved January 30, 2019, from https://www.seia.org/initiatives/net-metering

NOAA. (28 June 2018). What is eutrophication? Retrieved January 30, 2019, from https://oceanservice.noaa.gov/facts/eutrophication.html

Parida, B., Iniyan, S., & Goic, R. (April 2011). A review of solar photovoltaic technologies. *Renewable and Sustainable Energy Reviews*, *15*(3), 1625–1636. Retrieved February 11, 2019, from https://www.sciencedirect.com/science/article/pii/S1364032110004016?via%3Dihub

Peng, J., Lu, L., & Yang, H. (March 2013). Review on life cycle assessment of energy payback and greenhouse gas emission of solar photovoltaic systems. *Renewable and Sustainable Energy Reviews*, *19*, 255–274. Retrieved February 11, 2019, from https://www.sciencedirect.com/science/article/pii/S1364032112006478?via%3Dihub

Perlman, H. (02 December 2016). Runoff (surface water runoff). Retrieved January 30, 2019, from https://water.usgs.gov/edu/runoff.html

Perovskites and Perovskites Solar Cells: An Introduction. (n.d.). Retrieved January 30, 2019, from https://www.ossila.com/pages/perovskites-and-perovskite-solar-cells-an-introduction

Perovskite Solar Cell | Clean Energy Institute. (2019). Retrieved February 11, 2019, from https://www.cei.washington.edu/education/science-of-solar/perovskite-solar-cell/

Perovskite Solar Cells. (n.d.). Retrieved January 30, 2019, from https://www.energy.gov/eere/solar/perovskite-solar-cells

Perovskite Solar Cells. (n.d.). Retrieved January 30, 2019, from https://www.nrel.gov/pv/perovskite-solar-cells.html

Perovskite Solar Cells Fabrication Guide using I101 Perovskite Precursor Ink. (n.d.). Retrieved January 30, 2019, from https://www.ossila.com/pages/perovskite-solar-cells-fabrication-guide-using-i101-perovskite-precursor-ink

Philipps, D. S., Ise, F., Warmuth, W., Conferences, P., & GmbH, C. (27 August 2018). Photovoltaics Report, 47. Retrieved February 11, 2019, from https://www.ise.fraunhofer.de/content/dam/ise/de/documents/publications/studies/Photovoltaics-Report.pdf

Photovoltaics Manufacturing, Polysilicon | Solar Power. (2016). Retrieved February 11, 2019, from http://www.greenrhinoenergy.com/solar/technologies/pv_manufacturing.php

PV FAQS. (January 2004). Retrieved January 30, 2019, from https://www.nrel.gov/docs/fy04osti/35489.pdf

Pyrolysis. (n.d.). Retrieved January 30, 2019, from https://www.britannica.com/science/pyrolysis

Raghavan, S., Avasthi, S., Muralidharan, R., & Ramamurthy, P. C. (2018). Perovskite-like Solar Cells. Retrieved January 30, 2019, from http://www.cense.iisc.ac.in/research/solar-cells

Razza, S., Castro-Hermosa, S. A., Di Carlo, A., & Brown, T. (September 2016). Research Update: Large-area deposition, coating, printing, and processing techniques for the upscaling of perovskite solar cell technology. Retrieved January 30, 2019, from https://www.researchgate.net/publication/308345115_Research_Update_Large-area_deposition_coating_printing_and_processing_techniques_for_the_upscaling_of_perovskite_solar_cell_technology

Roos, C., Nelson, M., & Brockman, K. (October 2009). Solar Electric System Design, Operation and Installation. Retrieved January 30, 2019, from http://www.energy.wsu.edu/Documents/SolarPVforBuildersOct2009.pdf

Safarian, J., Tranell, G., & Tangstad, M. (2012). Processes for Upgrading Metallurgical Grade Silicon to Solar Grade Silicon. *Energy Procedia*, *20*, 88–97. Retrieved February 11, 2019, from https://www.sciencedirect.com/science/article/pii/S1876610212007412?via%3Dihub

Sarialtin, H. & Zafer, C. (December 2016). Life Cycle Assessment of Perovskite Solar Cells. Retrieved January 30, 2019, from https://www.researchgate.net/publication/309760432_Life_Cycle_Assessment_of_Perovskite_Solar_Cells

Schildgen, B. (21 March 2016). How much carbon do trees really store? Retrieved April 10, 2019, from https://www.sierraclub.org/sierra/2016-2-march-april/ask-mr-green/how-much-carbon-do-trees-really-store

Scott, A. (12 September 2018). Deeper understanding of perovskite formation. Retrieved February 11, 2019, from https://www.natureasia.com/en/nmiddleeast/article/10.1038/nmiddleeast.2018.107

Silica | Definition & Facts. (2019). Retrieved February 11, 2019, from https://www.britannica.com/science/silica

Smalley, J. (30 June 2015). What is a combiner box? Retrieved January 30, 2019, from https://www.solarpowerworldonline.com/2015/06/what-is-a-combiner-box/

Smith, C., & Barron, A. R. (21 May 2013) Synthesis and Purification of Bulk Semiconductors. Retrieved February 11, 2019, from https://cnx.org/contents/Q8JC6j42@7/Synthesis-and-Purification-of-Bulk-Semiconductors

Solar energy. (n.d.). Retrieved January 30, 2019, from https://www.iea.org/topics/renewables/solar/

Solar Industry Research Data. (2019). Retrieved February 11, 2019, from https://www.seia.org/solar-industry-research-data

Solar Maps. (2016). Retrieved April 8, 2019, from https://www.nrel.gov/gis/solar.html

Solar panel cleaning: what you should know. (28 February 2019). Retrieved March 1, 2019, from https://www.energysage.com/solar/solar-operations-and-maintenance/cleaning-your-solar-panels/

Sovacool, B. K. & Dworkin, M. H. (28 January 2015). Energy justice: Conceptual insights and practical applications. Retrieved April 10, 2019, from https://www.sciencedirect.com/science/article/pii/S0306261915000082

Srivastava, H. (August 2016). Crystalline Silicon PV Market by Type (Mono-Crystalline and Multi-Crystalline) and End-User (Residential and Commercial, Utility-Scale) - Global Opportunity Analysis and Industry Forecasts, 2014 - 2022. Retrieved February 11, 2019, from https://www.alliedmarketresearch.com/crystalline-silicon-photovoltaic-pv-market

Steel - Raw Materials. (2019). Retrieved February 11, 2019, from http://science.jrank.org/pages/6483/Steel-Raw-materials.html

Stehouwer, R. (15 September 2010). Lead in Residential Soils: Sources, Testing, and Reducing Exposure. Retrieved April 5, 2019, from https://extension.psu.edu/lead-in-residential-soils-sources-testing-and-reducing-exposure

Takiguchi, H. (27 April 2011). Global Flow Analysis of Crystalline Silicon. *Crystalline Silicon - Properties and Uses*. Retrieved February 11, 2019, from https://www.intechopen.com/books/crystalline-silicon-properties-and-uses/global-flow-analysis-of-crystalline-silicon

Taylor, N. T., Davis, K. M. D., Abad, H., McClung, M. R., & Moran, M. D. (October 2017). Ecosystem services of the Big Bend region of the Chiuanhuan Desert. Retrieved April 10, 2019, from https://www.sciencedirect.com/science/article/pii/S2212041617301869?via%3Dihub

Tress, W., Marinova, N., Inganas, O., Nazeeruddin, M. K., Zakeeruddin, S. M., & Graetzel, M. (08-13 June 2014). The role of the hole-transport layer in perovskite solar cells - reducing recombination and increasing absorption. Retrieved January 30, 2019, from https://ieeexplore.ieee.org/document/6925216/authors#authors

Tsao, J. (18 November 2016). Recycling Perovskite Solar Cells. Retrieved March 1, 2019, from https://greenchemuoft.wordpress.com/2016/11/18/recycling-perovskite-solar-cells/

Turconi, R., Boldrin, A., & Astrup, T. (December 2013). Life cycle assessment (LCA) of electricity generation technologies: Overview, comparability and limitations. *Renewable and Sustainable Energy Reviews*, *28*, 555–565. Retrieved February 11, 2019, from https://www.sciencedirect.com/science/article/pii/S1364032113005534?via%3Dihub

Understanding Global Warming Potentials. (14 February 2017). Retrieved January 30, 2019, from https://www.epa.gov/ghgemissions/understanding-global-warming-potentials

Uecker, R. (September 2014). The historical development of the Czochralski method. Retrieved February 11, 2019, from https://www.sciencedirect.com/science/article/pii/S0022024813008579

Uptmor, K. (n.d.). Cation & Anion Hydrolysis. Retrieved February 11, 2019, from http://study.com/academy/lesson/cation-anion-hydrolysis.html

U.S. Solar Market Insight. (13 December 2018). Retrieved January 30, 2019, from https://www.seia.org/us-solar-market-insight

Utility Scale Solar Farms in Wisconsin. (2018). Retrieved March 1, 2019, from https://www.renewwisconsin.org/solarfarms/

Utility-scale solar panel installations. (28 February 2019). Retrieved March 1, 2019, from https://www.energysage.com/solar/101/types-solar-installations/utility-scale-solar/

Utility-Scale Solar Photovoltaic Power Plants: A Project Developer's Guide (2015). Retrieved February 11, 2019, from https://www.ifc.org/wps/wcm/connect/f05d3e00498e0841bb6fbbe54d141794/IFC+Solar+Report_Web+_08+05.pdf?MOD=AJPERES

Vatalis, K. I., Charalambides, G., & Benetis, N. P. (2015). Market of High Purity Quartz Innovative Applications. *Procedia Economics and Finance*, *24*, 734–742. Retrieved February 11, 2019, from https://www.sciencedirect.com/science/article/pii/S2212567115006887?via%3Dihub

Vegetation. (2019). Retrieved January 30, 2019, from https://www.fecon.com/forestry/applications/vegetation-management/

Wander, M. (n.d.). Lead in Soils. Retrieved April 5, 2019, from https://web.extension.illinois.edu/bdo/downloads/24293.pdf

Water Use Management. (n.d.). Retrieved January 30, 2019, from https://www.seia.org/initiatives/water-use-management

Weckend, S., Wade, A., & Heath, G. (June 2016). End-of-Life Management: Solar Photovoltaic Panels. Retrieved January 30, 2019, from http://iea-pvps.org/fileadmin/dam/public/report/technical/IRENA_IEAPVPS_End-of-Life_Solar_PV_Panels_2016.pdf

Wesoff, E. (01 December 2015). The Mercifully Short List of Fallen Solar Companies: 2015 Edition. Retrieved January 30, 2019, from https://www.greentechmedia.com/articles/read/the-mercifully-short-list-of-fallen-solar-companies-2015-edition#gs.0iwh5d

What is Photovoltaic (PV) Wire? (2018). Retrieved January 30, 2019, from https://www.anixter.com/en_us/resources/literature/wire-wisdom/pv-wire.html

What is U.S. electricity generation by energy source? (01 March 2019). Retrieved March 9, 2019, from https://www.eia.gov/tools/faqs/faq.php?id=427&t=3

Why Clean Solar Panels? (n.d.). Retrieved January 30, 2019, from http://www.solar-panel-cleaners.com/why-clean-solar-panels

Winckler, G. (17 June 2010). Dust and its Impact on Earth's Climate System. Retrieved January 30,2019, from https://blogs.ei.columbia.edu/2010/06/17/dust-and-its-impact-on-earths-climate-system/

Wolkowski, R. & Lowery, B. (May 2008). Soil compaction: Causes, concerns, and cures. Retrieved January 30, 2019, from https://www.soils.wisc.edu/extension/pubs/A3367.pdf

Wu, W. (2017). Inorganic nanomaterials for printed electronics: a review. Retrieved January 30, 2019, from https://pubs.rsc.org/en/content/articlelanding/2017/nr/c7nr01604b/unauth#!divAbstract

Ydstie, B. E. & Du, J. (02 November 2011). Producing Poly-Silicon from Silane in a Fluidized Bed Reactor. Retrieved January 30, 2019, from https://www.intechopen.com/books/solar-cells-silicon-wafer-based-technologies/producing-poly-silicon-from-silane-in-a-fluidized-bed-reactor

Zadde, V. V., Pinov, A. B., Strebkov, D. S., Belov, E. P., Efimov, N. K., Lebedev, E. N., Korobkov, E. I. , Blake, D., & Touryan, K. (August 2002). New method for solar grade silicon production. Retrieved February 15, 2019, from https://www.nrel.gov/docs/fy02osti/35650.pdf

Zhou, Z. & Carbajales-Dale, M. (16 January 2018). Assessing the photovoltaic technology landscape: efficiency and energy return on investment (EORI). Retrieved April 8, 2019, from https://pubs.rsc.org/en/content/articlepdf/2018/ee/c7ee01806a

Zientara, B. (n.d.). Solar Panel Maintenance for Every Weather. Retrieved January 30, 2019, from https://www.solarpowerrocks.com/solar-questions/kind-maintenance-solar-panels-require/

Zuo, C., Vak, D., Angmo, D., Ding, L., & Gao, M. (April 2018). One-step roll-to-roll air processed high efficiency perovskite solar cells. Retrieved January 30, 2019, from https://www.sciencedirect.com/science/article/pii/S2211285518300454?via%3Dihub

Appendix I
Energy Requirements for Crystalline Silicon PV Production (Embodied Energy)

Note, I converted all energy calculations to kWh / m^2 for comparison purposes.

Alsema & Nieuwlaar (2000) calculated energy requirements for modules production on a step by step basis, the results are as follows.

- Estimated energy requirements for Siemens Process:

$$\frac{2200\ \text{MJ}}{1\ m^2\ \text{module material}} \times \frac{0.277778\ \text{kWh}}{1\ \text{MJ}} = \sim \frac{611\ \text{kWh}}{1\ m^2}$$

- Estimated energy requirements for the Czochralski Method:

$$\frac{1000\ \text{MJ}}{1\ m^2} \times \frac{0.277778\ \text{kWh}}{1\ \text{MJ}} = \sim \frac{278\ \text{kWh}}{1\ m^2}$$

- Estimated energy requirements for further module production:

$$\frac{1000\ \text{MJ}}{1\ m^2} \times \frac{0.277778\ \text{kWh}}{1\ \text{MJ}} = \sim \frac{278\ \text{kWh}}{1\ m^2}$$

- Estimated energy requirements for aluminum frame:

$$\frac{400\ \text{MJ}}{1\ m^2} \times \frac{0.277778\ \text{kWh}}{1\ \text{MJ}} = \sim \frac{111\ \text{kWh}}{1\ m^2}$$

- **Total** estimated embodied energy for crystalline silicon module manufacturing:

$$\frac{611\ \text{kWh}}{1\ m^2} + \frac{278\ \text{kWh}}{1\ m^2} + \frac{278\ \text{kWh}}{1\ m^2} + \frac{111\ \text{kWh}}{1\ m^2} = \mathbf{\frac{1278\ kWh}{1\ m^2}}$$

The National Renewable Energy Laboratory (NREL) conducted their own LCA of photovoltaics, resulting in information regarding embodied energy and EPBT. The results are as follows.

- **Total** embodied energy of crystalline silicon PV ranges from,

$$\mathbf{\frac{420\ kWh}{1\ m^2}\ to\ \frac{600\ kWh}{1\ m^2}}$$

- From PV FAQS (2004)

Nawaz & Tiwari (2006) calculated the energy requirements for crystalline silicon PV as well, the results as follows:

- **Estimated silicon material required for module production (this ratio is used for further calculations):**

$$\mathbf{\frac{0.724\ kg\ silicon}{1\ m^2\ PV\ module}}$$

- Estimated energy requirements for smelting to MG silicon:

$$\frac{20\ \text{kWh}}{1\ \text{kg MG-Si}} \times \frac{0.724\ \text{kg Si}}{1\ m^2} = \frac{14.48\ \text{kWh}}{1\ m^2}$$

- Estimated energy requirements for modified Siemens Process:

$$\frac{100\ \text{kWh}}{1\ \text{kg silicon}} \times \frac{0.724\ \text{kg Si}}{1\ m^2} = \frac{72.4\ \text{kWh}}{1\ m^2}$$

- Estimated energy requirements for Czochralski Method:

$$\frac{290\ \text{kWh}}{1\ \text{kg silicon}} \times \frac{0.724\ \text{kg Si}}{1\ m^2} = \frac{209.96\ \text{kWh}}{1\ m^2}$$

- Estimated energy requirements for further manufacturing processes:

$$\frac{190\ \text{kWh}}{1\ \text{m}^2\ \text{module material}}$$

- **Total** estimated embodied energy for crystalline silicon module manufacturing:

$$\frac{14.48\ \text{kWh}}{1\ \text{m}^2} + \frac{72.4\ \text{kWh}}{1\ \text{m}^2} + \frac{209.96\ \text{kWh}}{1\ \text{m}^2} + \frac{190\ \text{kWh}}{1\ \text{m}^2} = \mathbf{\frac{486.84\ \text{kWh}}{1\ \text{m}^2}}$$

Mann et al. (2013) contacted solar cell manufacturers to gather information on the embodied energy at each stage of the crystalline silicon PV production process, the results are as follows:

- Estimated energy requirements for modified Siemens Process:

$$\frac{545\ \text{MJp}}{1\ \text{kg silicon}} \times \frac{0.277778\ \text{kWh}}{1\ \text{MJ}} = \frac{151.389\ \text{kWh}}{1\ \text{kg Si}} \times \frac{0.724\ \text{kg Si}}{1\ \text{m}^2} = \frac{152.113\ \text{kWh}}{1\ \text{m}^2}$$

- Estimated energy requirements for Czochralski Method:

$$\frac{85.6\ \text{kWh}}{1\ \text{kg silicon}} \times \frac{0.724\ \text{kg Si}}{1\ \text{m}^2} = \frac{61.974\ \text{kWh}}{1\ \text{m}^2}$$

- Estimated energy requirements for manufacturing of complete solar module (including wafering, cell processing, and module encapsulation):

  Wafering:

$$\frac{51.4\ \text{kWh}}{1\ \text{m}^2\ \text{selected material}}$$

  Cell processing:

$$\frac{44.5\ \text{MJp}}{1\ \text{m}^2\ \text{selected material}} \times \frac{0.277778\ \text{kWh}}{1\ \text{MJ}} = \frac{12.36\ \text{kWh}}{1\ \text{m}^2\ \text{selected material}}$$

  Encapsulation:

$$\frac{66.7\ \text{MJp}}{1\ \text{m}^2\ \text{selected material}} \times \frac{0.277778\ \text{kWh}}{1\ \text{MJ}} = \frac{18.5278\ \text{kWh}}{1\ \text{m}^2\ \text{selected material}}$$

  Total for this section:

$$\frac{51.4\ \text{kWh}}{1\ \text{m}^2} + \frac{12.36\ \text{kWh}}{1\ \text{m}^2} + \frac{18.5278\ \text{kWh}}{1\ \text{m}^2} = \frac{82.2878\ \text{kWh}}{1\ \text{m}^2}$$

- **Total** estimate embodied energy for crystalline silicon PV manufacturing:

$$\frac{152.113\ \text{kWh}}{1\ \text{m}^2} + \frac{61.974\ \text{kWh}}{1\ \text{m}^2} + \frac{82.2878\ \text{kWh}}{1\ \text{m}^2} = \mathbf{\frac{296.3748\ \text{kWh}}{1\ \text{m}^2}}$$

Diaz, A. C. & Batalle, J. A. (2013-2014) calculated embodied energy using data from previously conducted LCAs. This article provides a range for energy requirements at each stage of production, the results are as follows.

- Estimated energy requirements for the Siemens Process:

  728 to 2397 MJ / m^2 (convert each to kWh for comparison of range)

$$\frac{728\ \text{MJ}}{1\ \text{m}^2} \times \frac{0.277778\ \text{kWh}}{1\ \text{MJ}} = \frac{202.2\ \text{kWh}}{1\ \text{m}^2}$$

$$\frac{2397\ \text{MJ}}{1\ \text{m}^2} \times \frac{0.277778\ \text{kWh}}{1\ \text{MJ}} = \frac{665.8\ \text{kWh}}{1\ \text{m}^2}$$

  NEW range: 202 to 666 kWh / m^2

- Estimated energy requirements for the Czochralski Method:

  432 to 2391 MJ / m^2 (convert)

$$\frac{432\ \text{MJ}}{1\ \text{m}^2} \times \frac{0.277778\ \text{kWh}}{1\ \text{MJ}} = \frac{120\ \text{kWh}}{1\ \text{m}^2}$$

$$\frac{2391\ MJ}{1\ m^2} \times \frac{0.277778\ kWh}{1\ MJ} = \frac{664.2\ kWh}{1\ m^2}$$

NEW range: 120 to 664 kWh / m^2

- Estimated energy requirements for further module production:

  684 to 1623 MJ / m^2 (convert)

  $$\frac{684\ MJ}{1\ m^2} \times \frac{0.277778\ kWh}{1\ MJ} = \frac{190\ kWh}{1\ m^2}$$

  $$\frac{1623\ MJ}{1\ m^2} \times \frac{0.277778\ kWh}{1\ MJ} = \frac{450.8\ kWh}{1\ m^2}$$

  NEW range: 190 to 451 kWh / m^2

- Estimated energy requirements for the aluminum frame:

  $$\frac{236\ MJ}{1\ m^2} \times \frac{0.277778\ kWh}{1\ MJ} = \frac{65.6\ kWh}{1\ m^2}$$

- **Total** range estimated embodied energy for crystalline silicon PV manufacturing:

  $$\frac{202.2\ kWh}{1\ m^2} + \frac{120\ kWh}{1\ m^2} + \frac{190\ kWh}{1\ m^2} + \frac{65.6\ kWh}{1\ m^2} = \frac{577.8\ kWh}{1\ m^2}$$

  $$\frac{665.8\ kWh}{1\ m^2} + \frac{664.2\ kWh}{1\ m^2} + \frac{450.8\ kWh}{1\ m^2} + \frac{65.6\ kWh}{1\ m^2} = \frac{1846.4\ kWh}{1\ m^2}$$

  $\frac{577.8\ kWh}{1\ m^2}$ to $\frac{1846.4\ kWh}{1\ m^2}$

Kim et al. (2014) calculated a range of energy requirements for the production of crystalline silicon PV modules.

- Total energy required for manufacturing ranges from, $\frac{123.1\ MJ}{1\ kg\ Si}$ to $\frac{518.4\ MJ}{1\ kg\ Si}$
- Convert to kWh / m^2

  $$\frac{123.1\ MJ}{1\ kg\ Si} \times \frac{0.724\ kg\ Si}{1\ m^2} \times \frac{0.277778\ kWh}{1\ MJ} = \frac{24.76\ kWh}{1\ m^2}$$

  $$\frac{518.4\ MJ}{1\ kg\ Si} \times \frac{0.724\ kg\ Si}{1\ m^2} \times \frac{0.277778\ kWh}{1\ MJ} = \frac{104.26\ kWh}{1\ m^2}$$

- **Total** range estimated embodied energy for crystalline silicon PV manufacturing:

  $\frac{24.76\ kWh}{1\ m^2}$ to $\frac{104.26\ kWh}{1\ m^2}$

As you can see, over the years, the energy requirements for crystalline silicon PV production have decreased drastically. These changes result following technological innovations in manufacturing, material processing, and so on. Table 4 on the following page is from the impact category sections.

Table 5: Energy Requirements for Crystalline Silicon PV Manufacturing (Embodied Energy)

Source	Carbon Smelting	Siemens Process	Czochralski Method	Further Manufacture Methods	Metal Frame	Total
Alsema & Nieuwlaar (2000)		~611 kWh / 1 m^2	~ 278 kWh / 1 m^2	~ 278 kWh / 1 m^2	~111 kWh / 1 m^2	~1278 kWh / 1 m^2
NREL's PV FAQS (2004)						~ 420 kWh / 1 m^2 to ~ 600 kWh / 1 m^2
Nawaz & Tiwari (2006)	~15 kWh / 1 m^2	~ 72 kWh / 1 m^2	~ 210 kWh / 1 m^2	~ 190 kWh / 1 m^2		~ 487 kWh / 1 m^2
Mann et al. (2013)		~152 kWh / 1 m^2	~ 62 kWh / 1 m^2	~ 82 kWh / 1 m^2		~ 296 kWh / 1 m^2
Diaz & Batalle (2013-2014) RANGE		~202 kWh / 1 m^2 to ~666 kWh / 1 m^2	~ 120 kWh / 1 m^2 to ~ 664 kWh / 1 m^2	~ 190 kWh / 1 m^2 to ~ 451 kWh / 1 m^2	~ 66 kWh / 1 m^2	~ 578 kWh / 1 m^2 to ~1846 kWh / 1 m^2
Kim et al. (2014)						~ 25 kWh / 1 m^2 to ~ 104 kWh / 1 m^2

To find an average embodied energy value, I eliminated the outliers from the following sources; Alsema & Nieuwlaar (2000), Diaz & Batalle (2013 – 2014), and Kim et al. (2014). This left me with information from four sources, NREL's PV FAQS (2004), Nawaz & Tiwari (2006), and Mann et al. (2013). My calculation is as follows

$$\frac{420\ \text{kWh}}{1\ \text{m}^2} + \frac{600\ \text{kWh}}{1\ \text{m}^2} + \frac{487\ \text{kWh}}{1\ \text{m}^2} + \frac{296\ \text{kWh}}{1\ \text{m}^2} = \frac{1803\ \text{kWh}}{1\ \text{m}^2}$$

$$\frac{1803\ \text{kWh} / 1\ \text{m}^2}{4} = \frac{450.75\ \text{kWh}}{1\ \text{m}^2}$$ average embodied energy for crystalline silicon PV

Appendix II
Energy Requirements for Perovskite PV Production (Embodied Energy)

Note, I converted all energy calculations to kWh / m^2 for comparison purposes.

Celik et al. (2016) used a similar research and comparative analysis as this study to compile data on the life cycle impacts associated with perovskite solar cells. The results are as follows.

- Solution processed perovskite cells had a **total** average energy requirement of,
  $\frac{665\ MJ}{1\ m^2} \times \frac{0.277778\ kWh}{1\ MJ} = \mathbf{\frac{184.72\ kWh}{1\ m^2}}$
- The authors also found a range of energy requirements within the EcoInvent database.
  $\frac{59\ MJ}{1\ m^2}$ to $\frac{484\ MJ}{1\ m^2}$
- Convert the range
  $\frac{59\ MJ}{1\ m^2} \times \frac{0.277778\ kWh}{1\ MJ} = \frac{16.39\ kWh}{1\ m^2}$
  $\frac{484\ MJ}{1\ m^2} \times \frac{0.277778\ kWh}{1\ MJ} = \frac{134.44\ kWh}{1\ m^2}$
- **New range:**
  $\frac{16.4\ kWh}{1\ m^2}$ to $\frac{134.4\ kWh}{1\ m^2}$

Ibn-Mohammed et al. (2017) assessed the embodied energy associated with perovskite solar cells through two different manufacturing methods, vapor deposition and spin coating, and the different raw materials for each. The results are as follows.

- Estimated energy requirements for vapor deposited perovskite PV:
  - Energy previously embedded in materials:
    $\frac{1.9\ MJ}{1\ m^2} \times \frac{0.277778\ kWh}{1\ MJ} = \frac{97.2\ kWh}{1\ m^2}$
  - Vapor deposition energy requirements (including ultrasonic cleaning, screen printing, etc.):
    $\frac{220.47\ MJ}{1\ m^2} \times \frac{0.277778\ kWh}{1\ MJ} = \frac{61.242\ kWh}{1\ m^2}$
    - Perovskite layer vapor deposition energy requirements account for 4.34 kWh of this 61.2 kWh
  - **Total** energy required for vapor deposited perovskite PV:
    $\frac{570.37\ MJ}{1\ m^2} \times \frac{0.277778\ kWh}{1\ MJ} = \mathbf{\frac{158.44\ kWh}{1\ m^2}}$
- Estimated energy requirements for spin coated perovskite PV:
  - Energy previously embedded in materials:
    $\frac{237.76J}{1\ m^2} \times \frac{0.277778\ kWh}{1\ MJ} = \frac{66.04\ kWh}{1\ m^2}$
  - Spin coating deposition energy requirements:
    $\frac{98.81\ MJ}{1\ m^2} \times \frac{0.277778\ kWh}{1\ MJ} = \frac{27.45\ kWh}{1\ m^2}$
    - ETL deposition energy requirements account for 3.31 kWh of 27.5 kWh

        - Semiconductor layer deposition energy requirements account for 1.64 kWh of 27.5 kWh
        - HTL and perovskite layer deposition energy requirements account for 0.8 kWh of 27.5 kWh
    - **Total** energy required for spin coated perovskite PV:
      $\frac{336.56\ MJ}{1\ m^2} \times \frac{0.277778\ kWh}{1\ MJ} = \mathbf{\frac{93.49\ kWh}{1\ m^2}}$
- According to this source, depending on the manufacturing process selected, embodied energy for perovskite PV can range from: **$\frac{93.5\ kWh}{1\ m^2}$ to $\frac{158.4\ kWh}{1\ m^2}$**

Table 7: Energy Requirements for Perovskite PV Manufacturing (Embodied Energy)

Source	**Manufacturing Process Analyzed**	**Material Embodied Energy**	**Deposition Energy Requirements**	**Total Embodied Energy**
Celik et al. (2016)	Solution Processing	-	-	~ $\frac{184.72\ kWh}{1\ m^2}$
Celik et al. (2016) RANGE from EcoInvent Database	Solution Processing	-	-	~ $\frac{16.4\ kWh}{1\ m^2}$ to ~ $\frac{134.4\ kWh}{1\ m^2}$
Ibn-Mohammed et al. (2017)	Vapor Deposition	$\frac{97.2\ kWh}{1\ m^2}$	$\frac{61.24\ kWh}{1\ m^2}$	~ $\frac{158.4\ kWh}{1\ m^2}$
Ibn-Mohammed et al. (2017)	Spin Coating	$\frac{66.04\ kWh}{1\ m^2}$	$\frac{27.45\ kWh}{1\ m^2}$	~ $\frac{93.5\ kWh}{1\ m^2}$

From these values, I calculated the average embodied energy of perovskite PV. The results are as follows.

$$\frac{184.72\ kWh}{1\ m^2} + \frac{16.4\ kWh}{1\ m^2} + \frac{134.4\ kWh}{1\ m^2} + \frac{158.4\ kWh}{1\ m^2} + \frac{93.5\ kWh}{1\ m^2} = \frac{587.42\ kWh}{1\ m^2}$$

$$\frac{587.42\ kWh/m^2}{5} = \frac{117.5\ kWh}{1\ m^2}$$

Appendix III
Energy Requirements for Utility Scale (and Rooftop) Solar Production (Embodied Energy)

Note, I converted all energy calculations to kWh / m^2 for comparison purposes.

Nawaz & Tiwari (2006) estimated the embodied energy for each type of solar installation, the results are as follows.

- Estimated energy requirements for BOS components for "open field installation" / utility scale solar:

$$\frac{500 \text{ kWh}}{1 \text{ m}^2 \text{ PV modules}}$$

- Estimated energy requirements for BOS components for rooftop solar installations:

$$\frac{200 \text{ kWh}}{1 \text{ m}^2 \text{ PV modules}}$$

- Decrease is primarily due to a rooftop solars decreased need for many support structures, etc.

Mason, Fthenakis, & Kim (2005) estimated that all BOS components for a utility scale solar site have an average embodied energy value of,

$$\frac{542 \text{ MJ}}{1 \text{ m}^2} \times \frac{0.277778 \text{ kWh}}{1 \text{ MJ}} = \frac{150.56 \text{ kWh}}{1 \text{ m}^2}$$

Zhou & Carbajales-Dale (2018) estimates that BOS components have an embodied energy range. This range is as follows.

- Low value:

$$\frac{37 \text{ kWh}}{1 \text{ m}^2}$$

- High value:

$$\frac{206 \text{ kWh}}{1 \text{ m}^2}$$

Using three of the four values provided above that are associated with utility scale solar, I calculated an average for utility scale embodied energy.

$$\frac{151 \text{ kWh}}{1 \text{ m}^2} + \frac{37 \text{ kWh}}{1 \text{ m}^2} + \frac{206 \text{ kWh}}{1 \text{ m}^2} = \frac{394 \text{ kWh}}{1 \text{ m}^2}$$

$$\frac{394 \text{ kWh/m}^2}{3} = \sim 131 \text{ kWh / m}^2$$

Due to the uncertainty associated with this calculation, the number will not be used for further analysis.

Appendix IV
Energy Payback Times (EPBT) of Crystalline Silicon and Perovskite PV

According to Nawaz & Tiwari (2006) and Bhandari et al. (2015), as well as most other studies, the EPBT is calculated using the following formula.

EPBT = Embedded energy
Energy output of system

In the previous Appendix I and II, I calculated the average embodied energy values for both crystalline silicon and perovskite PV. The results are as follows
Embedded energy:

- **Crystalline silicon: ~ 451 kWh/m^2**
- **Perovskite: ~ 118 kWh/m^2**

The energy output of the system is dependent on a variety of things.
Nawaz & Tiwari (2006) used the following formula to calculate the energy output $E_{(out)}$ of a PV system.

$E_{(out)}$ = insolation (kWh/m^2/year) x solar cell efficiency x packing factor x BOS efficiencies

Nawaz & Tiwari (2006) calculated an average insolation value of 3.95 kWh/m^2/year

For insolation averages, refer to the NREL-produced Map 1 on the following page. This map depicts the average 'Global Horizontal Solar Irradiance,' at locations throughout the United States, using data from 1998 to 2016. For the purpose of this study, we will look at the following four insolation values as they provide differing perspectives to the growing energy issues.

< 4.00 kWh/m^2/day, or 3.95 kWh/m^2/day from Nawaz & Tiwari (2006), for the purpose of this study

- This represents the northern region of the U.S., including Maine, New Hampshire, Vermont, New York, Pennsylvania, Michigan, Wisconsin, Minnesota, North Dakota, Montana, and Washington. Please see Map 1.
- Convert to per year for annual energy output

$$\frac{3.95\ \text{kWh}}{1\ \text{m}^2} \times \frac{365\ \text{days}}{1\ \text{year}} = \frac{1441.75\ \text{kWh}}{1\ \text{m}^2}$$

NEW value: **1442 kWh/m^2/year**
Let's call this low annual insolation areas

4.50 to 4.75 kwh/m^2/day, or 4.75 kWh/m^2/day, for the purpose of this study

- This represents the middle (horizontal) region of the U.S., spanning from North Carolina to Northern California/Southern Oregon. This includes, North Carolina, Arkansas, the northern halves of Georgia, Alabama, and Mississippi, as well as large portions of Kansas, Nebraska, Idaho, Wyoming, Oregon, and California. See Map 1.
- Convert to per year for annual energy output

$\frac{4.75 \text{ kWh}}{1 \text{ m}^2}$ x 365 days / year = $\frac{1733.75 \text{ kWh}}{1 \text{ m}^2}$

1 day 1 year

NEW value: **1734 kWh/m^2/year**

Let's call this medium to low annual insolation areas

5.0 to 5.50 kWh/m^2/day, or 5.25 kWh/m^2/day, for the purpose of this study

- This represents most of Florida, half of Texas, and large portions of Oklahoma, Colorado, Utah, Nevada, and California. See Map 1.
- Convert to per year for annual energy output

$\frac{5.25 \text{ kWh}}{1 \text{ m}^2}$ x 365 days / year = $\frac{1916.25 \text{ kWh}}{1 \text{ m}^2}$

1 day 1 year

NEW value: **1916 kWh/m^2/year**

Let's call this medium to high annual insolation areas

$\geq$ 5.75 kWh/m^2/day, or 6 kWh/m^2/day, for the purpose of this study

- This represents the southern-most portions of the western U.S., including the southern halves of New Mexico, Arizona, and California, as well as the southwest portion of Texas. See Map 1.
- Convert to per year for annual energy output

$\frac{6 \text{ kWh}}{1 \text{ m}^2}$ x 365 days / year = $\frac{2190 \text{ kWh}}{1 \text{ m}^2}$

1 day 1 year

NEW value: **2190 kWh/m^2/year**

Let's call this high annual insolation areas

Therefore, the four insolation values selected for this study are,

1. **1442 kWh/m^2/year – low annual insolation**
2. **1734 kWh/m^2/year – medium to low annual insolation**
3. **1916 kWh/m^2/year – medium to high annual insolation**
4. **2190 kWh/m^2/year – high annual insolation**

Map 1 (on the following page): "Global Horizontal Solar Irradiance," from *Solar Maps,* by NREL

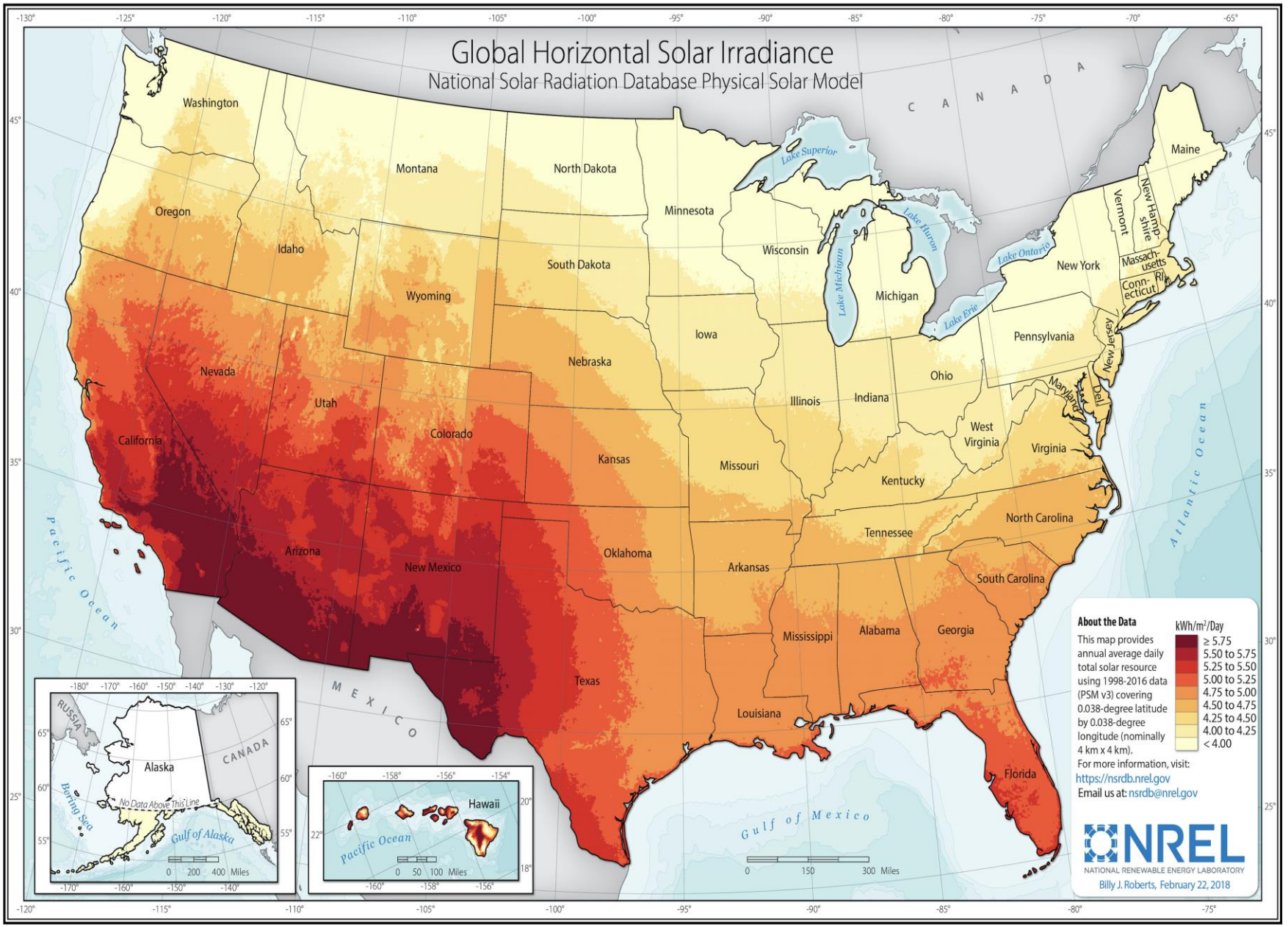
Global Horizontal Solar Irradiance
National Solar Radiation Database Physical Solar Model
CANADA
Washington
Oregon
California
Nevada
Idaho
Montana
Wyoming
Utah
Arizona
Colorado
New Mexico
North Dakota
South Dakota
Nebraska
Kansas
Oklahoma
Texas
Minnesota
Iowa
Missouri
Arkansas
Louisiana
Wisconsin
Illinois
Michigan
Indiana
Ohio
Kentucky
Tennessee
Mississippi
Alabama
Georgia
Florida
South Carolina
North Carolina
Virginia
West Virginia
Pennsylvania
New York
Maine
Vermont
New Hampshire
Massachusetts
Connecticut
RI
New Jersey
Maryland
Del
Lake Superior
Lake Michigan
Lake Huron
Lake Erie
Lake Ontario
Pacific Ocean
Atlantic Ocean
Gulf of Mexico
MEXICO
Alaska
RUSSIA
CANADA
No Data Above This Line
Bering Sea
Gulf of Alaska
Hawaii
Pacific Ocean
About the Data
This map provides annual average daily total solar resource using 1998-2016 data (PSM v3) covering 0.038-degree latitude by 0.038-degree longitude (nominally 4 km x 4 km).
For more information, visit:
https://nsrdb.nrel.gov
Email us at: nsrdb@nrel.gov
kWh/m²/Day
≥ 5.75
5.50 to 5.75
5.25 to 5.50
5.00 to 5.25
4.75 to 5.00
4.50 to 4.75
4.25 to 4.50
4.00 to 4.25
< 4.00
NREL
NATIONAL RENEWABLE ENERGY LABORATORY
Billy J. Roberts, February 22, 2018

$E_{(out)}$ = insolation (kWh/m^2/year) x solar cell efficiency x packing factor x BOS efficiencies

The insolation values chosen for this study are,

- **1442 kWh/m^2/year – low annual insolation**
- **1734 kWh/m^2/year – medium to low annual insolation**
- **1916 kWh/m^2/year – medium to high annual insolation**
- **2190 kWh/m^2/year – high annual insolation**
- To get a well-rounded understanding of the impacts of location on EPBT.

Solar Cell Efficiency Values were found as well.

- Crystalline Silicon:
  - According to the DOE, crystalline silicon PV energy conversion efficiencies range from 18% to 22%, therefore an average efficiency for this module is ~ 20%
  - However, researchers have found that this average increased to ~ 27% in 2019 (A decade of perovskite 2019)
  - With this new information, the energy conversion average would fall just below 24% (~23.5%)
  - For the purpose of this study, a value of **24%** is used.
- Perovskite:
  - Incredibly dependent on the material selected for production.
  - The following conversion efficiencies were collected from 'A decade of perovskite (2019)'
  - Perovskite/silicon solar cells have reached ~28%
  - Lead-halide perovskites were ~ 4% in 2009, but have grown to ~ 24%
  - For the purpose of this study, a value of **24%** is used

Packing Factor:

- Nawaz & Tiwari (2006) define the packing factor as the "ratio of the area occupied by PV cells in a module to the actual area of the same module i.e.:

Packing factor (PF) = Area of PV cells in a module / Actual area of module"

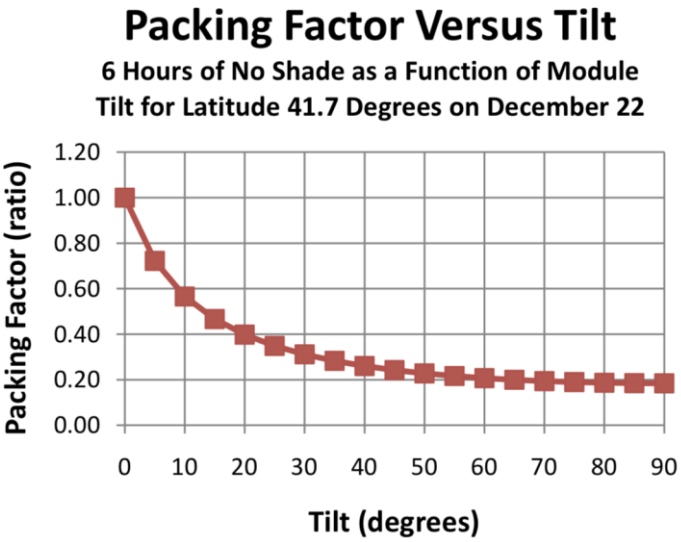

Figure 22: "Packing Factor Estimate Versus Tilt, from Feasibility Study of Economics and Performance of Solar Photovoltaic at Massachusetts Military Reservation, by Stafford, Robichaud, & Mosey 2011.

- Stafford, Robichaud, & Mosey (2011) define the packing factor as "the ratio of the row spacing divided by the row-to-row spacing." This article produced Figure 22 to illustrate packing factor as a function of the tilt of the PV module.
- Assuming this figure is accurate, the value chosen by Nawaz & Tiwari (2006) of 0.30 packing factor which coincides with ~ 35° tilt.
- From Marsh 2018, it is discovered that the degree of tilt coincides with the location of the solar site, i.e. the general rule of thumb is cloudier locations have increased tilts to maximize the amount of energy production during peak sunlight hours, whereas sunnier locations have decreased tilts to maximize energy production throughout the entire day.

- From Marsh 2018, it is discovered that the average panel tilt is ~38°, however it is dependent on the location of the solar site.
- For the purpose of this study, the values given by Marsh 2018 for solar panel tilt vs location are evaluated and applied towards their respective insolation values
- The locations and values from Marsh 2018 are placed into the following table next to their respective isolation value, based on the NREL Map 1 (note: the map is in kWh/m^2/day)

Table 11: Insolation Value vs Panel Tilt

Insolation Value	City, State	Optimal Solar Panel Tilt
1442 kWh/m^2/year	Boston, MA	42°
1442 kWh/m^2/year	Buffalo, NY	43°
1442 kWh/m^2/year	New York, New York	41°
1442 kWh/m^2/year	Newark, NJ	41°
1442 kWh/m^2/year	Portland, OR	46°
1442 kWh/m^2/year	Washington D.C.	39°
New Value		Average: 42°
1734 kWh/m^2/year	Austin, TX	30°
1734 kWh/m^2/year	Charlotte, NC	35°
1734 kWh/m^2/year	Denver, CO	40°
1734 kWh/m^2/year	Raleigh, NC	36°
1734 kWh/m^2/year	San Francisco, CA	38°
New Value		Average: 36°
1916 kWh/m^2/year	Alburquerque, MN	35°
1916 kWh/m^2/year	Los Angeles, CA	34°
1916 kWh/m^2/year	San Diego, CA	33°
New Value		Average: 34°
2190 kWh/m^2/year	Phoenix, AZ	33° (average)

- Use the averages from each insolation value selected to find the average packing factor in figure 23 on the previous page
- The pairing results are as follows,
    - **1442 kWh/m^2/year & 0.23 packing factor**
        - Low annual insolation
    - **1734 kWh/m^2/year & 0.29 packing factor**
        - Medium-low annual insolation
    - **1916 kWh/m^2/year & 0.31 packing factor**
        - Medium-high annual insolation
    - **2190 kWh/m^2/year & 0.32 packing factor**
        - High annual insolation
    - This assumes a 35° tilt coincides with 0.30 packing factor for calculation

$E_{(out)}$ = insolation (kWh/m^2/year) x solar cell efficiency x packing factor x BOS efficiencies

BOS component efficiencies:

- Nawaz & Tiwari (2006) suggest that BOS components have an average energy conversion efficiency of 80%
- Mason, Fthenakis, Hansen, & Kim (2005) suggest the efficiencies of these support structures can be as high as 99%
- For the purpose of this study, an average BOS efficiency level of 90% is assumed

With that, we can begin our energy output calculation based on four different locations.

$E_{(out)}$ = insolation (kWh/m^2/year) x solar cell efficiency x packing factor x BOS efficiencies

- **1442 kWh/m^2/year & 0.23 packing factor**
  - Low annual insolation areas
- **1734 kWh/m^2/year & 0.29 packing factor**
  - Medium-low annual insolation areas
- **1916 kWh/m^2/year & 0.31 packing factor**
  - Medium-high annual insolation areas
- **2190 kWh/m^2/year & 0.32 packing factor**
  - High annual insolation areas
- **Crystalline silicon and perovskite PV have calculated average energy conversion efficiency levels of 24%, so same values regardless of panel (complete EPBT calculation will be different based on different embodied energy values)**
- **BOS components have a calculated average efficiency level of 90%**
- The values are placed in the table below and multiplied together to calculate the total energy output of the panels at various insolation locations

Table 12: Total Energy Output vs Insolation

Insolation (kWh/m^2/year)	**Packing Factor**	**Solar Cell Efficiency**	**BOS Efficiency**	**Total Energy Output (kWh/m^2/year)**
1442 kWh/m^2/year (low)	0.23	0.24	0.90	~ 72 kWh/m^2/year
1734 kWh/m^2/year (medium-low)	0.29	0.24	0.90	~109 kWh/m^2/year
1916 kWh/m^2/year (medium-high)	0.31	0.24	0.90	~128 kWh/m^2/year
2190 kWh/m^2/year (high)	0.32	0.24	0.90	~151 kWh/m^2/year

Finally, we can use these values to calculate an EPBT range in years for each panel type (depending on location, i.e. insolation values)

EPBT = $\frac{\text{Embedded energy}}{\text{Energy output of system}}$

Embedded energy:

- **Crystalline silicon: ~ 451 kWh/m^2**
- **Perovskite: ~ 118 kWh/m^2**

Each panel's EPBT range is calculated on the following page.

Table 13: CRYSTALLINE SILICON EPBTs

Insolation	**Calculation**	**EPBT**
Low	$\frac{451\ kWh/m^2}{72\ kWh/m^2/year}$	~ 6 years
Medium-low	$\frac{451\ kWh/m^2}{109\ kWh/m^2/year}$	~ 4 years
Medium-high	$\frac{451\ kWh/m^2}{128\ kWh/m^2/year}$	~ 3.5 years
High	$\frac{451\ kWh/m^2}{151\ kWh/m^2/year}$	~ 3 years

From this table, it can be assumed that the EPBT of crystalline silicon PV can range anywhere between 3 and 6 years, aligning with previous calculations from other researchers, however there are some studies suggesting the EPBT of crystalline silicon can be as low as 2 years (Gerbinet, Belboom, & Leonard 2014 & Bhandari et al. 2015). Therefore, the EPBT for crystalline silicon PV ranges from 2 to 6 years depending on the processes used for manufacturing, etc. The EPBT is extremely location dependent as the energy output of the system strives off of incoming sunlight.

Table 14: PEROVSKITE EPBTs

Insolation	Calculation	EPBT
Low	$\frac{118\ kWh/m^2}{72\ kWh/m^2/year}$	~ 2 years
Medium-low	$\frac{118\ kWh/m^2}{109\ kWh/m^2/year}$	~ 1 year
Medium-high	$\frac{118\ kWh/m^2}{128\ kWh/m^2/year}$	~ 0.9 year
High	$\frac{118\ kWh/m^2}{151\ kWh/m^2/year}$	~ 0.8 year

The last two results for perovskite EPBT can be excluded for further analysis. Using data from outside sources, EPBTs of perovskite PV systems can be as low as 0.22 years (Gong, Darling, & You 2015, Kim et al. 2016, & Celik, et al. 2016). Therefore, it can be assumed that the EPBT of perovskite PV can range anywhere between 0.22 years and 2 years, aligning with previous calculations from other researchers. As stated previously, the EPBT is extremely location dependent due to variations in incoming sunlight.

Appendix V:
Average Global Warming Potentials of Crystalline Silicon and Perovskite PV

Table 9: Global Warming Potential of Crystalline Silicon PV

Source	**Global Warming Potential (g CO_2-eq. / kWh)**
Fthenakis, Kim, & Alsema (2007)	~ 30 to 45 g CO_2-eq. / kWh
Hsu, et al. (2012)	~ 57 g CO_2-eq. / kWh
Gerbinet, Belboom, & Leonard (2014)	~ 39 to 100 g CO_2-eq. / kWh
Gong, Darling, & You (2015)	~ 40 g CO_2-eq. / kWh
Leccisi, Raugei, & Fthenakis (2016)	~ 30 g CO_2-eq. / kWh

To figure out the average GWP of crystalline silicon PV, I used the following calculation.

30 g CO_2-eq./kWh + 45 g CO_2-eq./kWh + 57 g CO_2-eq./kWh + 39 g CO_2-eq./kWh + 100 g CO_2-eq./kWh + 40 g CO_2-eq./kWh + 30 g CO_2-eq./kWh = $\frac{341 \text{ g } CO_2\text{-eq.}}{\text{kWh}}$

$\frac{341 \text{ g } CO_2\text{-eq./kWh}}{7} = \frac{48.7 \text{ g } CO_2\text{-eq.}}{\text{kWh}}$

Table 10: Global Warming Potential of Perovskite PV

Source	**Global Warming Potential (g CO_2-eq. / kWh)**
Garcia-Valverde, Cherni, & Urbina (2010)	~ 55 to 110 g CO_2-eq. / kWh
Espinosa, et al. (2015)	~ 350 g CO_2-eq. / kWh
Gong, Darling, & You (2015)	~ 60 to 100 g CO_2-eq. / kWh
Celik, et al. (2016)	~ 99 to 147 g CO_2-eq. / kWh
Ibn-Mohammed, et al. (2017)	~ 90 to 160 g CO_2-eq. / kWh

To calculate the average global warming potential (GWP) for perovskite solar cells, I removed the outlier from Espinosa et al. (2015) first. Then, I added the low value points together and the high value points together and solved for the average. The calculation and results are as follows.

- Low value of range

  $\frac{55\ g\ CO_2\text{-eq.}}{kWh} + \frac{60\ g\ CO_2\text{-eq.}}{kWh} + \frac{99\ g\ CO_2\text{-eq.}}{kWh} + \frac{90\ g\ CO_2\text{-eq.}}{kWh} = \frac{304\ g\ CO_2\text{-eq.}}{kWh}$

  $\frac{304\ g\ CO_2\text{-eq.}\ /\ kWh}{4} = \frac{76\ g\ CO_2\text{-eq.}}{kWh}$

- High value of range

  $\frac{110\ g\ CO_2\text{-eq.}}{kWh} + \frac{100\ g\ CO_2\text{-eq.}}{kWh} + \frac{147\ g\ CO_2\text{-eq.}}{kWh} + \frac{160\ g\ CO_2\text{-eq.}}{kWh} = \frac{517\ g\ CO_2\text{-eq.}}{kWh}$

  $\frac{517\ g\ CO_2\text{-eq.}\ /\ kWh}{4} = \frac{129.25\ g\ CO_2\text{-eq.}}{kWh}$

- Average GWP range for perovskite PV:

  $\frac{76\ g\ CO_2\text{-eq.}}{kWh}$ to $\frac{129\ g\ CO_2\text{-eq.}}{kWh}$

- To get a single average GWP value, I calculated the following,

  $\frac{76\ g\ CO_2\text{-eq.}}{kWh} + \frac{129\ g\ CO_2\text{-eq.}}{kWh} = \frac{205\ g\ CO_2\text{-eq.}}{kWh}$

  $\frac{205\ g\ CO_2\text{-eq.}\ /\ kWh}{2} = \frac{102.5\ g\ CO_2\text{-eq.}}{kWh}$

Appendix VI:
Ecosystem Services

Using the EPA-produce map of North American Ecosystems below, I separated states into the following tables depending on insolation values determined previously from the NREL MAP.

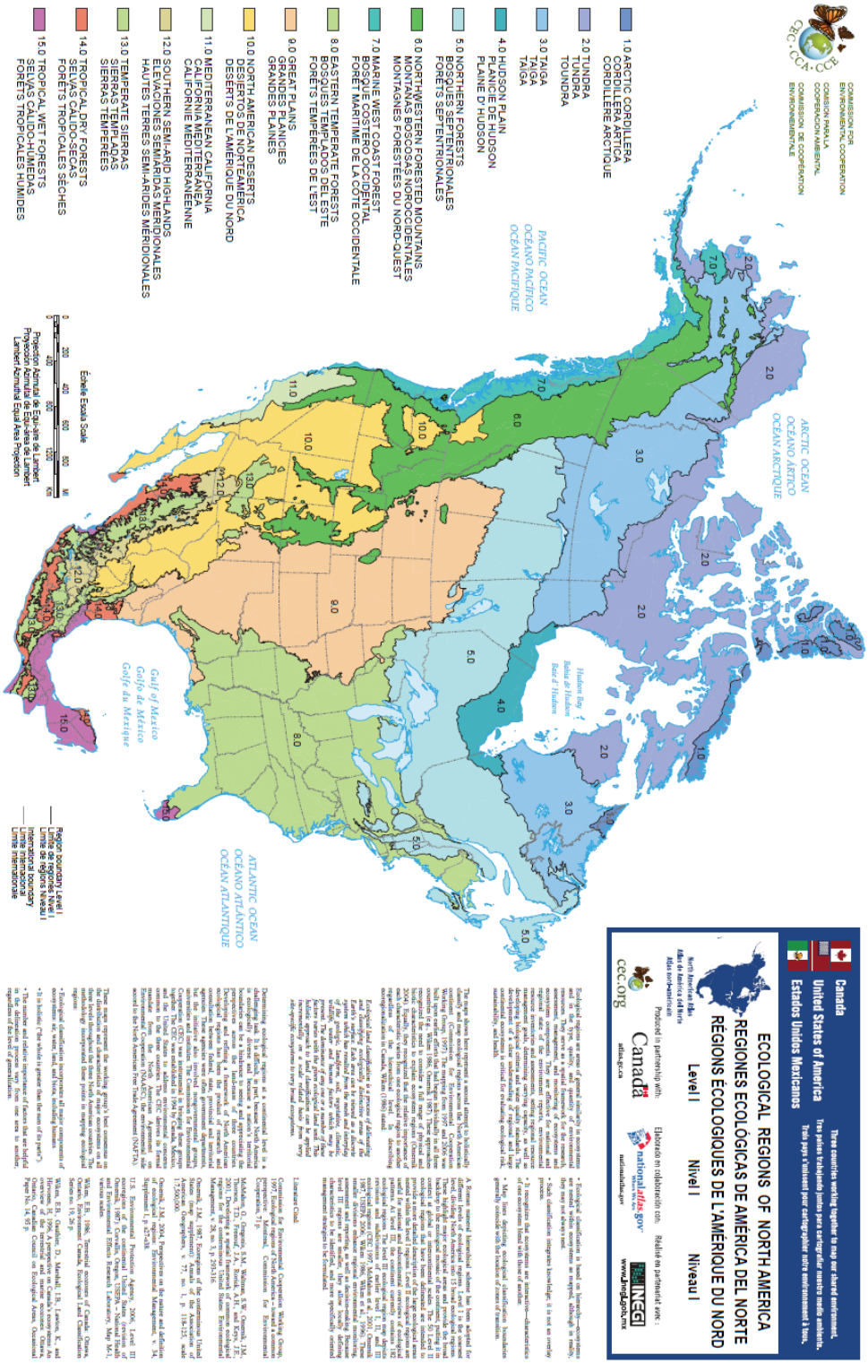

Map 2: Ecological Regions of North America, from *Ecoregions of North America*, by EPA

Table 15: Low insolation value state areas (~ 3.95 kWh/m^2/day, or ~ 1442 kWh/m^2/year)

State	Ecological Region 1	Ecological Region 2	Ecological Region 3
Maine	Northern Forests	Eastern Temperate Forests	
New Hampshire	Northern Forests	Eastern Temperate Forest	
Vermont	Northern Forests	Eastern Temperate Forest	
New York	Northern Forests	Eastern Temperate Forest	
Pennsylvania	Northern Forests	Eastern Temperate Forest	
Michigan	Northern Forests	Eastern Temperate Forest	
Wisconsin	Northern Forests	Eastern Temperate Forest	
Minnesota	Northern Forests	Eastern Temperate Forest	Great Plains
North Dakota	Great Plains		
Montana	Great Plains	Northwestern Forested Mountain	
Northern Idaho	Northwestern Forested Mountains		
Washington	Northwestern Forested Mountains	North American Deserts	Marine West Coast Forest

According to this table, low insolation areas are predominately associated with forested areas, including Northern Forests, Eastern Temperate Forests, and Northwestern Forested Mountains primarily.

Table 16: Medium-low insolation value state areas (~ 4.75 kWh/m^2/day, or ~ 1734 kWh/m^2/year)

State	Ecological Region 1	Ecological Region 2	Ecological Region 3
North Carolina	Eastern Temperate Forests		
Arkansas	Eastern Temperate Forests		
Northern Georgia	Eastern Temperate Forests		
Northern Alabama	Eastern Temperate Forests		
Northern Mississippi	Eastern Temperate Forests		
Kansas	Great Plains		

Nebraska	Great Plains		
Wyoming	Great Plains	Northwestern Forested Mountains	North American Deserts
Southern Idaho	North American Deserts	Northwestern Forested Mountains	
Southern Oregon	North American Deserts	Northwestern Forested Mountains	Marine West Coast Forest
Northern Colorado	North American Deserts	Northwestern Forested Mountains	Great Plains
Northern Utah	North American Deserts	Northwestern Forested Mountains	
Northern Nevada	North American Deserts		
Northern California	Northwestern Forested Mountains	Marine West Coast Forests	

According to this table, medium-low insolation areas are dominated nearly equally by both forests and deserts, including Eastern Temperate Forests and Northwestern Forested Mountains primarily, as well as the North American Deserts.

Table 17: Medium-high insolation value state areas (~5.25 kWh/m^2/day, or ~1916 kWh/m^2/year)

State	**Ecological Region 1**	**Ecological Region 2**	**Ecological Region 3**
Florida	Eastern Temperate Forests	Tropical Wet Forests	
Eastern Texas	Eastern Temperate Forests	Great Plains	
Oklahoma	Great Plains		
Colorado	North American Deserts	Northwestern Forested Mountains	Great Plains
Utah	North American Deserts	Northwestern Forested Mountains	
Nevada	North American Deserts		
California	Mediterranean California		

According to this table, medium-high insolation areas are dominated by North American Deserts and the Great Plains.

Table 18: High insolation value state areas (~ 6 kWh/m^2/day, or ~ 2190 kWh/m^2/year)

State	Ecological Region 1	Ecological Region 2	Ecological Region 3
Southwest Texas	Great Plains	North American Desert	
Southern New Mexico	North American Deserts	Temperate Sierras	
Southern Arizona	North American Deserts	Temperate Sierras	Southern Semi-Arid Highlands
Southern California	North American Deserts	Mediterranean California	

According to this table, high insolation value areas are dominated by the North American Deserts.

Therefore, we can assume the following,

- Low insolation areas are dominated by forested lands
- Medium-low insolation areas are dominated by both forested lands and the North American deserts
- Medium-high insolation areas are dominated by both North American Deserts and the Great Plains
- High insolation areas are dominated by the North American Deserts

Using data collected from this analysis, the following three ecosystem regions were chosen for further analysis in the land use impact category section;

1. **North American Forests (compiled information from Northern Forests, Eastern Temperate Forests, and Northwestern Forested Mountains)**
2. **North American Deserts**
3. **The Great Plains**